Pertanika Journal of

SCIENCE & TECHNOLOGY

JST

VOL. 33 (S5) 2025

A Special Issue devoted to

Global Food and Agriculture Recovery in the Post-Pandemic World

Guest Editors

Hazreen Haizi Harith, Rosnita A. Talib and Nazmi Mat Nawi

PERTANIKA JOURNALS

A scientific journal published by Universiti Putra Malaysia Press

Pertanika Journal of Science & Technology
Pertanika Journal of Science & Technology

PERTANIKA JOURNAL OF SCIENCE & TECHNOLOGY

About the Journal

Overview

Pertanika Journal of Science & Technology is an official journal of Universiti Putra Malaysia. It is an open-access online scientific journal. It publishes original scientific outputs. It neither accepts nor commissions third party content.

Recognised internationally as the leading peer-reviewed interdisciplinary journal devoted to the publication of original papers, it serves as a forum for practical approaches to improve quality on issues pertaining to science and engineering and its related fields.

Pertanika Journal of Science & Technology currently publishes 6 issues a year (*January, March, April*, *July, August,* and *October*). It is considered for publication of original articles as per its scope. The journal publishes in **English** and it is open for submission by authors from all over the world.

The journal is available world-wide.

Aims and scope

Pertanika Journal of Science & Technology aims to provide a forum for high quality research related to science and engineering research. Areas relevant to the scope of the journal include: bioinformatics, bioscience, biotechnology and bio-molecular sciences, chemistry, computer science, ecology, engineering, engineering design, environmental control and management, mathematics and statistics, medicine and health sciences, nanotechnology, physics, safety and emergency management, and related fields of study.

History

Pertanika Journal of Science & Technology was founded in 1993 and focuses on research in science and engineering and its related fields.

Vision

To publish a journal of international repute.

Mission

Our goal is to bring the highest quality research to the widest possible audience.

Quality

We aim for excellence, sustained by a responsible and professional approach to journal publishing. Submissions can expect to receive a decision within 90 days. The elapsed time from submission to publication for the articles averages 180 days. We are working towards decreasing the processing time with the help of our editors and the reviewers.

Abstracting and indexing of Pertanika

Pertanika Journal of Science & Technology is now over 33 years old; this accumulated knowledge and experience has resulted the journal being abstracted and indexed in SCOPUS (Elsevier), Journal Citation Reports (JCR-Clarivate), EBSCO, ASEAN CITATION INDEX, Microsoft Academic, Google Scholar, and MyCite.

Citing journal articles

The abbreviation for Pertanika Journal of Science & Technology is *Pertanika J. Sci. & Technol.*

Publication policy

Pertanika policy prohibits an author from submitting the same manuscript for concurrent consideration by two or more publications. It prohibits as well publication of any manuscript that has already been published either in whole or substantial part elsewhere. It also does not permit publication of manuscript that has been published in full in proceedings.

Code of Ethics

The *Pertanika* journals and Universiti Putra Malaysia take seriously the responsibility of all of its journal publications to reflect the highest in publication ethics. Thus, all journals and journal editors are expected to abide by the journal's codes of ethics. Refer to *Pertanika*'s **Code of Ethics** for full details, or visit the journal's web link at http://www.pertanika.upm.edu.my/code_of_ethics.php

Originality

The author must ensure that when a manuscript is submitted to *Pertanika*, the manuscript must be an original work. The author should check the manuscript for any possible plagiarism using any program such as Turn-It-In or any other software before submitting the manuscripts to the *Pertanika* Editorial Office, Journal Division.

All submitted manuscripts must be in the journal's acceptable similarity index range:

≤ 20% – PASS; > 20% – REJECT.

International Standard Serial Number (ISSN)

An ISSN is an 8-digit code used to identify periodicals such as journals of all kinds and on all media–print and electronic.

Pertanika Journal of Science & Technology: e-ISSN 2231-8526 (Online).

Lag time

A decision on acceptance or rejection of a manuscript is reached in 90 days (average). The elapsed time from submission to publication for the articles averages 180 days.

Authorship

Authors are not permitted to add or remove any names from the authorship provided at the time of initial submission without the consent of the journal's Chief Executive Editor.

Manuscript preparation

For manuscript preparation, authors may refer to Pertanika's **INSTRUCTION TO AUTHORS**, available on the official website of *Pertanika*.

Editorial process

Authors who complete any submission are notified with an acknowledgement containing a manuscript ID on receipt of a manuscript, and upon the editorial decision regarding publication.

Pertanika follows a **double-blind peer-review** process. Manuscripts deemed suitable for publication are sent to reviewers. Authors are encouraged to suggest names of at least 3 potential reviewers at the time of submission of their manuscripts to *Pertanika*, but the editors will make the final selection and are not, however, bound by these suggestions.

Notification of the editorial decision is usually provided within 90 days from the receipt of manuscript. Publication of solicited manuscripts is not guaranteed. In most cases, manuscripts are accepted conditionally, pending an author's revision of the material.

The journal's peer review

In the peer-review process, 2 to 3 referees independently evaluate the scientific quality of the submitted manuscripts. At least 2 referee reports are required to help make a decision.

Peer reviewers are experts chosen by journal editors to provide written assessment of the **strengths** and **weaknesses** of written research, with the aim of improving the reporting of research and identifying the most appropriate and highest quality material for the journal.

Operating and review process

What happens to a manuscript once it is submitted to *Pertanika*? Typically, there are 7 steps to the editorial review process:

1. The journal's Chief Executive Editor and the Editor-in-Chief examine the paper to determine whether it is relevance to journal needs in terms of novelty, impact, design, procedure, language as well as presentation and allow it to proceed to the reviewing process. If not appropriate, the manuscript is rejected outright and the author is informed.

2. The Chief Executive Editor sends the article-identifying information having been removed, to 2 to 3 reviewers. They are specialists in the subject matter of the article. The Chief Executive Editor requests that they complete the review within 3 weeks.

   Comments to authors are about the appropriateness and adequacy of the theoretical or conceptual framework, literature review, method, results and discussion, and conclusions. Reviewers often include suggestions for strengthening of the manuscript. Comments to the editor are in the nature of the significance of the work and its potential contribution to the research field.

Pertanika Journal of Science & Technology
Pertanika Journal of Science & Technology

Pertanika Journal of Science & Technology
Pertanika Journal of Science & Technology

3. The Editor-in-Chief examines the review reports and decides whether to accept or reject the manuscript, invite the authors to revise and resubmit the manuscript, or seek additional review reports. In rare instances, the manuscript is accepted with almost no revision. Almost without exception, reviewers' comments (to the authors) are forwarded to the authors. If a revision is indicated, the editor provides guidelines for attending to the reviewers' suggestions and perhaps additional advice about revising the manuscript.

4. The authors decide whether and how to address the reviewers' comments and criticisms and the editor's concerns. The authors return a revised version of the paper to the Chief Executive Editor along with specific information describing how they have addressed' the concerns of the reviewers and the editor, usually in a tabular form. The authors may also submit a rebuttal if there is a need especially when the authors disagree with certain comments provided by reviewers.

5. The Chief Executive Editor sends the revised manuscript out for re-review. Typically, at least 1 of the original reviewers will be asked to examine the article.

6. When the reviewers have completed their work, the Editor-in-Chief examines their comments and decides whether the manuscript is ready to be published, needs another round of revisions, or should be rejected. If the decision is to accept, the Chief Executive Editor is notified.

7. The Chief Executive Editor reserves the final right to accept or reject any material for publication, if the processing of a particular manuscript is deemed not to be in compliance with the S.O.P. of *Pertanika*. An acceptance letter is sent to all the authors.

   The editorial office ensures that the manuscript adheres to the correct style (in-text citations, the reference list, and tables are typical areas of concern, clarity, and grammar). The authors are asked to respond to any minor queries by the editorial office. Following these corrections, page proofs are mailed to the corresponding authors for their final approval. At this point, **only essential changes are accepted**. Finally, the manuscript appears in the pages of the journal and is posted on-line.

Pertanika Journal of

SCIENCE & TECHNOLOGY

A Special Issue devoted to
Global Food and Agriculture Recovery in the Post-Pandemic World

Vol. 33 (S5) 2025

Guest Editors
Hazreen Haizi Harith, Rosnita A. Talib and Nazmi Mat Nawi

A scientific journal published by Universiti Putra Malaysia Press

PJST
Pertanika Journal of Science & Technology
AN INTERNATIONAL PEER-REVIEWED JOURNAL

EDITORIAL OFFICE
JOURNAL DIVISION
Putra Science Park
1st Floor, IDEA Tower II
UPM-MTDC Technology Centre
Universiti Putra Malaysia
43400 Serdang, Selangor Malaysia.

General Enquiry
Tel. No: +603 9769 1622
E-mail:
executive_editor.pertanika@upm.edu.my
URL: http://www.pertanika.upm.edu.my

PUBLISHER
UPM Press
Universiti Putra Malaysia
43400 UPM, Serdang, Selangor, Malaysia.
Tel: +603 9769 8855
E-mail: dir.penerbit@upm.edu.my
URL: http://penerbit.upm.edu.my

ABSTRACTING AND INDEXING OF PERTANIKA JOURNALS

Pertanika Journal of Science & Technology is indexed in Journal Citation Reports (JCR-Clarivate), SCOPUS (Elsevier), EBSCO, ASEAN Citation Index, Microsoft Academic, Google Scholar and MyCite.

Pertanika Journal of Science & Technology
Vol. 33 (S5) 2025

Contents

Preface

We are pleased to present the second volume of the *Pertanika Journal of Science and Technology* Special Issue, featuring another selection of peer-reviewed articles presented at the **International Conference on Agricultural and Food Engineering 2023 (CAFEi 2023)**. Held under the theme *"Global Food and Agriculture Recovery in the Post-Pandemic World,"* the conference served as a vital forum for advancing knowledge and fostering innovation in rebuilding agri-food systems for greater sustainability, safety, and resilience.

This second volume continues to showcase the interdisciplinary strength of CAFEi2023 by highlighting original research from diverse fields, including food safety, agricultural biotechnology, postharvest engineering, environmental monitoring, and digital agriculture. The studies presented here reflect a shared regional and global commitment to addressing complex challenges in agriculture and food production through the application of science and technology.

Notable contributions in this volume include:

- **Environmental health and crop safety**, as explored in a study on heavy metal accumulation in crops near nickel mining areas in the Philippines.
- **Postharvest innovation**, focusing on research into drying kinetics and nutritional preservation of Pegaga (*Centella asiatica L.*) leaves using various pretreatment methods.
- **Digital and AI-enhanced agriculture**, demonstrated by the application of artificial neural networks for monitoring moisture levels in dried earthworms, highlights the integration of machine learning in agricultural process control.
- **Green bioprocessing and functional materials**, such as the use of liquid biphasic flotation for protein separation from *Azolla pinnata* and the development of biodegradable composite polymer materials for agricultural use.
- **Food quality and authenticity** were addressed using Vis-NIR spectroscopy and chemometrics to detect pork adulteration in beef and mutton products, emphasizing the importance of food traceability and consumer trust.
- **Engineering innovations in fermentation** through the development of a compact fermentation container with stirring mechanisms to improve cocoa bean quality.

Each of these studies represents a valuable contribution to the body of knowledge supporting sustainable and technology-driven transformations in the agricultural and food sectors.

We extend our deepest gratitude to all authors for their high-quality submissions, to the reviewers for their critical insights and timely evaluations, and to the editorial and publishing team at *Pertanika Journal of Science and Technology* for their unwavering support.

We hope that this volume, along with the first, will serve as a lasting reference for researchers, practitioners, and policymakers and continue to inspire collaborative innovation for a more sustainable and secure global agri-food future.

Guest Editors
Hazreen Haizi Harith (Dr.)
Rosnita A. Talib (Assoc. Prof. Dr.)
Nazmi Mat Nawi (Assoc. Prof. Dr.)

Pertanika J. Sci. & Technol. 33 (S5): 1 - 17 (2025)

PERTANIKA JOURNALS

SCIENCE & TECHNOLOGY

Journal homepage: http://www.pertanika.upm.edu.my/

Assessment of Heavy Metal Accumulation in Agricultural Crops in a Nickel Mining Site in Agusan Del Norte

Jobelle Jayoma Capilitan[1,2]* and Ian Dominic Flormata Tabañag[1,3]

[1]School of Engineering, University of San Carlos, Talamban, Cebu City, 6000, Philippines
[2]Caraga State University, Butuan City, Philippine
[3]Philippine Council for Industry, Energy, and Emerging Technology Research and Development, Department of Science and Technology (DOST-PCIEERD), Bicutan, Taguig City, 1631, Philippines

ABSTRACT

Ni laterite exploration by surface mining is destructive to the local biological landscape. A sustainable approach is mine restoration using vegetation. Nonetheless, substantial concentrations of heavy metals are present in areas impacted by anthropogenic activities, such as mining. Crops may absorb heavy metals from the soil, which can have adverse effects on the land, water, and human health. This study assesses the accumulation of heavy metals (Cr, Cu, Ni, Mn, and Zn) in the soil and the consumable parts of crops (roots, leaves, and fruits) at the nickel laterite mining site in Tubay, Agusan del Norte, along with the potential health risks associated with human intake. The concentration of heavy metals in the soil and crops significantly exceeds the maximum permissible limit (MPL) set by the FAO and WHO. The concentration of heavy metals in the edible sections is ranked as follows: Mn > Ni > Zn > Cr > Cu. The Target Hazard Quotient (THQ) assessed non-carcinogenic risks, indicating that Cr, Cu, Mn, and Ni exceeded 1. The THQ number signifies significant health risks associated with prolonged consumption of the plant's edible parts.

Keywords: Health risk, heavy metal accumulation, nickel mine, target hazard quotient, XRF

INTRODUCTION

Agriculture is essential to the nation's food security. In an agrarian country like the Philippines, agriculture constitutes the foundation of its economy. For many years, agriculture-related activities have been a primary source of income and employment (Philippine Statistics Authority, 2024).

Mining has also significantly contributed to nation-building, economic stability, and

ARTICLE INFO

Article history:
Received: 13 February 2025
Accepted: 28 May 2025
Published: 10 July 2025

DOI: https://doi.org/10.47836/pjst.33.S5.01

E-mail addresses:
jjcapilitan@carsu.edu.ph (Jobelle Jayoma Capilitan)
ian.tabanag@pcieerd.dost.gov.ph (Ian Dominic Flormata Tabañag)
* Corresponding author

technological advancements in the Philippines. In 2022, the Philippines led the global nickel (Ni) source market, accounting for an estimated 11%–12% of global output (GlobalData, 2022; Moon, 2024), ranking second among the world's nickel-producing countries (Moon, 2024). As of June 2024, the country has 36 operational metallic mines, primarily concentrated on nickel, with 24 mining companies located in the Caraga region (Mines and Geosciences Bureau, 2024). The Caraga region is recognized as the primary nickel producer, accounting for 46.57% of the overall metallic mineral production value. Nonetheless, the continuous effort to achieve economic stability, involving agriculture and mining operations as pivotal sectors in the region's development, presents threats to agricultural quality and the environment.

Mining operations, particularly the extraction of nickel (Ni) from laterite ores using open-pit methods, exacerbate the accumulation of heavy metals, leading to significant ecological and human health concerns (Setia et al., 2023) due to mine waste, including tailings, dams, and overburden waste rock sites (Apodaca et al., 2018; Gavhane et al., 2021). Mining activities are crucial in the release of numerous heavy metals into the environment, substantially contributing to contamination by copper, iron, manganese, and zinc (Haghighizadeh et al., 2024; Hu et al., 2024). Hence, in the absence of organic decomposition, they accumulate in the soil, endangering plants, human health, and the environment (Sadak, 2023).

Heavy metal contamination of soil can harm humans through direct ingestion or contact with contaminated soil and the food chain (Wuana & Okieimen, 2011). The conditions of the soil and land pollution are significant concerns regarding the safety of the food supply. The challenge of ensuring that food is safe to consume is essential worldwide. Compared to the routes of inhalation or skin contact exposure, food consumption is acknowledged as the principal means by which humans are exposed to various environmental toxins; this accounts for over 90 percent of the total intake (Akinyele & Shokunbi, 2015). It is fundamentally dependent on the condition of the soil, and the detrimental effects that contaminants such as heavy metals have had on crop quality have put human health at risk. The accumulation of heavy metals in crops is an increasing concern, as elevated levels of toxic elements can jeopardize plant health and present significant risks to human consumption. According to their potential nutritional functions, the World Health Organization (WHO) divided trace elements into three categories: potentially toxic heavy metals, elements of probable physiological importance, such as manganese (Mn) and nickel (Ni), and essential elements, like chromium (Cr), copper (Cu), and zinc (Zn) (Muñoz-Olivas & Cámara, 2007). However, as carcinogenic substances, excessive and continuous ingestion and exposure to these heavy metals may damage DNA, proteins, and lipids by creating free radicals (Gupta et al., 2022; Sadak, 2023).

Numerous studies have demonstrated that the accumulation of heavy metals is a risk to human health (Fodoué et al., 2022; Ghaneei-Bafghi et al., 2024; Haghighizadeh et al.,

2024; Hu et al., 2024; Setia et al., 2023). Concerns emerge when crop cultivation for mine rehabilitation is executed without prior evaluation of heavy metal pollution. The ramifications of heavy metal contamination in agriculture are substantial, underscoring the necessity for soil and crop compatibility evaluations, an essential component of post-mining operations.

This study evaluates the accumulation of chromium (Cr), copper (Cu), manganese (Mn), nickel (Ni), and zinc (Zn) on selected crops that were grown in the rehabilitated area at the nickel mining site in Tubay, Agusan del Norte. It compares the results to the recommended amounts for each element set by the World Health Organization (WHO) and the Food and Agriculture Organization (FAO).

An X-ray fluorescence (XRF) spectroscopy investigation of the soil is carried out to ascertain the level of heavy metals in the soil and the crops. According to a study by Peralta et al. (2020), in-situ soil studies using XRF spectroscopy have been proven to be an effective tool for detecting the amount of metal contamination. This technology can concurrently determine the overall concentration of several different elements at a relatively low running cost and with a minimal sample requirement (McComb et al., 2014). The technology known as X-ray fluorescence, which is more usually abbreviated as XRF, is both quick and non-destructive. These benefits are compared to ICP-OES and ICP-MS, which provide extensive preparation for solid samples. Comparative research demonstrates that XRF is an excellent method for analyzing contaminated soils and crops because it does not degrade samples during analysis (Kim et al., 2022; McComb et al., 2014).

This study also investigates the potential adverse health effects that may be caused by heavy metals in the edible parts of crops if ingested by adults, using the bioconcentration factor (BCF) and the Target Hazard Quotient (THQ). The health risk assessment (HRA) method, such as the THQ, has been utilized in the investigations concerning the intake of vegetables exposed to toxic metals in the area (Gupta et al., 2022; Kharazi et al., 2021; Li et al., 2018). This information, which has never bee

n investigated, is crucial to assessing and determining post-mining considerations and mine rehabilitation alternatives. This research is limited to the nickel mining site in Tubay, Agusan del Norte, focusing on the crops grown in the rehabilitated area.

MATERIALS AND METHODS

Study Area

The nickel mining site is located within the municipal boundaries of Tubay, Jabonga, and Santiago in Agusan del Norte of Region XIII (Caraga), Philippines (Figure 1). It lies 9°10’30” north and 125°29’30” east at an elevation ranging from 310 to 325 meters above sea level. The mining site is inside a 4,995-hectare region bordered by water features, including the Kaliniwan River to the east, Lake Mainit to the north, and Butuan Bay to the

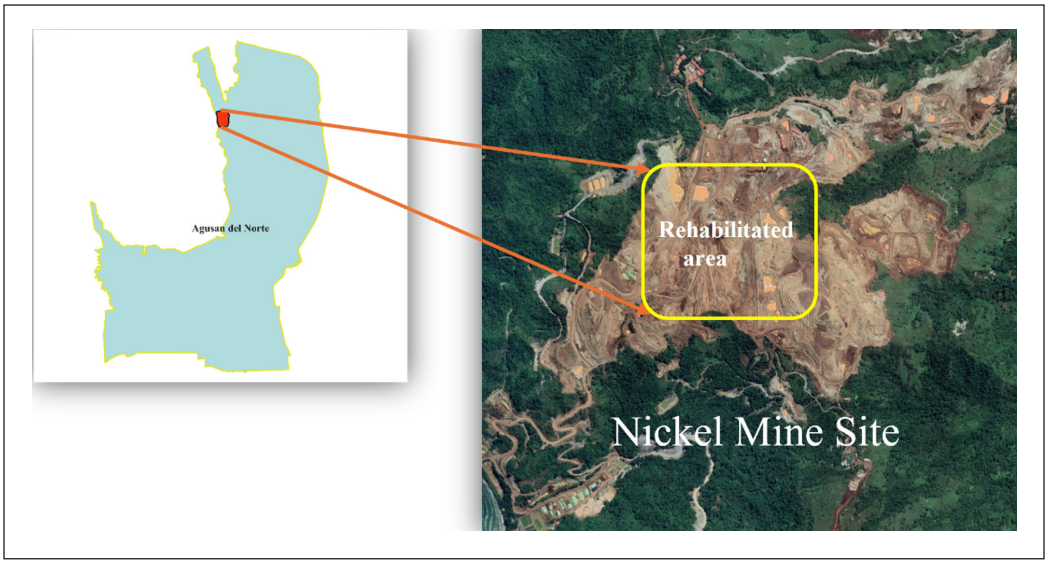

Figure 1. Study area

west. The site is characterized by a tropical climate, receiving an annual rainfall of 3,978.43 mm based on precipitation data from 2004 to 2024 (Climate Engine, 2024).

The surface mining and associated activities have caused significant land degradation at the site. As of 2021, the mine site has undergone post-mining operations, where approximately 20% of the mined-out area has been partially rehabilitated through cropping or growing agricultural plants for food consumption.

Sampling and Analysis

The nickel mine site has partially restored the excavated sections by cultivating crops intended for human consumption. Preliminary evaluation and suitability analysis, however, were not performed. This study collects plant samples at their harvesting stage at rehabilitated locations, including eggplant, lady's finger, Malabar spinach, taro, and tomato, and the edible portion of the plant (root, leaf, fruit) was saved for individual analysis. Subsequently, the samples were cleaned and rinsed with distilled water to eliminate contaminants. Plant specimens are chopped, air-dried for 16 hours, oven-dried at 80 degrees Celsius for one hour, and ground into powder. Representative samples for each crop weighing approximately 20 grams were enclosed in airtight plastic bags to avert moisture ingress and contamination prior to XRF analysis. Figure 2 shows the sample preparation and analysis.

Epson 1 EDXRF was utilized to determine chromium, copper, manganese, nickel, and zinc levels in the soil and the crop samples. Standard operating procedures and calibration protocols were meticulously followed during the laboratory XRF analysis. Approximately

0.5 g of the powdered samples (soil and crops) were placed in a 3.6 µm transparent Mylar film and inserted into a 30-mm container cup. This technique examines loose powdered substances, offering the X-ray analyzer a level surface and elevating the sample above the beam. Finely ground samples demonstrate increased homogeneity and reduced void spaces, improving analytical precision.

To determine if the levels of the heavy metals are within limits, the maximum allowable limits for Cr, Cu, Mn, Ni, and Zn in soil and vegetables are listed in Table 1 (Food and Agriculture Organization, 2004; World Health Organization, 1996).

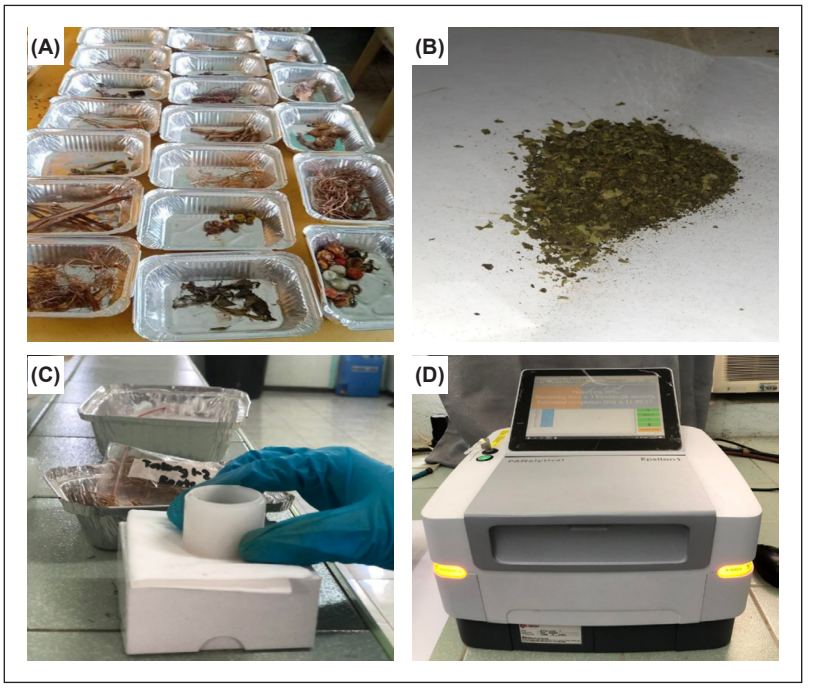

Figure 2. Sampling preparation and analysis: (A) Plant samples separated by parts while edible portions are subjected to analysis; (B) Plant samples in decreased particle size; (C) Samples placed in the 30-mm container cup for analysis; (D) Epson 1 EDXRF for X-ray Fluorescence spectroscopy analysis

Table 1
Maximum Permissible Limit (MPL) of heavy metal concentrations in soil and vegetables according to WHO/FAO

Heavy metal	Maximum permissible level in soil in mg/kg	Maximum permissible level in vegetables in mg/kg
Chromium (Cr)	110	1.3
Copper (Cu)	100	10
Manganese	2000	500
Nickel (Ni)	50	10
Zinc (Zn)	200	99.4

Statistical Analysis

The relationship between heavy metals is determined using Pearson's correlation analysis, while a simple linear regression approach assessed the relationships between heavy metals in the soil and crops.

Bioconcentration Factor (BCF)

According to Li et al. (2012), the accumulation factor predicts the possible transfer of contaminants, such as heavy metals, from the soil to the portion of crops humans consume. If the BCF is less than 1, the plant can only ingest metals and cannot accumulate them. In any other case, if BCF is less than 1, the plant will store metals in the soil (Kharazi et al., 2021; Sulaiman & Hamzah, 2018). Based on Equation 1, BCF is given by:

$$BCF = \frac{metal\ concentration\ in\ the\ edible\ part\ of\ the\ crop\ (dw)}{metal\ concentration\ in\ root - soil\ (dw)} \quad [1]$$

Health Risk Assessment

The potential health risk of heavy metals in crops was assessed using the target hazard quotient (THQ), using the estimated daily intake (EDI) and oral reference dose (RfD) (Khan et al., 2013; Kharazi et al., 2021; USEPA, 1989). The maximum tolerable daily intake is shown in Table 2. The THQ describes the non-carcinogenic health risk associated with the hazardous element. Non-carcinogenic health consequences are unlikely if THQ is <1. If the THQ is >1, health issues may occur. Non-carcinogenic health consequences are not statistically likely, with a THQ greater than 1 (Antoine et al., 2017). THQ is calculated as illustrated in the studies of (Antoine et al., 2017; Khan et al., 2013; Kharazi et al., 2021) presented in Equation 2, while EDI is calculated using Equation 3 for ingested substrate:

$$THQ = \frac{EDI}{RfD} \quad [2]$$

$$EDI = \frac{E_{FR} \times Ed \times IR \times C}{BWa \times ATn} \times 10^{-3} \quad [3]$$

Where EFR is the exposure frequency to heavy metal (350 days/year), Ed is the exposure duration (40 years for non-carcinogenic effects), IR is the crop ingestion rate (65 g/day), C is the concentration in a wet weight of the trace element in the crop, BWa as the body weight reference for an adult of 70 kg, and the exposure time considering 365 days in 40 years, for ATn (Antoine et al., 2017; Hassan et al., 2022). Ma Reference dose (RfD) values for ingested elements are listed in Table 3.

Table 2
Maximum tolerable daily intake

Heavy Metal	MTDI (mg/day)
Chromium (Cr)	0.035–0.2
Copper (Cu)	2.5–3
Manganese (Mn)	2–5
Nickel (Ni)	0.1–0.3
Zinc (Zn)	60–65

Source: Gebeyehu & Bayissa, 2020

Table 3
Reference dose (RfD) values

Heavy Metal	RfD_{ing} (mg/kg/day)
Chromium (Cr)	3.00×10^{-3}
Copper (Cu)	3.00×10^{-4}
Manganese (Mn)	$1.4.00 \times 10^{-1}$
Nickel (Ni)	2.00×10^{-2}
Zinc (Zn)	3.00×10^{-1}

Source: Zheng et al., 2015

RESULTS AND DISCUSSIONS

Heavy Metal Level in the Soil

Table 4 presents the amounts of heavy metals in the soil, as determined by X-ray fluorescence (XRF) spectroscopy, specifically for chromium, copper, manganese, nickel, and zinc. The values were contrasted with the Maximum Permissible Limit (MPL) set by the World Health Organization (WHO) and the Food and Agriculture Organization (FAO). The data reveal that all soil samples have levels exceeding the permissible limits.

WHO/FAO stipulates that the maximum allowable limit for chromium (Cr) in soil is 110 mg/kg. The data presented in Table 4 indicate that the chromium concentration in the soil significantly exceeds the threshold across all samples, varying from 4,460 mg/kg to 10,276.67 mg/kg, which is 40–93 times higher than the safe limits.

The elevated concentration of copper indicates a marginal exceedance of the permissible threshold of 100 mg/kg established by WHO/FAO for all soil samples. Copper values in the soil samples range from 111.03 to 165.73 mg/kg, 1.1 to 1.6 times above the permissible limit. Although the Cu content is slightly lower than that of other heavy metals under study, it is still a cause of concern due to the possible crop accumulation and long-term degradation. The manganese content in the soil also presents a slight exceedance of the MPL, which is 1.2 to 2.3 times greater than the WHO/FAO limit of 2,000 mg/kg. Mn in the soil ranges from 2390 mg/kg to 4516.67 mg/kg.

Table 4
Heavy metal levels in the soil in comparison to the Maximum Permissible Limit (MPL)

Soil samples	Cr	Cu	Mn	Ni	Zn
$S_{Eggplant}$	10,276.67	165.73	4,330.00	8,623.33	404.23
$S_{Lady's\ Finger}$	4,460.00	111.03	2,390.00	3,666.67	597.40
$S_{Malabar\ spinach}$	7,160.00	143.57	4,516.67	5,356.67	450.00
S_{Taro}	9,313.33	143.70	4,413.33	9,483.33	438.30
S_{Tomato}	7,110.00	159.30	3,570.00	4,943.33	337.77
MPL	110.00	100.00	2,000.00	50.00	200.00

Nickel concentrations in soil samples markedly exceed the maximum allowable limit of 50 mg/kg, categorizing it as a serious pollutant. XRF data reveal that nickel concentrations are raised by a factor of 73 to 189, ranging from 3,666.67 to 9,483.33 mg/kg. Zinc concentrations surpassed the maximum permissible limit by 1.7 to 3 times, with values between 337.77 mg/kg and 597.40 mg/kg.

Cr and Ni levels are critically high, while Cu, Mn, and Zn, although exceeding the limits, are significantly less hazardous than Cr and Ni. A strong positive correlation is observed between Cr and Ni (0.90), Cr and Mn (0.90), Cr and Cu (0.78), and Cu and Mn (0.76), as illustrated in Figure 3. Conversely, Zn exhibits negative correlations with Mn (-0.54), Cr (-0.52), and Cu (-0.49). The negative results signify that an increase in Zn concentration correlates with a drop in the levels of these metals.

The regression analysis establishes that there is a significant positive correlation between Cr and Ni ($r = .90$, $p<0.05$), Cr and Mn ($r = .90$, $p<0.05$), Cr and Cu ($r = .78$, $p<0.05$), and Cu and Mn ($r = .76$, $p<0.05$). This information suggests they share the same geochemical behavior or identical contamination sources. On the contrary, there is a weak negative correlation for Mn and Zn ($r = .54$, $p<0.05$) and Cr and Zn ($r = .52$, $p<0.05$), suggesting that higher Zn levels correspond to lower Mn and Cr levels, respectively, due to competitive interactions or distinct source of contamination. While Cu and Zn ($r = 0.49$, $p>0.05$), Ni and Zn ($r = .22$, $p<0.05$) exhibit non-significant correlations, indicating that Cu and Ni are not predictors of Zn in the soil.

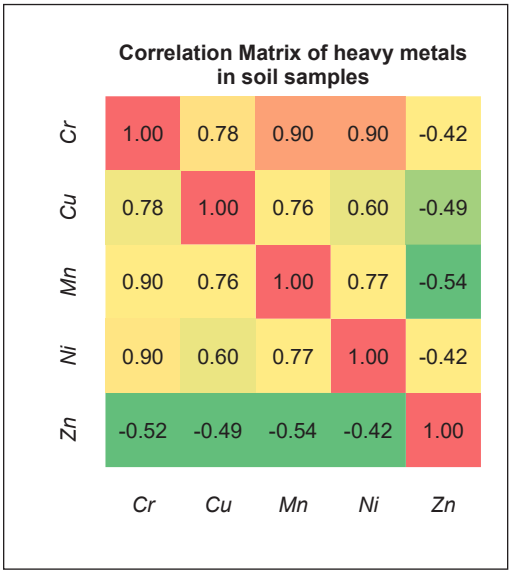

Figure 3. Correlation matrix of heavy metals in soil samples

Heavy Metal Levels in the Crops

Concentrations of heavy metals in the edible portions of selected crops, as ascertained by X-ray fluorescence (XRF) spectroscopy, such as the Cr, Cu, Mn, Ni, and Zn, are listed in Table 5. The Maximum Permissible Limit (MPL) was established by the World Health Organization (WHO), and the Food and Agriculture Organization (FAO) served as a reference point for comparison. The readings indicate that the concentration of heavy metals present in the edible portions of the crop has significantly surpassed the maximum allowed limit.

Table 5
Heavy metal levels in the crops in comparison to the Maximum Permissible Limit (MPL)

Crop Samples	Cr	Cu	Mn	Ni	Zn
Eggplant	133.67	44.73	285.27	168.67	84.97
Lady's finger	58.73	20.73	159.43	62.07	101.03
Malabar spinach	183.57	-	785.77	408.23	143.8
Taro	90.73	45.1	118.47	114.33	152.43
Tomato	90.27	45.63	161.87	86.67	108.77
MAL	**1.3**	**10**	**500**	**10**	**99.4**

Chromium (Cr) has exceeded the limit by about 45 to 141 times the MPL of 1.3 mg/kg. The Cr content in crops ranges from 58.73 to 183.57 mg/kg, where eggplant dominates the Cr accumulation in its edible portions. Chromium (VI) compounds have severe and potentially deadly effects on the respiratory, cardiovascular, gastrointestinal, hepatic, renal, and neurological systems when ingested in significant quantities for an extended period (Tchounwou et al., 2012; UK Health Security Agency, 2022). According to research by the U.S. Department of Health and Human Services (2012), individuals who unintentionally or purposefully ingested high doses of chromium (VI) compounds experienced severe effects on their respiratory systems, cardiovascular systems, gastrointestinal systems, hematological systems, hepatic systems, renal systems, and neurological systems, which either resulted in death or required medical treatment.

A slight exceedance of the permissible limit of copper is noted in the edible components of the sample crops. Approximately, Cu content is 2 to 4.5 times exceeding the threshold established by the WHO/FAO, with values ranging from 20.73 mg/kg to 45.63 mg/kg. There was no detected Cu in Malabar spinach. The consumable portion of the eggplant possesses the highest Cu content. This matches a Bangladeshi study that found no copper in Malabar spinach (Fahad et al., 2015). At higher concentrations, copper is stored in the liver, brain, and kidneys (Royer & Sharman, 2023). Copper poisoning is a leading contributor to the development of Wilson's disease. Oxidative stress, DNA damage, and reduced cell development are all caused by an excess of copper (Oe et al., 2016).

The permissible limit of manganese (Mn) in the crops by WHO/FAO indicates that the Mn level of Malabar spinach of 785.77 mg/kg is above the 500 mg/kg limit by 1.5 times. All other crops examined have exhibited reduced Mn values. Excessive manganese consumption leads to motor dysfunction and reduced neurotransmitter levels, as manganese primarily impacts the central nervous system, similar to Parkinson's disease (Flora, 2014; Keen et al., 2012).

Ni level in the edible portions for all sample crops highly exceeded the MPL by 6 to 40 times the permissible limit of 10 mg/kg. The highest Ni content is at 408.23 mg/kg for Malabar spinach. Acute exposure to nickel compounds can result in nausea, vomiting,

diarrhea, dizziness, cough, and shortness of breath, while a lethal overdose of nickel compounds can occur (Das et al., 2019; Genchi et al., 2020; Public Health England, 2009). Nickel exposure ranges from acute skin contact to occupational inhalation (Chen et al., 2017). Ni is found in both natural sources and anthropogenic activities and is present in many applications due to its unique physicochemical properties (Genchi et al., 2020).

Zinc level in crops is limited to 99.4 mg/kg by the WHO/FAO. All Zn content in the crops surpassed the limit except eggplant (84.97 mg/kg). Taro has the highest Zn content, at 152.43 mg/kg, approximately 1.5 times the MPL. Apparent signs of Zn toxicity are nausea, vomiting, epigastric discomfort, lethargy, and weariness. (Nazir et al., 2015; Sandstead, 2015; Wallig & Keenan, 2013), acute poisoning caused by zinc can cause abdominal pain, nausea, and disorientation. The zinc amount used to induce vomiting ranged from 225 to 400 mg.

Cr and Ni levels in the crops pose severe health risks, with high exceedance of the limit, while Cu and Zn exceeded the MPL moderately. Malabar spinach has the highest amounts of Cr, Mn, and Ni. This is because leafy vegetables absorb more heavy metals than roots and fruit vegetables (Mishra & Kumari, 2021; Sultana et al., 2022). This helps explain why fruit vegetables such as eggplant, lady's finger, and tomato have reduced Cr, Mn, and Ni contents. Studies suggest that root crops like taro are high in Cr and Ni (Mishra & Kumari, 2021; Sultana et al., 2022).

Figure 4 depicts the average concentration of heavy metals (Cr, Cu, Mn, Ni, and Zn) in the consumable portions of the crops and their variability in the samples. Manganese exhibits the highest concentration, accompanied by considerable diversity among crops. Furthermore, Ni has a high concentration with considerable variability, suggesting distinct accumulating patterns across all crops. Cr, Ni, and Zn values present moderate

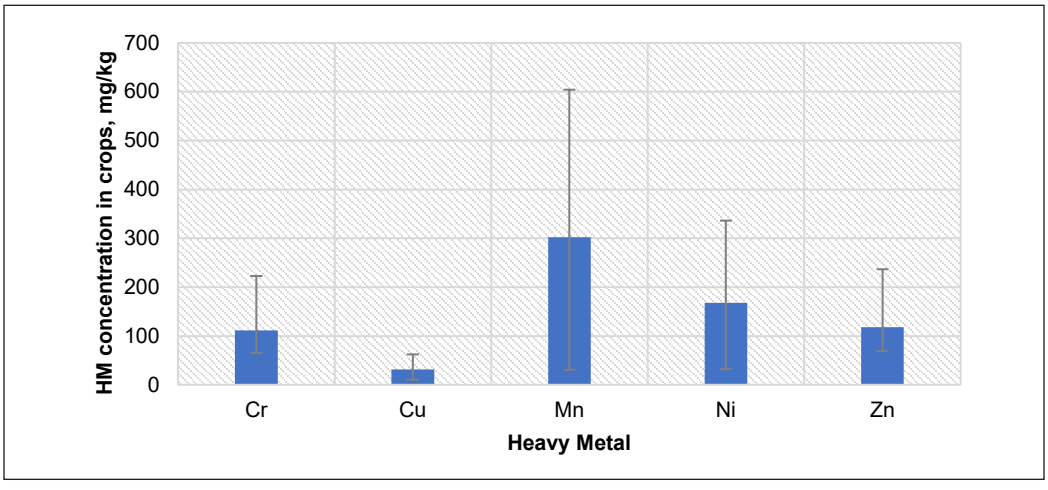

Figure 4. Heavy metal concentrations in the edible portion of the crops

concentration and variability, while Cu has the lowest concentration with noticeable variations within the crop. The heavy metal in edible portions of the crops follows the order Mn>Ni>Zn>Cr>Cu.

Bioconcentration Factor

Figure 5 shows the bioavailable metal fraction or the Bioconcentration Factor (BCF) for the edible portions under study. The BCF refers to the total quantity of metal the crop takes from the soil. It is the principal pathway for potentially hazardous metals to enter the food chain, concerning food safety (Akinyele & Shokunbi, 2015; Gebeyehu & Bayissa, 2020). Eggplants have the lowest BCF for Cu concentration at 0.004, which means less copper accumulates in their edible portion. The calculated BCF in eggplant is highest for Mn at 0.028, followed by Ni (0.016), Cr (0.013), and Zn (0.008). Mn (0.06) and Zn (0.023) BCF values of the lady's finger are relatively higher among the elements present in its edible portions, which suggests that Mn and Zn are absorbed more in the lady's finger compared to Cu (0.005), Cr (0.013), and Ni (0.014). Notably, Mn, Ni, and Cr BCF levels in Malabar spinach are highest at 0.110, 0.057, and 0.026. Zn (0.020) is also notably high in Malabar spinach. This shows that Malabar spinach absorbs more heavy metals than other assessed crops in this study. The BCF values for taro are lowest for Cu (0.005), followed by Cr (0.010), Ni (0.012), Mn (0.013), and Zn (0.016). In tomatoes, Cu also has the lowest BCF (0.006), with the highest at Ni (0.023). Calculated values for Cr, Ni, and Zn are 0.013, 0.0.12, and 0.015, respectively. For all crops, Cu BCF is the lowest.

These findings indicate that at BCF< 1, the bioavailability of the Cr, Cu, Mn, Ni, and Zn in the edible portions of the crop samples under study is minimal. Plants do not store the metals in their tissues but only absorb them.

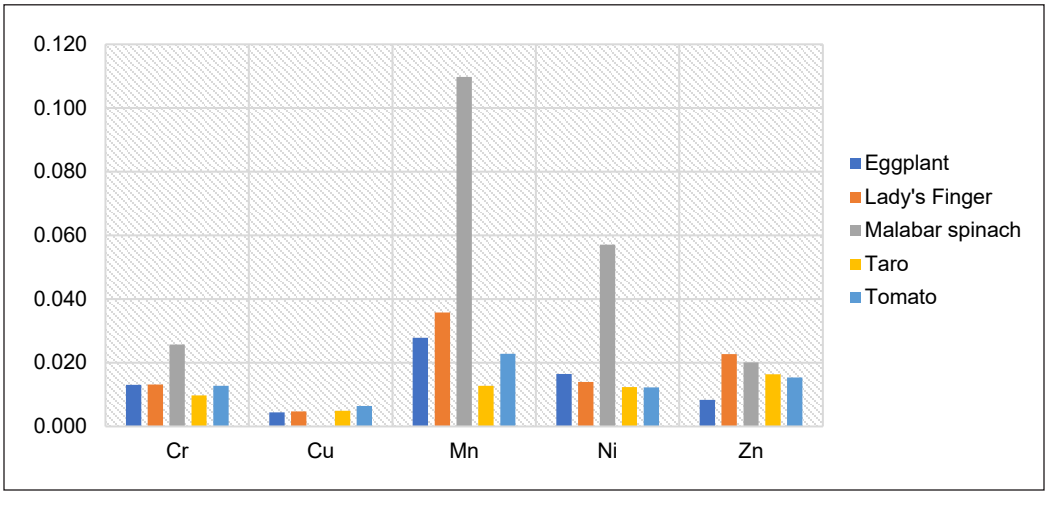

Figure 5. Bioconcentration Factor (BCF)

Health Risk Assessment

Table 6 shows the estimated daily intake (EDI) calculation, considering the adult population exposed for 40 years, assuming a daily intake of 65 g of the crops under study. Based on the result, Cr values are a little over the MTDI values, while Cu, Mn, Ni, and Zn values for all crops are below the suggested maximum tolerable intake values in the study presented by Gebeyehu and Bayissa (2020). However, when crops are consumed altogether in a day, Ni and Cr exhibit a total EDI of 0.75 mg/day and 0.5 mg/day, respectively, exceeding the MTDI for Ni and Cr. The combined EDI in the crops is still below the maximum limit for Mn, Cu, and Zn.

In Table 7, THQ calculation revealed that most crops have THQ>1, which means there is a high potential for damaging health effects if consumed over an extended period. Copper THQ values for all crops are significantly larger than the other metals under investigation and are most concerning. The highest THQ value was found for tomatoes (135.44) and taro (133.44). When consumed excessively, copper toxicity may lead to oxidative stress, DNA damage, and cell development suppression (Oe et al., 2016).

THQ values for Cr, Mn, and Ni are also significantly above 1 and are alarming due to their substantial health effects. The human respiratory, cardiovascular, gastrointestinal, hepatic, renal, and neurological systems can all be adversely affected by chromium (Cr-VI),

Table 6
Estimate Daily Intake (EDI) values in comparison to Maximum Tolerable Daily Intake (MTDI) in mg/day

Crop samples	Estimate Daily Intake (EDI) mg/day				
	Cr	**Cu**	**Mn**	**Ni**	**Zn**
Eggplant	0.12	0.04	0.25	0.15	0.08
Lady's finger	0.05	0.02	0.14	0.06	0.09
Malabar spinach	0.16	0.00	0.70	0.36	0.13
Taro	0.08	0.04	0.11	0.10	0.14
Tomato	0.08	0.04	0.14	0.08	0.10
Total EDI for all crops	*0.50*	*0.14*	*1.35*	*0.75*	*0.53*
MTDI (mg/day)	*0.035–0.2*	*2.5–3*	*2.0–5.0*	*0.1–0.3*	*60–65*

Table 7
Target Hazard Quotient (THQ) of individual metals

Crop samples	Cr	Cu	Mn	Ni	Zn
Eggplant	39.67	132.77	1.81	7.51	0.25
Lady's finger	17.43	61.54	1.01	2.76	0.30
Malabar spinach	54.48	-	5.00	18.17	0.43
Taro	26.93	133.86	0.75	5.09	0.45
Tomato	26.79	135.44	1.03	3.86	0.32

with some of these reactions having the potential to be fatal (Tchounwou et al., 2012; UK Health Security Agency, 2022) while nickel toxicity can cause nausea, vomiting, diarrhea, dizziness, cough, and shortness of breath, and may lead to death (Das et al., 2019; Genchi et al., 2020; Public Health England, 2009). Values for Zn, however, are less than 1.

A Hazard Quotient is a dimensionless figure representing the likelihood of an individual experiencing adverse health impacts. The elevated THQ values for Cu, Cr, Ni, and Mn in the crop samples indicate a possible long-term health hazard associated with their consumption. The data suggest that regular intake of these crops may pose a considerable health risk, particularly to the community and local consumers who are exposed to them.

CONCLUSION

The X-ray fluorescence (XRF) spectroscopy analysis determines heavy metals in the soil and crops. The heavy metal accumulation (Cr, Cu, Mn, Ni, Zn) in the soil is high and beyond the maximum allowable limit by the World Health Organization (WHO). These accumulations are translated to the crops, and the edible portions are analyzed to determine the levels of heavy metals. Cr, Cu, Mn, Ni, and Zn display values that exceed the maximum permissible values by the WHO. Cr and Ni levels in the crops pose severe health risks, with high exceedance of the limit, while Cu and Zn exceeded the permissible limit moderately. Manganese is most significant in the edible portions of the sample crops, following the order Mn>Ni>Zn>Cr>Cu. Malabar spinach, a leafy vegetable, has the most Cr, Mn, and Ni since leafy vegetables absorb more heavy metals than roots and fruits. The BCF for all crops is below 1, signifying that crops do not amass significant concentrations of heavy metals in their consumable parts. The Health Risk Assessment (HRA) using Target Hazard reveals elevated levels of Cu, Cr, Ni, and Mn. This suggests that consuming substantial quantities of crops daily may have long-term health risks. This study reveals that the assessed crops (eggplant, lady's finger, Malabar spinach, taro, and tomato) pose a health hazard and are unsuitable for growing in the mined-out nickel mine site. Consequently, the intentional rehabilitation of the mine for agricultural purposes may not be an optimal solution for the present condition of the mining site. Additional research may be required to advance crop production using soil enhancers that are appropriate for agricultural practices.

Despite being profitable, growing edible crops can have many adverse effects. Mining companies should have a thorough evaluation, feasibility study, and soil assessment to ensure that crops are suitable and safe for consumption. Creating a database of crops suited for rehabilitation would be beneficial, and creating maps that match those crops' suitability will provide more specific information regarding the management of mine revegetation and planning. Phytomining and renewable energy (solar and wind) sourcing will be good alternatives, as this will help minimize health risks in the food chain. However, data on this is not yet available on the site. Further studies and site validation are needed.

ACKNOWLEDGMENT

Through its Engineering Research for Development and Technology (ERDT) program, the Department of Science and Technology (DOST) provides financial assistance for this research study.

REFERENCES

Akinyele, I. O., & Shokunbi, O. S. (2015). Concentrations of Mn, Fe, Cu, Zn, Cr, Cd, Pb, Ni in selected Nigerian tubers, legumes and cereals and estimates of the adult daily intakes. *Food Chemistry*, *173*, 702–708. https://doi.org/10.1016/j.foodchem.2014.10.098

Antoine, J. M. R., Fung, L. A. H., & Grant, C. N. (2017). Assessment of the potential health risks associated with the aluminium, arsenic, cadmium and lead content in selected fruits and vegetables grown in Jamaica. *Toxicology Reports*, *4*, 181–187. https://doi.org/10.1016/j.toxrep.2017.03.006

Apodaca, D. C., Domingo, J. P. T., David, C. P. C., & David, S. D. (2018). Siltation load contribution of nickel laterite mining on the coastal water quality of Hinadkaban Bay, Surigao Provinces, Philippines. *IOP Conference Series: Earth and Environmental Science*, *191*(1), Article 012048. https://doi.org/10.1088/1755-1315/191/1/012048

Chen, Q. Y., Brocato, J., Laulicht, F., & Costa, M. (2017). Mechanisms of nickel carcinogenesis. In A. Mudipalli & J. T. Zelifoff (Eds.) *Essential and non-essential metal* (pp. 181–197). Humana Press. https://doi.org/10.1007/978-3-319-55448-8_8

Climate Engine. (2024). *Desert research institute and University of California, merced*. Climateengine. https://app.climateengine.org/climateEngine

Das, K. K., Reddy, R. C., Bagoji, I. B., Das, S., Bagali, S., Mullur, L., Khodnapur, J. P., & Biradar, M. S. (2019). Primary concept of nickel toxicity - An overview. *Journal of Basic and Clinical Physiology and Pharmacology*, *30*(2), 141–152. https://doi.org/10.1515/jbcpp-2017-0171

Fahad, S. M., Islam, A. F. M. M., Ahmed, M., Uddin, N., Alam, M. R., Alam, M. F., Khalik, M. F., Hossain, M. S., Hossain, M. L., & Abedin, M. J. (2015). Determination of elemental composition of Malabar spinach, lettuce, spinach, hyacinth bean, and cauliflower vegetables using proton induced X-Ray emission technique at Savar subdistrict in Bangladesh. *BioMed Research International, 2015*(1), Article 128256. https://doi.org/10.1155/2015/128256

Flora, S. J. S. (2014). Metals. In R. C. Gupta (Ed.) *Biomarkers in toxicology* (pp. 485-519). Academic Press. https://doi.org/10.1016/B978-0-12-404630-6.00029-4

Fodoué, Y., Ismaila, A., Yannah, M., Wirmvem, M. J., & Mana, C. B. (2022). Heavy metal contamination and ecological risk assessment in soils of the pawara gold mining area, Eastern Cameroon. *Earth*, *3*(3), 907–924. https://doi.org/10.3390/earth3030053

Food and Agriculture Organization. (2004). *Maximum limits for dangerous substances in soil and groundwater* (No. 12). Food and Agriculture Organization

Gavhane, S. K., Sapkale, J. B., Susware, N. K., & Sapkale, S. J. (2021). Impact of heavy metals in riverine and estuarine environment: A review. *Research Journal of Chemistry and Environment*, *25*(5), 226–233.

Gebeyehu, H. R., & Bayissa, L. D. (2020). Levels of heavy metals in soil and vegetables and associated health risks in mojo area, Ethiopia. *PLoS ONE*, *15*(1), Article 0227883. https://doi.org/10.1371/journal.pone.0227883

Genchi, G., Carocci, A., Lauria, G., & Sinicropi, M. S. (2020). Nickel: Human health and environmental toxicology. *International Journal of Environmental Research and Public Health*, *17*(3), 679–700.

Ghaneei-Bafghi, M. J., Feiznia, S., Mokhtari, A. R., Jaafari, M., Tavili, A., & Khodaeian, Z. (2024). Agricultural soil contamination and degradation near a mining area in an arid region. *Journal of Geochemical Exploration*, *256*, Article 107349. https://doi.org/https://doi.org/10.1016/j.gexplo.2023.107349

GlobalData. (2022). *Nickel mining market analysis including reserves, production, operating, developing and exploration assets, demand drivers, key players and forecasts, 2021-2026*. GlobalData. https://www.globaldata.com/store/report/nickel-mining-market-analysis

Gupta, N., Yadav, K. K., Kumar, V., Prasad, S., Cabral-Pinto, M. M. S., Jeon, B. H., Kumar, S., Abdellattif, M. H., & Alsukaibia, A. K. D. (2022). Investigation of heavy metal accumulation in vegetables and health risk to humans from their consumption. *Frontiers in Environmental Science*, *10*, Article 791052. https://doi.org/10.3389/fenvs.2022.791052

Haghighizadeh, A., Rajabi, O., Nezarat, A., Hajyani, Z., Haghmohammadi, M., Hedayatikhah, S., Asl, S. D., & Beni, A. A. (2024). Comprehensive analysis of heavy metal soil contamination in mining environments: Impacts, monitoring techniques, and remediation strategies. *Arabian Journal of Chemistry*, *17*(6), Article 105777. https://doi.org/10.1016/j.arabjc.2024.105777

Hassan, W., Rahman, S., Ara, A., Saadi, S., & Afridi, H. K. (2022). Evaluation and health risk assessment of five toxic metals concentration in soil, water and seasonal vegetables and fruits from Pakistan-Afghanistan border, Torkham. *Letters in Applied NanoBioScience*, *11*(4), 4089–4104. https://doi.org/10.33263/LIANBS114.40894104

Hu, Y., Wang, J., Yang, Y., Li, S., Wu, Q., Nepovimova, E., Zhang, X., & Kuca, K. (2024). Revolutionizing soil heavy metal remediation: Cutting-edge innovations in plant disposal technology. *Science of The Total Environment*, *918*, Article 170577. https://doi.org/https://doi.org/10.1016/j.scitotenv.2024.170577

Keen, C. L., Ensunsa, J. L., Lönnerdal, B., & Zidenberg-Cherr, S. (2012). Manganese. *Encyclopedia of Human Nutrition*, *3–4*, 148–154. https://doi.org/10.1016/B978-0-12-375083-9.00182-3

Khan, K., Lu, Y., Khan, H., Ishtiaq, M., Khan, S., Waqas, M., Wei, L., & Wang, T. (2013). Heavy metals in agricultural soils and crops and their health risks in swat district, Northern Pakistan. *Food and Chemical Toxicology*, *58*, 449–458. https://doi.org/10.1016/j.fct.2013.05.014

Kharazi, A., Leili, M., Khazaei, M., Alikhani, M. Y., & Shokoohi, R. (2021). Human health risk assessment of heavy metals in agricultural soil and food crops in Hamadan, Iran. *Journal of Food Composition and Analysis*, *100*, Article 103890. https://doi.org/10.1016/j.jfca.2021.103890

Kim, Y., Rudasingwa, G., Cho, S. H., McWilliams, A., Kang, C. M., Kim, S., & Kim, S. (2022). Comparison of the concentrations of heavy metals in PM2.5 analyzed in three different global research institutions using x-ray fluorescence. *Applied Sciences*, *12*(9), Article 4572. https://doi.org/10.3390/app12094572

Li, Q. S., Chen, Y., Fu, H. B., Cui, Z. H., Shi, L., Wang, L. L., & Liu, Z. F. (2012). Health risk of heavy metals in food crops grown on reclaimed tidal flat soil in the Pearl River Estuary, China. *Journal of Hazardous Materials*, *227–228*, 148–154. https://doi.org/10.1016/j.jhazmat.2012.05.023

Li, X., Li, Z., Lin, C. J., Bi, X., Liu, J., Feng, X., Zhang, H., Chen, J., & Wu, T. (2018). Health risks of heavy metal exposure through vegetable consumption near a large-scale Pb/Zn smelter in central China. *Ecotoxicology and Environmental Safety*, *161*, 99–110. https://doi.org/10.1016/j.ecoenv.2018.05.080

McComb, J. Q., Rogers, C., Han, F. X., & Tchounwou, P. B. (2014). Rapid screening of heavy metals and trace elements in environmental samples using portable X-ray fluorescence spectrometer, A comparative study. *Water Air Soil Pollution*, *176*(3), 139–148. https://doi.org/10.1007/s11270-014-2169-5

Mines and Geosciences Bureau. (2024). *59 operating metallic mines in the Philippines* (Issue June). Mines and Geosciences Bureau https://mgb.gov.ph/images/Mineral_Statistics/mining_facts_and_figures_updated_22_June_2020_final.pdf

Mishra, A., & Kumari, S. (2021). Heavy metal contamination. In M. L. Larramendy & S. Soloneski (Eds.) *Soil contamination - Threats and sustainable solutions* (Chaper 1). IntechOpen. https://doi.org/10.5772/intechopen.93412

Moon, J. W. (2024). *Area reports—International—Asia and the Pacific: Minerals yearbook 2022.* U.S. Geological Survey. https://doi.org/10.3133/70178411

Muñoz-Olivas, R., & Cámara, C. (2007). Speciation related to human health. In L. Ebdon, L. Pitts, R. Cornelis, H. Crews, O. F. X. Donard & P. Quevauviller (Eds.) *Trace element speciation for environment, food and health* (pp. 331–353). Royal Society of Chemistry. https://doi.org/10.1039/9781847552204-00331

Nazir, R., Khan, M., Masab, M., Rehman, H. U., Rauf, N. U., Shahab, S., Ameer, N., Sajed, M., Ullah, M., Rafeeq, M., & Shaheen, Z. (2015). Accumulation of heavy metals (Ni, Cu, Cd, Cr, Pb, Zn, Fe) in the soil, water and plants and analysis of physico-chemical parameters of soil and water collected from Tanda Dam Kohat. *Journal of Pharmaceutical Sciences and Research*, *7*(3), 89–97.

Oe, S., Miyagawa, K., Honma, Y., & Harada, M. (2016). Copper induces hepatocyte injury due to the endoplasmic reticulum stress in cultured cells and patients with Wilson disease. *Experimental Cell Research*, *347*(1), 192–200. https://doi.org/10.1016/j.yexcr.2016.08.003

Peralta, E., Pérez, G., Ojeda, G., Alcañiz, J. M., Valiente, M., López-Mesas, M., & Sánchez-Martín, M. J. (2020). Heavy metal availability assessment using portable X-ray fluorescence and single extraction procedures on former vineyard polluted soils. *Science of the Total Environment*, *726*, Article 138670. https://doi.org/10.1016/J.SCITOTENV.2020.138670

Philippine Statistics Authority. (2024). *Technical notes on the 2022 annual survey of Philippine business and industry (ASPBI) - Agriculture, forestry, and fishing section: Preliminary results*. Philippine Statistics Authority. https://psa.gov.ph/statistics/agriculture/aspbi

Public Health England. (2009). *Nickel: Toxicological overview*. Public Health England

Royer, A., & Sharman, T. (2023). *Copper toxicity*. Stat Pearls Publication.

Sadak, O. (2023). Chemical sensing of heavy metals in water. In A. Barhoum & Z. Altintas (Eds.) *Advanced sensor technology* (pp. 565–591). Elsevier. https://doi.org/10.1016/B978-0-323-90222-9.00010-8

Sandstead, H. H. (2015). Zinc. In G. F. Nordberg, B. A. Fowler & M. Nordberg (Eds.) *Handbook on the toxicology of metals* (4th ed., pp. 1369–1385). Academic Press. https://doi.org/10.1016/B978-0-444-59453-2.00061-5

Setia, R., Dhaliwal, S. S., Singh, R., Singh, B., Kukal, S. S., & Pateriya, B. (2023). Ecological and human health risk assessment of metals in soils and wheat along Sutlej river (India). *Chemosphere*, *312*, Article 137331. https://doi.org/10.1016/j.chemosphere.2022.137331

Sulaiman, F. R., & Hamzah, H. A. (2018). Heavy metals accumulation in suburban roadside plants of a tropical area (Jengka, Malaysia). *Ecological Processes*, *7*(1), Article 28. https://doi.org/10.1186/s13717-018-0139-3

Sultana, R., Tanvir, R. U., Hussain, K. A., Chamon, A. S., & Mondol, M. N. (2022). Heavy metals in commonly consumed root and leafy vegetables in Dhaka City, Bangladesh, and assessment of associated public health risks. *Environmental Systems Research*, *11*(1), Aticle 15. https://doi.org/10.1186/s40068-022-00261-9

Tchounwou, P. B., Yedjou, C. G., Patlolla, A. K., & Sutton, D. J. (2012). Heavy metals toxicity and the environment. *Molecular, Clinical and Environmental Toxicology*, *101*, 133–164. https://doi.org/10.1007/978-3-7643-8340-4

U.S. Department of Health and Human Services. (2012). *Toxicological profile for chromium.* U.S. Department of Health and Human Services.

UK Health Security Agency. (2022). *Chromium: Toxicological overview*. UK Health Security Agency.

USEPA. (1989). *Risk assessment guidance for superfund volume I human health evaluation manual* (Part A). United States Environmental Protection Agency.

Wallig, M. A., & Keenan, K. P. (2013). Nutritional toxicologic pathology. In W. M. Haschek, C. G. Rousseaux, M. A. Wallig & B. Balon (Eds.) *Haschek and rousseaux's handbook of toxicologic pathology* (pp. 105-180). Academic Press. https://doi.org/10.1016/B978-0-12-415759-0.00036-4

World Health Organization. (1996). *Permissible limits of heavy metals in soil and plants*. World Health Organization.

Wuana, R. A., & Okieimen, F. E. (2011). Heavy metals in contaminated soils: A review of sources, chemistry, risks and best available strategies for remediation. *International Scholarly Research Notices, 2011*(1), Article 402647. https://doi.org/10.5402/2011/402647

Zheng, X., Zhao, W., Yan, X., Shu, T., Xiong, Q., & Chen, F. (2015). Pollution characteristics and health risk assessment of airborne heavy metals collected from Beijing bus stations. *International Journal of Environmental Research and Public Health*, *12*(8), 9658–9671. https://doi.org/10.3390/ijerph120809658

Pertanika J. Sci. & Technol. 33 (S5): 19 - 42 (2025)

PERTANIKA JOURNALS

SCIENCE & TECHNOLOGY

Journal homepage: http://www.pertanika.upm.edu.my/

Effect of Different Pre-treatments on Vacuum Oven Drying of Pegaga (*Centella Asiatica* L.) Leaves: Drying Kinetics, Nutritional Qualities, and Antioxidant Capacity

Nazurah Mohd Yunos[1], Siti Hajar Ariffin[1,2]*, Yus Aniza Yusof[1,2], Faiqa Shazeaa Mohd Salleh[1] and Rabitah Zakaria[1]

[1]Department of Process and Food Engineering, Faculty of Engineering, Universiti Putra Malaysia, 43400 Serdang, Selangor, Malaysia
[2]Laboratory of Halal Services, Halal Products Research Institute, Universiti Putra Malaysia, 43400 Serdang, Selangor, Malaysia

ABSTRACT

Recent reports have indicated that a broad variety of phytochemicals, particularly those with antioxidant activity, can be found in fruits and vegetables, which has drawn considerable interest. However, due to its delicate texture and high water content, it is prone to damage and has a short shelf life. Drying is the most frequent practice for minimizing moisture content and, consequently, water activity to a safe level that extends longevity. The current commercial potential of pegaga, particularly in dried form, has not been adequately investigated. The effect of various pre-treatments (water blanching, steam blanching, vacuum blanching, and microwave blanching) on the vacuum oven drying of pegaga leaves was examined in this study. These pre-treatments were selected because they offer distinct advantages that can enhance the drying process and preserve the nutritional quality of the leaves. Pegaga leaves were vacuum oven-dried for 90 minutes at 60 °C at 0.01 MPa. The total phenolic content (TPC), total flavonoid content (TFC), and antioxidant activity of pegaga leaves were determined before pre-treatment, after pre-treatment, or before drying and after the drying process. Using the 2,2-diphenyl-1-picrylhydrazyl (DPPH) test, the antioxidant activities of the methanolic extract solution were assessed. The Midilli Kucuk model was selected and fitted with the drying data to understand the drying kinetics of pegaga leaves. The results showed that vacuum blanching increased the TPC and TFC of pegaga leaves. The highest DPPH inhibition value was observed in control pegaga leaves after vacuum oven drying. Therefore, the combination of pre-treatments and

ARTICLE INFO

Article history:
Received: 13 February 2025
Accepted: 28 May 2025
Published: 10 July 2025

DOI: https://doi.org/10.47836/pjst.33.S5.02

E-mail addresses:
nazurahyunos@gmail.com (Nazurah Mohd Yunos)
hajarariffin@upm.edu.my (Siti Hajar Ariffin)
yus.aniza@upm.edu.my (Yus Aniza Yusof)
faiqazea@upm.edu.my (Faiqa Shazeaa Mohd Salleh)
rabitah@upm.edu.my (Rabitah Zakaria)
* Corresponding author

e-ISSN: 2231-8526

vacuum oven-dried pegaga leaves may retain their antioxidant and phenolic component content, which would be beneficial to local farmers and fresh produce industries by helping to minimize the loss of quality in dried pegaga leaf manufacturing.

Keywords: Antioxidant capacity, blanching pre-treatment, drying kinetics, nutritional properties, pegaga leaves, vacuum oven drying

INTRODUCTION

Pegaga (*Centella Asiatica* L.) leaves are a perennial herb belonging to the Apiaceae family (Idris et al., 2020). The plant has been widely recognized for its medicinal properties and is traditionally used in various culinary and therapeutic applications due to its antioxidant and pharmacological properties (Fadzil et al., 2020). Among its parts, the leaves of pegaga are particularly valued for their potential nutritional benefits (Rahim et al., 2021). They are high in bioactive substances, such as phenolic compounds and flavonoids, which contribute to their antioxidant behavior (Idris & Nadzir, 2021). However, keeping the nutritional value and antioxidant capacity of pegaga leaves throughout processing is quite difficult, especially during the drying phase, which is essential for increasing shelf life and retaining the medicinal properties of pegaga leaves.

In recent years, several pre-treatments have been explored to optimize the retention of bioactive compounds in various plant materials. Blanching is a common pre-treatment procedure that includes providing plant material with a short heat treatment to destroy the presence of enzymes, decrease the microbial load, and improve product stability (Tomar & Gururani, 2019). Pre-treatments, including steam, water, vacuum, and microwave blanching, are frequently used before drying to get around these restrictions. By lowering the starting moisture content and altering the tissue structure, these pre-treatments can improve drying efficiency and result in more consistent moisture removal. Additionally, they are essential for maintaining the physicochemical characteristics of dried products, such as their color, texture, and nutritional value (Deng et al., 2019). In contrast, microwave blanching can speed up the drying process by preheating the leaves, enhancing the overall quality of the dried product (Babu et al., 2018). For example, it has been discovered that steam blanching inactivates the enzymes that lead to browning (Xiao et al., 2017). The combination of these pre-treatments and vacuum oven drying can, therefore, greatly improve the efficacy and efficiency of the drying process while guaranteeing that the dried leaves maintain the appropriate quality characteristics.

Drying pegaga leaves is a widespread technique in certain cultures for traditional medicinal and culinary purposes. The benefit of drying pegaga leaves is that they preserve their beneficial characteristics for subsequent use. Drying pegaga leaves reduces the amount of moisture, which helps prevent microbial growth, mold, and other microorganisms that can cause deterioration. Because of the prolonged shelf life, the leaves may be preserved and

utilized for a longer period (Rahim et al., 2021). Pegaga leaves have a high concentration of active substances such as triterpenoids, flavonoids, and other phytochemicals (Zainol et al., 2009). The chemicals are concentrated when the leaves are dried, making them more effective. This is significant for their traditional medical use since the concentrated chemicals are thought to provide a variety of health advantages. While drying pegaga leaves can provide these benefits, the exact techniques and conditions of drying may influence the quality of the end products. To ensure that the leaves maintain as much of their color, taste, fragrance, and beneficial ingredients as possible, proper drying processes should be used (Babu et al., 2018). The preservation of these valuable compounds during pre-treatment and drying methods is crucial to retain the nutritional quality of pegaga leaves (Mohapatra et al., 2022).

The choice of drying method is equally important, as it directly influences the preservation of bioactive compounds in pegaga leaves (Márquez-Cardozo et al., 2021). Some researchers have performed drying of pegaga leaves using a tray and heat pump-assisted dehumidified drying (Trirattanapikul & Phoungchandang, 2014), hot air drying (Hiranvarachat et al., 2015; Zainol et al., 2009; Ng et al., 2020), freeze-drying (Rahim et al., 2021; Zainol et al., 2009), oven drying (Rahim et al., 2021; Zainol et al., 2009), dehydration drying (Rahim et al., 2021), vacuum oven (Tripathy & Srivastav, 2023) and microwave drying (Ng et al., 2020). However, there is limited research on the drying of pegaga leaves using a vacuum oven in terms of their nutritional content.

Vacuum oven drying, a low-temperature drying technique, has gained popularity due to its ability to maintain the nutritional content of heat-sensitive compounds compared to conventional drying methods (Hasan et al., 2019). Some types of green leaves have been dried in a vacuum oven. Dried products include collard leaves (Alibas, 2009), stevia leaves (Lemus-Mondaca et al., 2018), olive leaves (Şahin et al., 2018), lemon myrtle dried leaves (Saifullah et al., 2019), basil leaves (Telfser & Galindo, 2019), and Amaranthus leaves (Nighitha & Mathew, 2019). Vacuum oven drying has benefits, but it also has limitations. These include the need for longer drying periods and the possibility of uneven drying since moisture is removed more slowly at lower temperatures. This may lead to a final product that is not as good as it could be, especially in terms of color, texture, and ability to rehydrate (Zielinska et al., 2020).

Mathematical modeling is a useful technique for drying process simulation and gives optimal operating conditions for the equipment design of drying goods with higher rehydration qualities (Bishnoi et al., 2020). These fundamental models, also known as thin-layer models, are used to explore drying kinetics and predict mass transfer during drying (Lemus-Mondaca et al., 2021). Thus, the purpose of this study was to investigate the effect of vacuum oven drying pegaga leaves by modeling drying kinetics and assessing the effect of each pre-treatment.

The selection of a pre-treatment before drying can have a substantial impact on the drying kinetics as well as the antioxidant and nutritional content preservation. While a variety of drying techniques have been investigated, limited studies have been conducted on how diverse pre-treatments, such as microwave, steam, vacuum, and water blanching, combine with vacuum oven drying. Although the comparative effects of these pre-treatments are still unknown, they may change the microstructure of the leaves, improve drying efficiency, and retain nutritional characteristics.

This work aims to examine the effects of several pre-treatments on the vacuum oven drying process of pegaga leaves, emphasizing the drying kinetics, nutritional value, and antioxidant capacity. This study compares the water blanching, steam blanching, vacuum blanching, and microwave blanching methods systematically to determine which pre-treatment technique maximally preserves bioactive compounds during the drying process. Comprehending these impacts will yield significant knowledge for refining food and pharmaceutical industry processing methods, increasing the use of pegaga leaves as a functional component in a range of applications. Using common assays, the antioxidant activity in this study, as well as the drying behavior of pegaga leaves after each pre-treatment, and the retention of important nutritional elements, will be examined. As well as adding to our understanding of pegaga leaves, the results of this study will provide useful advice for producing high-quality dried goods that retain their beneficial qualities.

MATERIALS AND METHODS

Plant Material and Preparation

Fresh pegaga leaves were obtained from Laman Sayur, Malaysia Agro Exposition Park Serdang (MAEPS), Selangor, Malaysia. The leaves were carefully selected, free from any visual defects or damage. They were then washed thoroughly with tap water to remove any dirt or impurities. The leaves were air-dried after rinsing to eliminate extra moisture. Figure 1 shows the flow chart of drying pegaga leaves with different pre-treatments.

Pre-treatments

The pre-treatments applied to the pegaga leaves included water blanching, steam blanching, vacuum blanching, and microwave blanching. The blanching parameters were fixed for all blanching techniques with minor modifications, as it obtained a green chlorophyll color and minimized the loss of soluble components (Minh, 2014). The following pre-treatments, which were altered from earlier research, were used to blanch around 10 g of pegaga leaves. The blanching process is conducted in a closed system. The following procedures were followed for each pre-treatment:

(i) Control leaves (CL): Leaves were washed and drained.

(ii) Water-blanched leaves (WB): Pegaga leaves were immersed in a 1 L beaker at

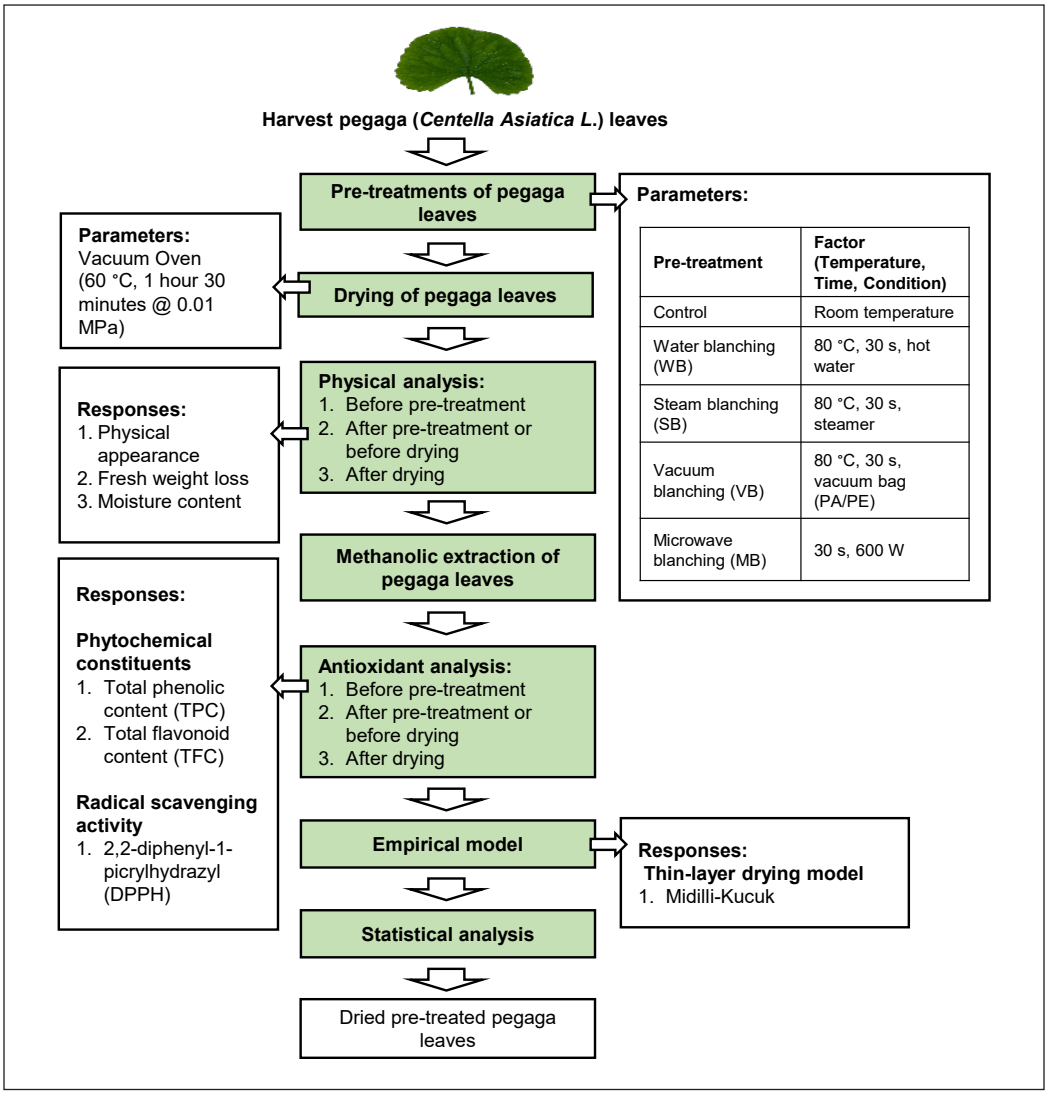

Figure 1. Flow chart of drying pegaga leaves with different pre-treatment

80 °C for 30 seconds on a hot plate. The blanched leaves were then drained and air-dried.

(iii) Steam-blanched leaves (SB): Pegaga leaves were placed in the steamer and steamed at 80 °C for 30 seconds by spreading a single layer of leaves in a steamer. The blanched leaves were then drained and air-dried.

(iv) Vacuum-blanched leaves (VB): Pegaga leaves were placed in a vacuum bag (polyamide/polyethylene). The bag was sealed, and vacuum pressure was applied. The bag with the leaves was then immersed at 80 °C for 30 seconds. The blanched leaves were removed from the bag, drained, and air-dried.

(v) Microwave-blanched leaves (MB): Pegaga leaves were microwaved at 600 W for 30 seconds. The microwaved leaves were drained and air-dried.

Drying Method

Vacuum oven drying (OV-12, Medline Scientific™ Jeio Tech, Malaysia) was employed to dry the pre-treated pegaga leaves. The pre-treated leaves were evenly spread on trays suitable for vacuum oven drying. The trays were then placed in a vacuum oven. The drying process was conducted at a temperature of 60 °C for 1 hour and 30 minutes under a vacuum pressure of 0.01 MPa. The drying parameters were used according to the method described by Şahin et al. (2018), Saifullah et al. (2019), and Nighitha and Mathew (2019) with slight modifications as it gives better preservation, reduced drying time at high temperature, retained higher phytochemical levels and antioxidant properties including ideal moisture content. The dried leaves were taken out of the oven and set aside to cool down at ambient temperature. The dried leaves were stored in airtight containers until further analysis.

Image Acquisition

An image of the samples was taken inside a black box (Figure 2). An LED ring light was placed on top of the box with the following settings: light, power 7-14W, and white color. Images were taken by using a digital camera with a fixed setting (Table 1). The images were taken before pre-treatment, after pre-treatment or before drying and after drying of Pegaga leaves. The physical appearance of the samples was observed.

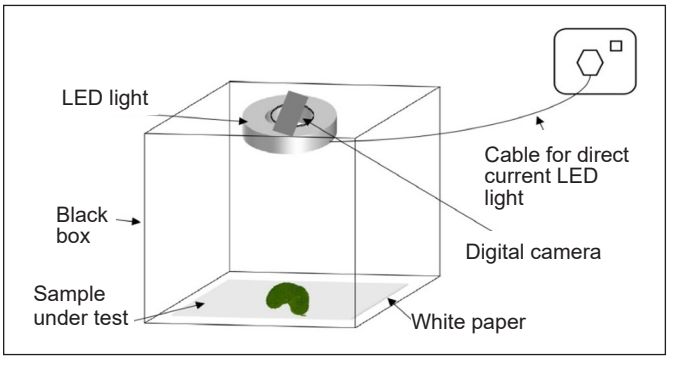

Figure 2. Conceptual design of the black box

Table 1
Digital camera setting for a physical image of pegaga leaves

Options	Settings
Megapixels	12 MP
Aperture size	F2.2
Focal length	29 m
Shutter speed	½ s
Flash	Off
Focus pixel	Autofocus

Moisture Content

The moisture content of pegaga leaves before pre-treatment, after pre-treatment or before drying and after vacuum oven drying was measured using a moisture analyzer (105 °C) (MX-50, AnD, Malaysia). The samples were placed on a small aluminum tray for testing. The time required for each sample to dry completely ranged from 4 to 20 minutes.

Fresh Weight Loss

After vacuum oven drying, pegaga leaves were weighed using an electronic weighing scale (SB12001, Mettler Toledo, Malaysia). Seven replications for each pegaga leaf used in this study were prepared. The percentage of fresh weight loss was calculated based on the initial weight of the pegaga leaves before drying and after pre-treatment (g) and the weight of the pegaga leaves after drying (g), as shown in Equation 1.

$$W_{loss} = \frac{W_{initial} - W_{final}}{W_{initial}} \times 100 \quad [1]$$

Moisture Ratio

The moisture ratio is calculated based on the moisture content at any random time, the equilibrium moisture content, and the initial moisture content, as shown in Equation 2.

$$MR = \frac{M_t - M_e}{M_0 - M_e} \quad [2]$$

Drying Kinetics and Modelling

The weight loss of the sample was recorded for seven intervals. The experiments were stopped when no weight loss was observed after three consecutive weighing. All the experiments were conducted in triplicate. The drying curves were fitted using a thin-layer model. The model is commonly used in most kinds of food and biological components (Zambra et al., 2021), specifically the Midilli Kucuk model. The drying kinetics of pegaga leaves were predicted using this model (Equation 3). The Midilli Kucuk model has been developed to accurately clarify the dehydration characteristics of several crops (Zambra et al., 2021). This model requires the calculation of the dimensionless moisture ratio from Equation 2.

$$Moisture\ Ratio\ (MR) = a\ exp(-kt)^n + bt \quad [3]$$

Where k is the kinetic parameter (min^{-1}); n, a, and b are empirical constants of the mathematical models.

SOLVER was used to do regression studies (MS Excel 2021, MS Office, USA). For the Midilli Kucuk model, the reduced chi-squared (χ^2) (Equation 4), the root mean square error (RMSE) (Equation 5) and the determination coefficient (R^2) were defined. Where N is the number of observations, z is the number of constants for each model, and $MR_{exp,i}$ and $MR_{pre,i}$ are the experimental data. The greatest R^2, lowest chi-square, and lowest RMSE values served as the selection criteria for the best-fit model (Hii & Ogugo, 2014). To obtain precise findings, the experiment was conducted three times.

$$\chi^2 = \left(\frac{\sum_{i=1}^{N} \left(MR_{pre,i} - MR_{exp,i} \right)^2}{N - z} \right) \quad [4]$$

$$RMSE = \sqrt{\frac{\sum_{i=1}^{N} \left(MR_{exp,i} - MR_{pre,i} \right)^2}{N}} \quad [5]$$

Nutritional and Antioxidant Properties

The dried leaves were ground separately into fine powder using a dry grinder. 10 g powder, dry pegaga leaves were immersed in 160 mL of 80% methanol and agitated for 2 hours at 50 °C in a water bath solution (Almey et al., 2010). Whatman No. 1 filter paper was used to filter the extract. The extracts were filled in the bottles and stored at 4 °C until further use.

Total Phenolic Content (TPC)

The TPC was measured using the Folin-Ciocalteu method with minor modifications (Bakar et al., 2022). 3.16 mL distilled water and 0.2 mL Folin-Ciocalteau reagent were dissolved together. Then, 0.6 mL of 20% sodium carbonate (Na_2CO_3) was mixed with 40 µl of pegaga extract. The tubes were incubated at room temperature for 2 hours. Absorbance was measured using a UV-Vis spectrophotometer (GENESYS™ 180 UV-Vis Spectrophotometer, Malaysia) at 765 nm using a mixture of distilled water, Folin-Ciocalteau reagent and sodium carbonate as the blank. The standard curve was constructed using gallic acid as the standard and represented as milligram gallic acid equivalent per gram of extract sample (mg GAE/g extract). All samples and readings have been obtained and evaluated in triplicate. The calibration curve equation was calculated based on the absorbance of light and the concentration of the compound, shown in Equation 6. The determination coefficient was $R^2 = 0.999$. Where Y was the absorbance of light, and X was the concentration of the compound.

$$Y = 0.004X + 0.021 \quad [6]$$

Total Flavonoid Content (TPC)

The TFC of pegaga extract was determined using a previously published technique with slight modifications (Mahirah et al., 2018). 1 mL of pegaga extract was mixed with 4 mL of distilled water. At zero time, 0.3 mL of 5% sodium nitrate ($NaNO_3$) was introduced to the test tubes, followed by 0.3 mL of 10% aluminum chloride ($AlCl_3$) after 5 minutes. After 1 minute, 2 mL of 1M sodium hydroxide (NaOH) was added, followed by 10 mL of distilled water. Absorbance was measured at 510 nm using a UV-Vis spectrophotometer

(GENESYS™ 180 UV-Vis Spectrophotometer, Malaysia). All samples and readings have been obtained and evaluated in triplicate. The standard curve was established using quercetin, and the results were represented as milligrams of quercetin equivalents per gram of extract sample (mg QUE/g extract). The calibration curve equation was calculated based on the absorbance of light and the concentration of the compound, as shown in Equation 7. The determination coefficient was $R^2 = 0.994$. Where Y was the absorbance of light, and X was the concentration of the compound.

$$Y = 0.001X + 0.013 \quad [7]$$

2, 2-diphenyl-1-picrylhydrazyl (DPPH) Assay

Pegaga extract was evaluated using the 2, 2-Diphenyl-1-picrylhydrazyl (DPPH) assay technique with minimal modifications (Almey et al., 2010). 250 µL of pegaga extract was combined with 5 mL of 0.1 mM DPPH solution and incubated in the dark for 30 minutes. The percentage inhibition of DPPH by extracts was calculated by UV-Vis spectrophotometer (GENESYS™ 180 UV-Vis Spectrophotometer, Malaysia), and its absorbance was recorded at 517 nm. All samples and readings have been obtained and evaluated in triplicate to ensure precise, reliable and consistent results. It offers a more comprehensive dataset for evaluating the antioxidant activity of pegaga leaves, which is essential for evaluating their possible uses and health advantages.

Statistical Analysis

Experiment data were analyzed using Microsoft Excel (MS Excel 2021, MS Office, USA) and Minitab version 21 software. Significant differences between samples for moisture content were analyzed using analysis of variance (ANOVA) and Tukey's multiple-range test ($P<0.05$). Data obtained were reported as mean ± standard deviation.

RESULTS AND DISCUSSION

Physical Image

Physical image is an important indicator that can be utilized to make quality inferences, which may subsequently be used to predict decisions (Makhal et al., 2021). In some cases, quality degradation results in a product being rejected, while in others, it decreases customer acceptability (Qin et al., 2014). Makhal et al. (2021) also stated that fresh vegetables are a good example of this because they are either offered loose or in clear packaging, leaving appearance as the primary criterion for determining quality. The physical images of pegaga leaves before pre-treatment, after pre-treatment or before and after drying in a vacuum drying oven are shown in Table 2. Steam blanching was able to retain its shape after drying

in a vacuum oven, whereas control, water blanching, vacuum blanching, and microwave blanching resulted in a smaller shape than the actual leaves. Shrinkage occurs after the leaves have been dried (Velić et al., 2007). Slices of red bell pepper that had been steam-blanching showed the least shrinkage (Jeevitha et al., 2013). The enhanced shrinkage may be attributed to moisture loss during blanching and the release of trapped oxygen in tissues after drying, resulting in cell structure breakdown in porous materials (Jeevitha et al., 2013). Velić et al. (2007) claimed that the blanching caused apples to shrink by about 23%. Microwave blanching caused *Moringa Oleifera* L. leaves to shrink the most (Champaneri et al., 2020). This might be because pre-treatment at a greater temperature raises contractile stress in the cellular structure, causing tissue shrinking (Srimagal et al., 2017). The bitter gourd samples used as controls showed the greatest shrinking (Srimagal et al., 2017).

Table 2
The physical image of pegaga leaves before pre-treatment, after pre-treatment or before drying and after drying in a vacuum drying oven

Drying Temperature	**60 °C**		
Drying Time	**1 hour 30 mins**		
Pre-treatment	**Before Pre-treatment**	**After Pre-treatment / Before Drying**	**After Drying**
Control			
Water Blanching			
Steam Blanching			
Vacuum Blanching			
Microwave Blanching			

Moisture Content

Fresh pegaga leaves had a wet basis moisture content of 84.37±0.01%. Table 3 presents the drying time, drying temperature, and moisture content of pegaga leaf samples vacuum-dried using various pre-treatment techniques. The results showed that pre-treatments have a significant impact on the ultimate moisture content of pegaga leaves after drying. The term "ultimate moisture content" describes the final moisture content of pegaga leaves during the drying process. After the leaves have completely dried, this is the amount of moisture that is still present. The moisture content of water-blanching pegaga leaves causes certain soluble components to leach, but it can also aid in lowering moisture content by weakening cell walls, which can promote faster drying (Sledz et al., 2016). Water-blanched leaves showed a decrease from 85.97±0.39% to 5.38±0.49% and showed a significant ($P<0.05$) decrease, which proved that certain soluble components are leaching from the pegaga leaves. In comparison to water blanching, steam blanching can conserve more nutrients because it causes less direct leaching and may result in a different moisture retention profile. Wickramasinghe et al. (2020) studied that steam blanching can more softly permeate plant tissues than water blanching, resulting in partial loss of moisture and heat-induced alterations. Steam blanching softens and improves the elasticity of plant material, allowing for improved moisture dispersion during drying (Wickramasinghe et al., 2020). Steam-blanched leaves showed a decrease from 85.79±0.01% to 8.86±0.09% and showed a significant difference ($P<0.05$), which proved that there is less direct leaching from the pegaga leaves compared to water blanching. Vacuum blanching can lower the required temperature and perhaps lead to a lower moisture content because of a faster rate of heat penetration and less cell damage (Xiao et al., 2017). Vacuum-blanched leaves showed a decrease from 84.66±0.14% to 9.21±0.24%, which was significant ($P<0.05$), resulting in lower moisture content compared to before drying. Microwave blanching is a highly quick and effective method; however, because of the rapid heating and loss of moisture, it may result in a reduced final moisture content.

Champaneri et al. (2020) claimed that microwave blanching resulted in the lowest moisture content of *Moringa Oleifera* L. leaves (6.78%), a difference from the result shown in Table 3. This may be due to the changes in humidity during drying and pre-treatment. The moisture content of the *Moringa Oleifera* L. leaves dropped as the power level increased, which might be due to moisture evaporation caused by microwave volumetric heating (Champaneri et al., 2020). Heat-induced alterations in plant tissues can occur when microwave or other heat treatments are used prior to drying (Gonzalez & Barrett, 2010). These changes include the enlargement of air spaces inside the tissue, which can aid in the evaporation of moisture during drying. Due to localized heating, microwaves can also cause some water to evaporate inside the tissues, enabling moisture removal during the subsequent drying stage (Ni et al., 1999).

Table 3
Moisture content remained of pegaga leaves before pre-treatment, after pre-treatment or before drying, and after drying in a vacuum drying oven

Drying Temperature	**60 °C**		
Drying Time	**1 hour 30 mins**		
Treatment	**Before Pre-treatment (%)**	**After Pre-treatment / Before Drying (%)**	**After Drying (%)**
Control	84.37±0.01	84.37±0.44	11.74±0.57
Water Blanching		85.97±0.39	5.38±0.49
Steam Blanching		85.79±0.01	8.86±0.09
Vacuum Blanching		84.66±0.14	9.21±0.24
Microwave Blanching		83.71±0.01	8.53±0.09

Pre-treatments can change moisture content scientifically by influencing water movement, diffusion, and evaporation during drying. This pre-treatment may damage cell walls and enhance cell membrane permeability, allowing for quicker water removal during drying (Ando et al., 2016). Except for the control samples, the moisture content of the dried pegaga leaves was less than 10%. 'T Hag et al. (2020) asserted, however, that the microbiological safe moisture level of Native African leafy vegetables (ALVs) was less than 14% on a dry basis. Dried vegetables must contain no more than 8% water (Food Regulations, 1985). Drying reduced the moisture content of *Moringa oleifera* L. leaves from 80% to less than 10%, allowing the leaves to be stored without infection by microbes (Nobosse et al., 2017). Mold should develop quickly when the moisture concentration is greater than 11%, and color loss should occur when the moisture content is less than 4% (Anoraga et al., 2018). From the results obtained, it was verified that drying conditions for pegaga leaves were 60 °C and 1 hour and 30 minutes.

Fresh Weight Loss

Figure 3 shows the percentage of fresh weight loss after drying in a vacuum drying oven for control, water blanching, steam blanching, vacuum blanching, and microwave blanching of pegaga leaves. All the samples were dried until they reached a constant weight, and the drying time for each treatment was recorded. It was noticed that the percentage fresh weight loss of all pre-treated pegaga leaves showed an increasing trend with the increment of drying time. The moisture content of plant leaves can be affected by biological and processing factors (Żbik et al., 2023). Żbik et al. (2023) reported that the weight loss differences between species are caused by differences in the leaf tissue morphology, which is most likely due to structural changes that facilitate water transport in the tissues or differences in epidermal permeability (Żbik et al., 2023). Indeed, various pre-treatment procedures can cause structural changes in pegaga leaves, which can have a major impact on their future drying behavior and final attributes.

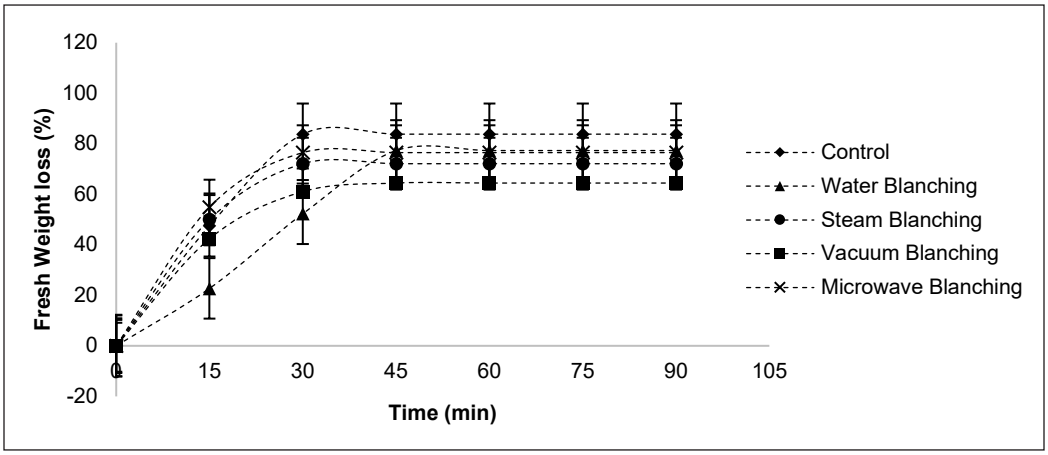

Figure 3. Percentage of fresh weight loss after drying in a vacuum drying oven for control, water blanching, steam blanching, vacuum blanching, and microwave blanching of pegaga leaves

These variations are caused by the unique processes involved in each pre-treatment approach. The maximum weight loss (66.61%) was shown by the pegaga leaves sample treated with no pre-treatments, followed by microwave blanching (62.46%), steam blanching (58.61%), and water blanching (54.87%). Pegaga leaves stay mainly intact when there are no pre-treatments on the leaves. Cell walls, cell membranes, and cellular components are undamaged, and the leaves retain their original qualities (Thamkaew et al., 2021). At the same time, the least weight loss (51.57%) was exhibited by the vacuum-blanched pegaga leaves. Vacuum blanching is the process of applying a vacuum to plant material while it is exposed to steam. Because the decreasing pressure reduces the boiling point of water, moisture evaporates even at lower temperatures. This combination of steam and lowered pressure can result in faster and more regulated cell expansion and moisture removal, resulting in structural changes that are a mix of steam and vacuum effects.

Drying Kinetics and Modelling

The coefficient of determination (R^2) and drying rate (k) values for the models are shown in Table 4. Figure 4 shows the comparison of experimental data and predicted moisture ratio using the Midilli Kucuk Model for pegaga leaves. The greatest R^2, lowest χ^2 and RMSE values for the Midilli Kucuk model varied throughout all trials by vacuum-blanched pegaga leaves. The Midilli Kucuk model, in particular, was found adequate to represent the vacuum-drying behavior of pegaga leaves. Similarly, Bialik et al. (2020) in the article on vacuum-dried kiwi berry, green seaweed (*Ulva spp.*) (Vega-Gálvez et al., 2022) *Stevia rebaudiana* leaves (Hidar et al., 2020), *Kageneckia oblong* leaves (Zambra et al., 2021), and golden berries (Kipçak, 2023), as well as many other researchers, concluded that the Midilli-Kucuk model satisfactorily describes the drying behavior of food products.

Table 4
Kinetics parameters for drying kinetics of pegaga leaves using the Midilli Kucuk model

Pre-treatment	Model Coefficients		Statistical Parameters		
		a	R^2	χ^2	RMSE
Control	a	451.9760	0.9672	4.001×10^{-3}	2.858×10^{-3}
	k	4.0832			
	n	0.1531			
	b	0.0001			
Water Blanching	a	2.1703	0.9504	3.960×10^{-3}	2.829×10^{-3}
	k	0.1724			
	n	0.7473			
	b	0.0006			
Steam Blanching	a	445.3704	0.9630	2.666×10^{-3}	1.904×10^{-3}
	k	4.0560			
	n	0.1621			
	b	0.0001			
Vacuum Blanching	a	438.9299	0.9990	0.0807×10^{-3}	0.0576×10^{-3}
	k	4.0865			
	n	0.1598			
	b	0			
Microwave Blanching	a	2.9134	0.9754	2.066×10^{-3}	1.476×10^{-3}
	k	0.2383			
	n	0.6624			
	b	0.0009			

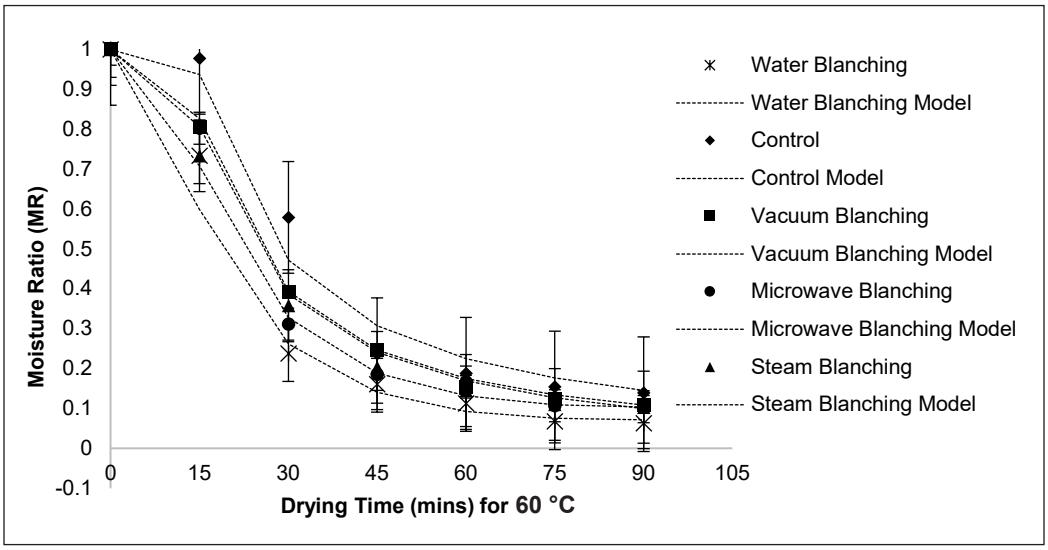

Figure 4. Comparison of experimental data and predicted moisture ratio using the Midilli Kucuk Model for pegaga leaves

Nutritional and Antioxidant Properties

Effect of Different Pre-treatments on Total Phenolic Content (TPC)

The major component of pegaga leaves is phenolic compounds (Bakar et al., 2022). The total phenolic content (TPC) in fresh pegaga was 0.02 mg GAE/g extract (Figure 5), which changed differently with varying pre-treatments. Among the pre-treated dried pegaga leaves, vacuum blanching of dried pegaga leaves had the highest TPC (0.09 mg GAE/g extract), followed by steam blanching (0.08 mg GAE/g extract), water blanching (0.07 mg GAE/g extract), microwave blanching (0.06 mg GAE/g extract) and control leaves (0.05 mg GAE/g extract). The vacuum blanching method prevented direct contact of the pegaga leaves with boiling water, whereas the water blanching, steam blanching, microwave blanching, and control leaf samples were all directly contacted with pre-treatments. However, the change in TPC observed following vacuum blanching and subsequent drying can be due to various metabolic events that occur throughout these procedures. Phenolic compounds are a type of secondary metabolite found in plants that are recognized for their antioxidant and health-promoting qualities (Nurzyńska-Wierdak, 2023). Certain phenolic compounds can degrade at high temperatures, even under low pressure (Minatel et al., 2017). Minatel et al. (2017) reported that some phenolics may undergo chemical modifications that alter their structure and limit their detection during TPC analysis, depending on the temperature and period of vacuum blanching. The concentration of phenolic chemicals in the residual tissue rises when water is removed from the plant material during drying (Chua et al., 2019). While the absolute number of water-soluble chemicals may decrease, phenolic compounds become more

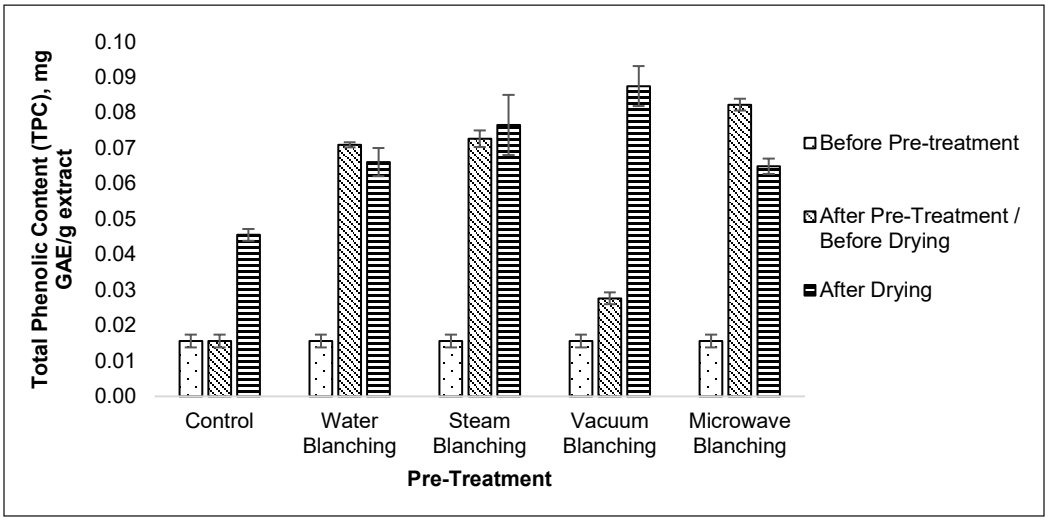

Figure 5. Total phenolic content (TPC) of pegaga leaves before pre-treatment, after pre-treatment or before drying, and after drying in a vacuum drying oven

concentrated in dried material, perhaps contributing to an increase in TPC (Hapsari et al., 2022). The rise in TPC during the pre-treatment process may be attributed to the higher temperature, as boiling water increases the permeability of the cell membrane, allowing bioactive compounds to be released during heat contact (Klungboonkrong et al., 2018). The TPC results of vacuum blanching pre-treated dried pegaga leaves in this investigation were consistent with the findings of Borines et al. (2020), who stated that vacuum-drying onion leaves gave the greatest TPC. Long-term exposure to air and light may accelerate the oxidation of several phenolic compounds, as previously noted in the literature (Klungboonkrong et al., 2018). Longer drying times decreased TPC in olive (*Olea europaea* L.) leaves (Filgueira-Garro et al., 2022).

Effect of Different Pre-treatments on Total Flavonoid Content (TFC)

The effect of pre-treatment and drying processes on the total flavonoid content (TFC) of pegaga leaves is depicted in Figure 6. The vacuum oven drying procedures had nearly the same effect on the TFC as they did on the TPC of the pegaga leaves. The TFC in fresh pegaga was 0.44 mg QUE/g extract, which changed differently with varying pre-treatments. Among the pre-treated dried pegaga leaves, vacuum blanching of dried pegaga leaves had the highest TFC (2.22 mg QUE/g extract), followed by microwave blanching (2.04 mg QUE/g extract), water blanching (1.95 mg QUE/g extract), steam blanching (1.62 mg QE/g extract) and control leaves (1.17 mg QUE/g extract). The observed phenomenon in which the initial Total Flavonoid Content (TFC) of pegaga leaves was low after vacuum blanching but increased significantly after vacuum oven

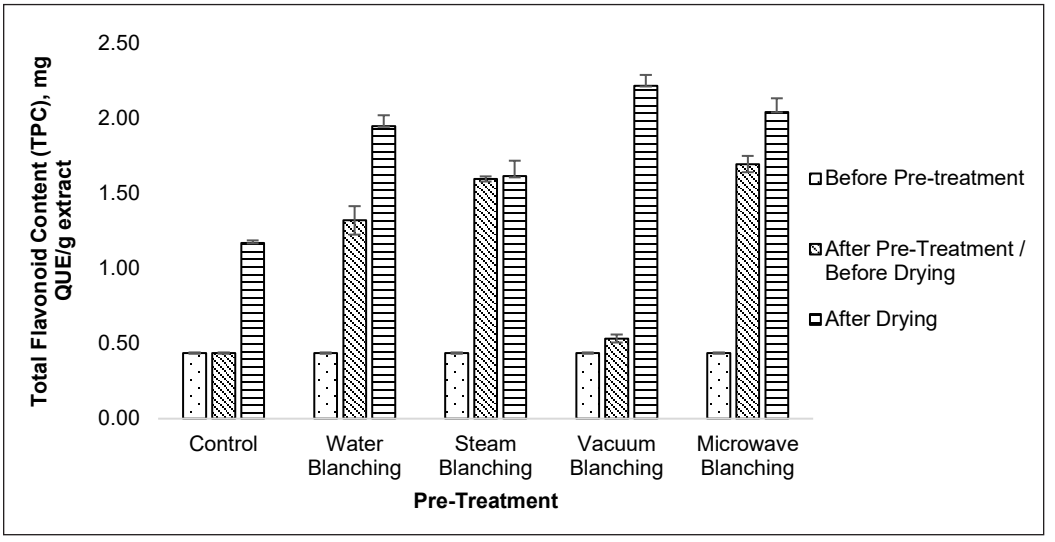

Figure 6. Total flavonoid content (TFC) of pegaga leaves before pre-treatment, after pre-treatment or before drying and after drying in a vacuum drying oven

drying can be explained by several factors related to the effects of vacuum blanching and subsequent vacuum oven drying on the flavonoid content and the chemistry of the plant material. Vacuum blanching can enhance the loss of volatile substances such as flavonoids (Xiao et al., 2017). Flavonoids are a class of bioactive chemicals that are heat, steam, and vacuum-sensitive (Tacer-Caba et al., 2015). Due to the presence of steam and the lower-pressure environment, certain flavonoids with smaller molecular weights or structures that are more prone to vaporization may be lost during vacuum blanching (ElGamal et al., 2023).

At lower temperatures, the vacuum atmosphere allows for the release of volatile chemicals, which can include flavonoids (Żbik et al., 2023). Lower pressure settings may allow for more effective and gentle extraction of flavonoids from plant material during drying (Jha & Sit, 2022). The value of TFC reported for vacuum oven-dried Ocimum basilicum leaves with methanol extract is high (Mahirah et al., 2018) compared to the experiment. According to Mahirah et al. (2018), flavonoids having a benzo-γ-pyrone structure form a significant category of polyphenolic chemicals found in plants. The presence of flavonoids contributes to the high antioxidant activity of green leafy vegetables (Hue et al., 2012). Consumption of flavonols, namely quercetin, found in onions, lowers the risk of diseases (Ribeiro et al., 2023). Total phenolic content (TPC) and TFC assay results followed a similar trend, with the vacuum oven-dried sample for pegaga leaves having the highest TPC and TFC, and the control leaves having the least TPC and TFC. The most frequent kind of plant phenol is flavonoid (Mahirah et al., 2018). Do et al. (2014) reported a significant relationship (0.923) between the polyphenolic contents (TPC and TFC) of the *Limnophila aromatica* plant. The results of this study supported the conclusion that flavonoid is the most common chemical in the phenolic category.

Effect of Different Pre-treatments on 2,2-diphenyl-1-picrylhydrazyl (DPPH) Assay

2,2-diphenyl-1-picrylhydrazyl (DPPH) assay of fresh pegaga leaves is 0.53%, but it decreased after pre-treatment and vacuum-drying of pegaga leaves. These results agree with Filgueira-Garro et al. (2022), where vacuum-drying olive leaves reduced DPPH. This reduction in DPPH might have been produced by polyphenol oxidases (PPO) that were active during vacuum drying. According to Filgueira-Garro et al. (2022), the presence of apparent browning in vacuum-dried olive leaves could mean that PPO activity has reduced the phenolic component and its antioxidant properties. The greatest proportion of DPPH was found in control leaves (0.30%), followed by water blanching (0.05%), vacuum blanching (0.05%), microwave blanching (0.05%), and steam blanching (0.04%) (Figure 7). Antioxidants counteract the damaging effects of free radical damage in our surroundings, where it is commonly found in herbal remedies and traditional treatments. (Bakar et al., 2022).

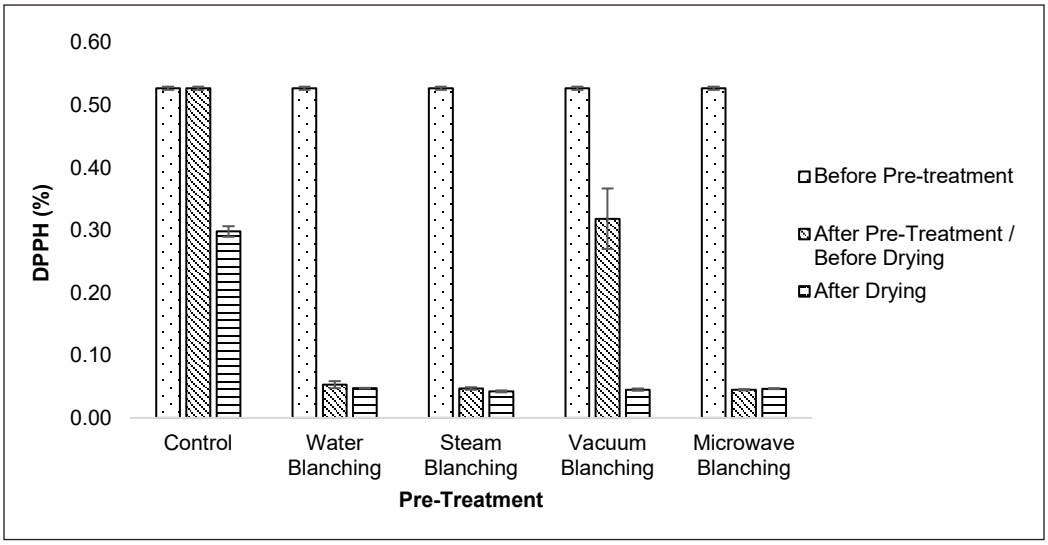

Figure 7. DPPH scavenging activity of pegaga leaves before pre-treatment, after pre-treatment or before drying and after drying in a vacuum drying oven

CONCLUSION

The drying properties of pegaga leaves were tested using a vacuum oven at 60 °C for 1 hour and 30 minutes under 0.01 MPa. During the decrease in rate period, the drying process happened, but not during the steady rate period. R^2, χ^2, and RMSE were used to assess the quality of fit of the experimental data to the thin layer drying model. The Midilli Kucuk model can appropriately represent the thin-layer drying behavior of pegaga leaves, according to the results. The most appropriate pre-treatment for drying pegaga leaves based on the above analysis was found to be vacuum blanching, microwave blanching, steam blanching, control, and water blanching, respectively.

In general, it was found that the pre-treatment before drying pegaga leaves significantly affected the nutritional qualities and antioxidant activities of the pegaga leaves. Vacuum blanching resulted in relatively high TPC (0.09 mg GAE/g extract) and TFC (2.22 mg QUE/g extract) while decreasing the 2,2-diphenyl-1-picrylhydrazyl (DPPH) assay value (0.05%) after vacuum oven drying. Thus, the vacuum blanching and vacuum oven drying method is the best method to preserve or enhance the nutritional content of pegaga leaves based on this study. Improved pre-treatments and drying techniques can lead to more uniform quality in terms of appearance, phytochemicals, and antioxidant properties, which are crucial for marketability, customer acceptability, and applications in functional foods, supplements, and herbal products. Utilizing more of the pegaga leaves efficiently and minimizing waste may be achieved by maximizing the drying process to avoid over- or under-drying. The research might lead to improvements in food processing and

preservation methods by providing fresh perspectives on the efficacy of various drying and pre-treatment methods. However, the specific phenolic compounds or other substances responsible for the antioxidant capabilities of the extracts are yet unclear. Since previous and present research suggests that pegaga leaves offer potential as natural antioxidant sources, additional study is needed to identify and describe antioxidant compounds from extracts that may be contributing to the high antioxidant properties. The findings may serve as a basis for further investigation into formulation strategies, extraction processes, and novel applications related to the processing of pegaga leaves. Thus, this study can enhance the utilization of pre-treated dried pegaga leaves as a valuable natural resource in various applications.

ACKNOWLEDGEMENTS

The authors thank Geran Inisiatif Putra Muda (GP-IPM/2020/9689800) for funding the project and the facilities provided by Universiti Putra Malaysia to conduct research activities.

REFERENCES

Alibas, I. (2009). Microwave, vacuum, and air drying characteristics of collard leaves. *Drying Technology*, *27*(11), 1266–1273. https://doi.org/10.1080/07373930903267773

Ando, Y., Maeda, Y., Mizutani, K., Wakatsuki, N., Hagiwara, S., & Nabetani, H. (2016). Impact of blanching and freeze-thaw pretreatment on drying rate of carrot roots in relation to changes in cell membrane function and cell wall structure. *LWT-Food Science and Technology*, *71*, 40–46. https://doi.org/10.1016/j.lwt.2016.03.019

Anoraga, S. B., Sabarisman, I., & Ainuri, M. (2018). Effect of different pretreatments on dried chilli (*Capsicum annum* L.) quality. *IOP Conference Series: Earth and Environmental Science*, *131*(1), Article 012014. https://doi.org/10.1088/1755-1315/131/1/012014

Almey, A. A. A., Khan, C. A. J., Zahir, I. S., Suleiman, K. M., Aisyah, M. R., & Rahim, K. K. (2010). Total phenolic content and primary antioxidant activity of methanolic and ethanolic extracts of aromatic plants' leaves. *International Food Research Journal*, *17*(4), 1077–1084.

Babu, A. K., Kumaresan, G., Raj, V. A. A., & Velraj, R. (2018). Review of leaf drying: Mechanism and influencing parameters, drying methods, nutrient preservation, and mathematical models. *Renewable and Sustainable Energy Reviews*, *90*, 536–556. https://doi.org/10.1016/j.rser.2018.04.002

Bakar, I. N. A., Ibrahim, M. F., Hakiman, M., Abd-Aziz, S., Prasongsuk, S., Tin, L. C. Y., & Jenol, M. A. (2022). Characterization of asiaticoside concentration, total phenolic compounds, and antioxidant activity of different varieties of *Centella asiatica* (L.) and essential oil extraction using hydro-distillation with enzyme assisted. *Biocatalysis and Agricultural Biotechnology*, *44*, Article 102474. https://doi.org/10.1016/J.BCAB.2022.102474

Bialik, M., Wiktor, A., Witrowa-Rajchert, D., Samborska, K., Gondek, E., & Findura, P. (2020). Osmotic dehydration and freezing as a suitable pretreatment in the process of vacuum drying kiwiberry: Drying

kinetics and microstructural changes. *International Agrophysics*, *34*(2), 265–272. https://doi.org/10.31545/INTAGR/118859

Bishnoi, S., Chhikara, N., Singhania, N., & Ray, A. B. (2020). Effect of cabinet drying on nutritional quality and drying kinetics of fenugreek leaves (*Trigonella foenum-graecum* L.). *Journal of Agriculture and Food Research*, *2*, Article 100072. https://doi.org/10.1016/j.jafr.2020.100072

Borines, M. G., Demafelis, R. B., Capunitan, J. A., Stephanie, L., Dizon, H., Joyce, R., Landoy, B., & Rodriguez, R. C. (2020). Effects of dehydration on the bioactive compounds of waste onion leaves. *Philippine Journal of Crop Science*, *45*(1), 21–33.

Champaneri, D. D., Mayani, J. M., Pancholi, H. N., Patel, J. B., & Bangoria, U. V. (2020). Effect of different blanching methods on physical and colour characteristics of *Moringa Oleifera* L. dry leaf powder. *International Journal of Latest Trends in Engineering and Technology* , *16*(1), 34–37. http://dx.doi.org/10.21172/1.162.03

Chua, L. Y. W., Chua, B. L., Figiel, A., Chong, C. H., Wojdyło, A., Szumny, A., & Choong, T. S. Y. (2019). Antioxidant activity, and volatile and phytosterol contents of strobilanthes crispus dehydrated using conventional and vacuum microwave drying methods. *Molecules*, *24*(7), Article 1397. https://doi.org/10.3390/molecules24071397

Deng, L. Z., Mujumdar, A. S., Zhang, Q., Yang, X. H., Wang, J., Zheng, Z. A., Gao, Z. J., & Xiao, H. W. (2019). Chemical and physical pretreatments of fruits and vegetables: Effects on drying characteristics and quality attributes–a comprehensive review. *Critical Reviews in Food Science and Nutrition*, *59*(9), 1408–1432. https://doi.org/10.1080/10408398.2017.1409192

Do, Q. D., Angkawijaya, A. E., Tran-Nguyen, P. L., Huynh, L. H., Soetaredjo, F. E., Ismadji, S., & Ju, Y. H. (2014). Effect of extraction solvent on total phenol content, total flavonoid content, and antioxidant activity of Limnophila aromatica. *Journal of Food and Drug Analysis*, *22*(3), 296–302. https://doi.org/10.1016/j.jfda.2013.11.001

ElGamal, R., Song, C., Rayan, A. M., Liu, C., Al-Rejaie, S., & ElMasry, G. (2023). Thermal degradation of bioactive compounds during drying process of horticultural and agronomic products: A comprehensive overview. *Agronomy*, *13*(6), Article 1580. https://doi.org/10.3390/agronomy13061580

Fadzil, N. F., Bakar, M. F. A., Yusop, M. H. M., & Bakar, F. I. A. (2020). Sensorial and physicochemical characteristics of herbal noodle enriched with centella asiatica. *Food Research*, *4*(4), 1030–1037. https://doi.org/10.26656/fr.2017.4(4).408

Filgueira-Garro, I., González-Ferrero, C., Mendiola, D., & Marín-Arroyo, M. R. (2022). Effect of cultivar and drying methods on phenolic compounds and antioxidant capacity in olive (*Olea europaea* L.) leaves. *AIMS Agriculture and Food*, *18*(1), 250–264. https://doi.org/10.3934/agrfood.2022016

Food Regulations (1985). *Food regulations 1985*. International Law Book Services.

Gonzalez, M. E., & Barrett, D. M. (2010). Thermal, high pressure, and electric field processing effects on plant cell membrane integrity and relevance to fruit and vegetable quality. *Journal of Food Science*, *75*(7), R121-R130. https://doi.org/10.1111/j.1750-3841.2010.01763.x

Hapsari, S., Yohed, I., Kristianita, R. A., Jadid, N., Aparamarta, H. W., & Gunawan, S. (2022). Phenolic and flavonoid compounds extraction from Calophyllum inophyllum leaves. *Arabian Journal of Chemistry*, *15*(3), Article 103666. https://doi.org/10.1016/j.arabjc.2021.103666

Hasan, M. U., Malik, A. U., Ali, S., Imtiaz, A., Munir, A., Amjad, W., & Anwar, R. (2019). Modern drying techniques in fruits and vegetables to overcome postharvest losses: A review. *Journal of Food Processing and Preservation*, *43*(12), Article e14280. https://doi.org/10.1111/jfpp.14280

Hidar, N., Ouhammou, M., Mghazli, S., Idlimam, A., Hajjaj, A., Bouchdoug, M., Jaouad, A., & Mahrouz, M. (2020). The impact of solar convective drying on kinetics, bioactive compounds and microstructure of stevia leaves. *Renewable Energy*, *161*, 1176–1183. https://doi.org/10.1016/j.renene.2020.07.124

Hii, C. L., & Ogugo, J. F. (2014). Effect of pre-treatment on the drying kinetics and product quality of star fruit slices. *Journal of Engineering Science and Technology*, *9*(1), 122–134.

Hiranvarachat, B., Devahastin, S., & Soponronnarit, S. (2015). Comparative evaluation of atmospheric and vacuum microwave-assisted extraction of bioactive compounds from fresh and dried *Centella asiatica* L. leaves. *International Journal of Food Science and Technology*, *50*(3), 750–757. https://doi.org/10.1111/ijfs.12669

Hue, S. M., Boyce, A. N., & Somasundram, C. (2012). Antioxidant activity, phenolic and flavonoid contents in the leaves of different varieties of sweet potato (Ipomoea batatas). *Australian Journal of Crop Science*, *6*(3), 375–380.

Idris, F. N., & Nadzir, M. M. (2021). Comparative studies on different extraction methods of centella asiatica and extracts bioactive compounds effects on antimicrobial activities. *Antibiotics*, *10*(4), Article 457. https://doi.org/10.3390/antibiotics10040457

Idris, F. N., Nadzir, M. M., & Abd Shukor, S. R. (2020). Optimization of solvent-free microwave extraction of Centella asiatica using Taguchi method. *Journal of Environmental Chemical Engineering*, *8*(3), Article 103766. https://doi.org/10.1016/j.jece.2020.103766

Jeevitha, G. C., Hebbar, H. U., & Raghavarao, K. S. M. S. (2013). Electromagnetic radiation-based dry blanching of red bell peppers: A comparative study. *Journal of Food Process Engineering*, *36*(5), 663–674. https://doi.org/10.1111/jfpe.12030

Jha, A. K., & Sit, N. (2022). Extraction of bioactive compounds from plant materials using combination of various novel methods: A review. *Trends in Food Science & Technology*, *119*, 579–591. https://doi.org/10.1016/J.TIFS.2021.11.019

Kıpçak, E. (2023). The investigation of oven and vacuum oven drying kinetics and mathematical modelling of golden berries. *Journal of the Turkish Chemical Society Section B: Chemical Engineering*, *6*, 1–8. https://doi.org/10.58692/jotcsb.1190201

Klungboonkrong, V., Phoungchandang, S., & Lamsal, B. (2018). Drying of Orthosiphon aristatus leaves: Mathematical modeling, drying characteristics, and quality aspects. *Chemical Engineering Communications*, *205*(9), 1239–1251. https://doi.org/10.1080/00986445.2018.1443080

Lemus-Mondaca, R., Vega-Gálvez, A., Rojas, P., Stucken, K., Delporte, C., Valenzuela-Barra, G., Jagus, R. J., Agüero, M. V., & Pasten, A. (2018). Antioxidant, antimicrobial and anti-inflammatory potential of

Stevia rebaudiana leaves: Effect of different drying methods. *Journal of Applied Research on Medicinal and Aromatic Plants*, *11*, 37–46. https://doi.org/10.1016/j.jarmap.2018.10.003

Lemus-Mondaca, R., Zura-Bravo, L., Ah-Hen, K., & Di Scala, K. (2021). Effect of drying methods on drying kinetics, energy features, thermophysical and microstructural properties of Stevia rebaudiana leaves. *Journal of the Science of Food and Agriculture*, *101*(15), 6484–6495. https://doi.org/10.1002/jsfa.11320

Mahirah, Y. S., Rabeta, M. S., & Antora, R. A. (2018). Effects of different drying methods on the proximate composition and antioxidant activities of ocimum basilicum leaves. *Food Research*, *2*(5), 421–428. https://doi.org/10.26656/fr.2017.2(5).083

Makhal, A., Robertson, K., Thyne, M., & Mirosa, M. (2021). Normalising the "ugly" to reduce food waste: Exploring the socialisations that form appearance preferences for fresh fruits and vegetables. *Journal of Consumer Behaviour*, *20*(5), 1025-1039. https://doi.org/10.1002/cb.1908

Márquez-Cardozo, C. J., Caballero-Gutiérrez, B. L., Ciro-Velázquez, H. J., & Restrepo-Molina, D. A. (2021). Effect of pretreatment and temperature on the drying kinetics and physicochemical and techno-functional characteristics of pumpkin (Cucurbita maxima). *Heliyon*, *7*(4), Article e06802. https://doi.org/10.1016/j.heliyon.2021.e06802

Minatel, I. O., Borges, C. V., Borges, C. V., Alonzo, H., Hector, G., Gomez, G., Chen, C. O., Chen, C. O., Pace, G., & Lima, P. (2017). Phenolic compounds: Functional properties, impact of processing and bioavailability. In M. Soto-Hernandez, M. Palma-Tenango & M. D. R. Garcia-Mateos (Eds.) *Phenolic compounds - Biological activity* (pp. 1–24). IntechOpen. https://doi.org/10.57772/66368

Minh, N. P. (2014). Effects of blanching and drying treatment on extraction of soluble components from dried Centella asiatica. *International Journal of Multidisciplinary Research and Development, 1*(2), 77–82.

Mohapatra, P., Ray, A., Jena, S., Nayak, S., & Mohanty, S. (2022). Influence of various drying methods on physicochemical characteristics, antioxidant activity, and bioactive compounds in *Centella asiatica* L. leaves: A comparative study. *Biotechnologia*, *103*(3), 235–247. https://doi.org/10.5114/bta.2022.118666

Ng, Z. X., Yong, P. H., & Lim, S. Y. (2020). Customized drying treatments increased the extraction of phytochemicals and antioxidant activity from economically viable medicinal plants. *Industrial Crops and Products*, *155*, Article 112815. https://doi.org/10.1016/j.indcrop.2020.112815

Ni, H., Datta, A. K., & Torrance, K. E. (1999). Moisture transport in intensive microwave heating of biomaterials: A multiphase porous media model. *International Journal of Heat and Mass Transfer*, *42*(8), 1501–1512. https://doi.org/10.1016/S0017-9310(98)00123-9

Nighitha, M. T., & Mathew, S. M. (2019). The effect of drying on the shelflife amaranthus leaves. *International Research Journal of Engineering and Technology, 6*(2), 219–222.

Nobosse, P., Fombang, E. N., & Mbofung, C. M. F. (2017). The effect of steam blanching and drying method on nutrients, phytochemicals and antioxidant activity of moringa (*Moringa oleifera* L.) leaves. *American Journal of Food Science and Technology, 5*(2), 53-60. https://doi.org/10.12691/ajfst-5-2-4

Nurzyńska-Wierdak, R. (2023). Phenolic compounds from new natural sources—Plant genotype and ontogenetic variation. *Molecules*, *28*(4), Article 1731. https://doi.org/10.3390/molecules28041731

Qin, Y., Wang, J., & Wei, C. (2014). Joint pricing and inventory control for fresh produce and foods with quality and physical quantity deteriorating simultaneously. *International Journal of Production Economics*, *152*, 42-48. https://doi.org/10.1016/j.ijpe.2014.01.005

Rahim, M. S. A. A., Baharudin, N. A., Nazri, I. A. A., Mohamad, S., & Muazzam, K. A. A. R. (2021). Effect of different drying methods on the antioxidant properties of leaves of Centella asiatica. *IOP Conference Series: Earth and Environmental Science*, *756*(1), 6–13. https://doi.org/10.1088/1755-1315/756/1/012054

Ribeiro, T. B., Melo, A., Vilas-Boas, A. A., & Pintado, M. (2023). Flavonoids. In M. Carocho, S. A. Heleno & L. Barros (Eds.) *Natural secondary metabolites: From nature, through science, to industry* (pp. 73–105). Springer. https://doi.org/10.1007/978-3-031-18587-8_4

Şahin, S., Elhussein, E., Bilgin, M., Lorenzo, J. M., Barba, F. J., & Roohinejad, S. (2018). Effect of drying method on oleuropein, total phenolic content, flavonoid content, and antioxidant activity of olive (Olea europaea) leaf. *Journal of Food Processing and Preservation*, *42*(5), Article e13604. https://doi.org/10.1111/jfpp.13604

Saifullah, M., McCullum, R., McCluskey, A., & Vuong, Q. (2019). Effects of different drying methods on extractable phenolic compounds and antioxidant properties from lemon myrtle dried leaves. *Heliyon*, *5*(12), Article e03044. https://doi.org/10.1016/j.heliyon.2019.e03044

Sledz, M., Wiktor, A., Rybak, K., Nowacka, M., & Witrowa-Rajchert, D. (2016). The impact of ultrasound and steam blanching pre-treatments on the drying kinetics, energy consumption and selected properties of parsley leaves. *Applied Acoustics*, *103*, 148–156. https://doi.org/10.1016/j.apacoust.2015.05.006

Srimagal, A., Mishra, S., & Pradhan, R. C. (2017). Effects of ethyl oleate and microwave blanching on drying kinetics of bitter gourd. *Journal of Food Science and Technology*, *54*(5), 1192–1198. https://doi.org/10.1007/s13197-017-2518-7

Tacer-Caba, Z., Nilufer-Erdil, D., & Ai, Y. (2015). Chemical composition of cereals and their products. In P. C. K. Cheung & B. M. Mehta (Eds.) *Handbook of food chemistry* (pp. 301-330). Springer. https://doi.org/10.1007/978-3-642-36605-5_33

Telfser, A., & Galindo, F. G. (2019). Effect of reversible permeabilization in combination with different drying methods on the structure and sensorial quality of dried basil (*Ocimum basilicum* L.) leaves. *LWT*, *99*, 148–155. https://doi.org/10.1016/j.lwt.2018.09.062

Thamkaew, G., Sjöholm, I., & Galindo, F. G. (2021). A review of drying methods for improving the quality of dried herbs. *Critical Reviews in Food Science and Nutrition*, *61*(11), 1763–1786. https://doi.org/10.1080/10408398.2020.1765309

Tomar, M. S., & Gururani, P. (2019). Microwave assisted blanching of fruits and vegetables : A mini review. *Octa Journal of Biosciences, 7*(2), 105–107.

Tripathy, S., & Srivastav, P. P. (2023). Effect of dielectric barrier discharge (DBD) cold plasma-activated water pre-treatment on the drying properties, kinetic parameters, and physicochemical and functional properties of Centella asiatica leaves. *Chemosphere*, *332*, Article 138901. https://doi.org/10.1016/J.CHEMOSPHERE.2023.138901

Trirattanapikul, W., & Phoungchandang, S. (2014). Microwave blanching and drying characteristics of *Centella asiatica* (L.) urban leaves using tray and heat pump-assisted dehumidified drying. *Journal of Food Science and Technology*, *51*(12), 3623–3634. https://doi.org/10.1007/s13197-012-0876-8

'T Hag, L. V., Danthe, J., Handschin, S., Mutuli, G. P., Mbuge, D., & Mezzenga, R. (2020). Drying of African leafy vegetables for their effective preservation: The difference in moisture sorption isotherms explained by their microstructure. *Food and Function*, *11*(1), 955–964. https://doi.org/10.1039/c9fo01175g

Vega-Gálvez, A., Uribe, E., Gómez-Pérez, L. S., García, V., Mejias, N., & Pastén, A. (2022). Drying kinetic modeling and assessment of mineral content, antimicrobial activity, and potential α-glucosidase activity inhibition of a green seaweed (Ulva spp.) subjected to different drying methods. *ACS Omega*, *7*(38), 34230–34238. https://doi.org/10.1021/acsomega.2c03617

Velić, D., Bilić, M., Tomas, S., Planinić, M., Bucić-Kojić, A., & Aladić, K. (2007). Study of the drying kinetics of "Granny Smith" apple in tray drier. *Agriculturae Conspectus Scientificus*, *72*(4), 323–328.

Wickramasinghe, Y. W. H., Wickramasinghe, I., & Wijesekara, I. (2020). Effect of steam blanching, dehydration temperature & time, on the sensory and nutritional properties of a herbal tea developed from moringa oleifera leaves. *International Journal of Food Science, 2020*(1), Article 5376280. https://doi.org/10.1155/2020/5376280

Xiao, H. W., Pan, Z., Deng, L. Z., El-Mashad, H. M., Yang, X. H., Mujumdar, A. S., Gao, Z. J., & Zhang, Q. (2017). Recent developments and trends in thermal blanching – A comprehensive review. *Information Processing in Agriculture*, *4*(2), 101–127. https://doi.org/10.1016/j.inpa.2017.02.001

Zainol, M. K. M., Abdul-Hamid, A., Bakar, F. A., & Dek, S. P. (2009). Effect of different drying methods on the degradation of selected flavonoids in Centella asiatica. *International Food Research Journal*, *16*(4), 531–537.

Zambra, C., Hernández, D., Reyes, H., Riveros, N., & Lemus-Mondaca, R. (2021). Kageneckia oblonga leaves subjected to different drying methods: Drying kinetics, energy consumption and interesting compounds. *Frontiers in Sustainable Food Systems*, *5*, Article 641858. https://doi.org/10.3389/fsufs.2021.641858

Żbik, K., Górska-Horczyczak, E., Onopiuk, A., Kurek, M., & Zalewska, M. (2023). Vacuum and convection drying effects on volatile compounds profile and physicochemical properties of selected herbs from Lamiaceae family. *European Food Research and Technology*, *249*(10), 2569-2581. https://doi.org/10.1007/s00217-023-04309-7

Zielinska, M., Ropelewska, E., Xiao, H. W., Mujumdar, A. S., & Law, C. L. (2020). Review of recent applications and research progress in hybrid and combined microwave-assisted drying of food products: Quality properties. *Critical Reviews in Food Science and Nutrition*, *60*(13), 2212–2264. https://doi.org/10.1080/10408398.2019.1632788

Pertanika J. Sci. & Technol. 33 (S5): 43 - 58 (2025)

PERTANIKA JOURNALS

SCIENCE & TECHNOLOGY

Journal homepage: http://www.pertanika.upm.edu.my/

Application of Artificial Neural Networks for Classifying Earthworms (*Eudrilus eugeniae*) Moisture Content During the Drying Process

Yusuf Hendrawan*, Mei Lusi Ambarwati, Anang Lastriyanto, Retno Damayanti, Dimas Firmanda Al Riza, Mochamad Bagus Hermanto and Sandra Malin Sutan

Department of Biosystems Engineering, Faculty of Agricultural Technology, Brawijaya University, Veteran St., Malang, East Java, ZIP 65145, Indonesia

ABSTRACT

Earthworms (*Eudrilus eugeniae*) have many benefits for the health and animal feed industries. The drying process of earthworms is necessary to extend their shelf life, yet conventional gravimetric moisture tests are slow and destructive. The purpose of this study was to classify the moisture content of earthworms using machine vision and artificial neural networks (ANN) during the drying process, with classified worms into wet (> 40% wb), semi-dry (40%–12%), and dry (< 12%) states. RGB images (n = 450) were acquired every 15 min during cabinet drying at 60 °C; reference moisture was obtained gravimetrically. Nine color and texture features were extracted and ranked in WEKA; then, the top eight features were retained**.** An external feed-forward ANN implemented in MATLAB with 8-40-3 architecture, TrainLM optimiser, logsig–logsig–purelin transfer functions yielded MSE = 0.0733 (training) and 0.086058 (validation) and R = 0.95309 (training) and 0.92962 (validation). The modest MSE gap reflects class imbalance rather than overfitting, as classification metrics on the unseen test set match the validation results.

Keywords: Artificial neural networks, drying process, earthworms, machine vision

ARTICLE INFO

Article history:
Received: 13 February 2025
Accepted: 28 May 2025
Published: 10 July 2025

DOI: https://doi.org/10.47836/pjst.33.S5.03

E-mail addresses:
yusuf_h@ub.ac.id (Yusuf Hendrawan)
mlusi1072@gmail.com (Mei Lusi Ambarawati)
anangl@ub.ac.id (Anang Lastriyanto)
damayanti@ub.ac.id (Retno Damayanti)
dimasfirmanda@ub.ac.id (Dimas Firmanda Al Riza)
mbhermanto@ub.ac.id (Mochamad Bagus Hermanto)
sandra.msutan@ub.ac.id (Sandra Malin Sutan)
* Corresponding author

INTRODUCTION

Earthworms (*Eudrilus eugeniae*) are a great source of protein for animal feed with a protein content of 65.4%, 19% nitrogen, 11% fat, and 6% ash, and also contain 9 essential amino acids and 4 non-essential amino acids (Deepika et al., 2018). The nutritional content makes earthworms widely used in the livestock, cosmetic, and pharmaceutical industries (Azmi et al.,

2014; Sun, 2015). The addition of earthworms to animal feed as the main or additive feed has been proven to increase the productivity of eggs and meat, and the livestock becomes more resistant to bacteria, viruses, and fungi (Mohanta et al., 2016; Musyoka et al., 2019). Several types of earthworms that can be used for animal feed are *Lumbricus rubellus*, *Eudrilus eugeniae*, and *Eisenia fetida* (Antonova et al., 2021). Earthworms are processed into dried earthworms for the shipping process because living earthworms are sensitive to environmental changes such as soil moisture, soil pH, and temperature (Wu et al., 2019). Earthworms that have been dried have a longer shelf life as well as nutritional content that is still maintained (Fortu Jr et al., 2019).

Conventional production relies on cabinet ovens heated by gas stoves, where temperature control is coarse, and drying must continue for ≥12 h; this often produces overly dark material with uncertain moisture content (Letner & Kajtar, 2018). Moisture content can be used as the main parameter in determining the quality of dried earthworm products (Kröncke et al., 2019). Moisture content is an important parameter in dry matter because it greatly affects the activity of microorganisms that can cause spoilage (Zambrano et al., 2019). Decay bacteria can grow well at a moisture content of 46%–16% (Uyeh et al., 2021). Dried earthworms must have a moisture content below the point of growth of these spoilage bacteria to maintain their quality during shipping and storage. The moisture content test is commonly analyzed with a gravimetric test. The standard gravimetric test is time-consuming and destructive: a sample is weighed repeatedly until mass stabilizes at 60 °C, then re-dried at 105 °C for 3 h to obtain the residual water mass (Carneiro et al., 2018). This two-stage protocol can take half a day and may denature heat-labile proteins, making it impractical for in-process control. This analysis is inefficient because it must be carried out in every production process, and the protein content is likely to be damaged above 100 °C (Suryana et al., 2022).

Accordingly, a rapid and non-destructive alternative is required. Machine-vision techniques offer real-time moisture estimation because the color and surface texture of biomaterials changes predictably with water loss (Prilianti et al., 2021). Sandra et al. (2021) demonstrated that color-texture features coupled with image analysis describe moisture dynamics in cassava chips during drying. Artificial neural networks (ANNs) further enhance predictive performance when suitably optimized (Damayanti et al., 2021; Hendrawan et al., 2019, 2023; Rohmatulloh et al., 2022). Prior work using ANN and feature selection achieved an $R^2 \approx 0.9$ for cassava-chip moisture prediction (Hendrawan et al., 2018) and markedly improved coffee bean quality estimation (Hendrawan, Widyaningtyas et al., 2019).

Building on these findings, the present study develops a machine-vision system that combines color and grey-level co-occurrence-matrix (GLCM) texture descriptors, ranks them using the Waikato Environment for Knowledge Analysis (WEKA) feature-selection toolkit (Hall et al., 2009), and feeds the optimal subset into an ANN to classify *E. eugeniae* into wet (>40%), semi-dry (40%–12%), and dry (<12%) states. The purpose of this study

was to classify the moisture content of earthworms using machine vision and ANN during the drying process. This study developed digital image analysis, which included color and texture with ANN models to predict the moisture content of dried earthworms.

MATERIAL AND METHODS

Samples of fresh earthworms were obtained from Malang City, East Java, Indonesia. The oven process and image data collection were carried out at the Laboratory of Biosystem Mechatronics, Faculty of Agricultural Technology, Universitas Brawijaya, Indonesia. The tools used in this research were as follows: a modified 400-watt Kirin oven with the addition of a Pt100 thermocouple temperature sensor with an Autonic TCN4S controller; a computer with Intel Core i3-4150 CPU @3.50GHz (4 CPUs) 10 GB RAM to run ANN programs; Canon DSLR 700D camera (EF 110 mm macro lens for capturing image data, effective pixel of 18 MP, CMOS sensor, sensor size of 22.3 × 14.9 mm); 4 LED spotlights 50W, 110-220V coated with PL Filter CPL 72 mm with an average light intensity of 1394 lux and lens distance to object 280 mm; a standard color card containing 24 colors (85 × 55 mm) used for color correction and white balance reference; and a digital scale (0.001 g) for gravimetric measurements. Prior to drying, worms were harvested, rinsed under running water, blanched for 10 s at 90 °C to stabilize tissue (Gunya et al., 2016), cooled, and cut to a length of 40 mm of earthworms from the head (Sivasubramaniam, 2021). Image acquisition inside the tray dryer is illustrated in Figure 1.

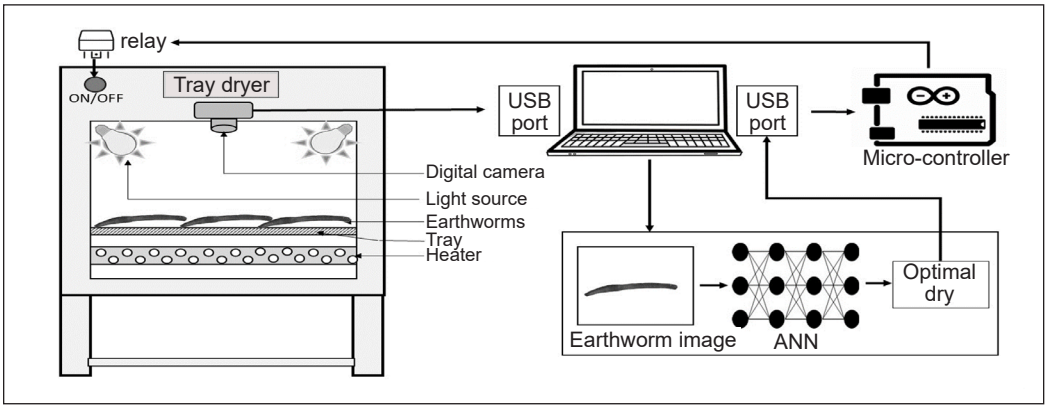

Figure 1. Earthworm drying machine model with moisture content monitoring system

Experimental Design

This study uses 450 earthworm images, which are divided into three classifications: i.e., dry (moisture content > 40%) of 150 images, semi-dry (moisture content between 40%–12%) of 150 images, and wet (< 12%) of 150 images as shown in Figure 2. The semi-dry class was an optimal moisture content condition for animal feed products; however, the storage

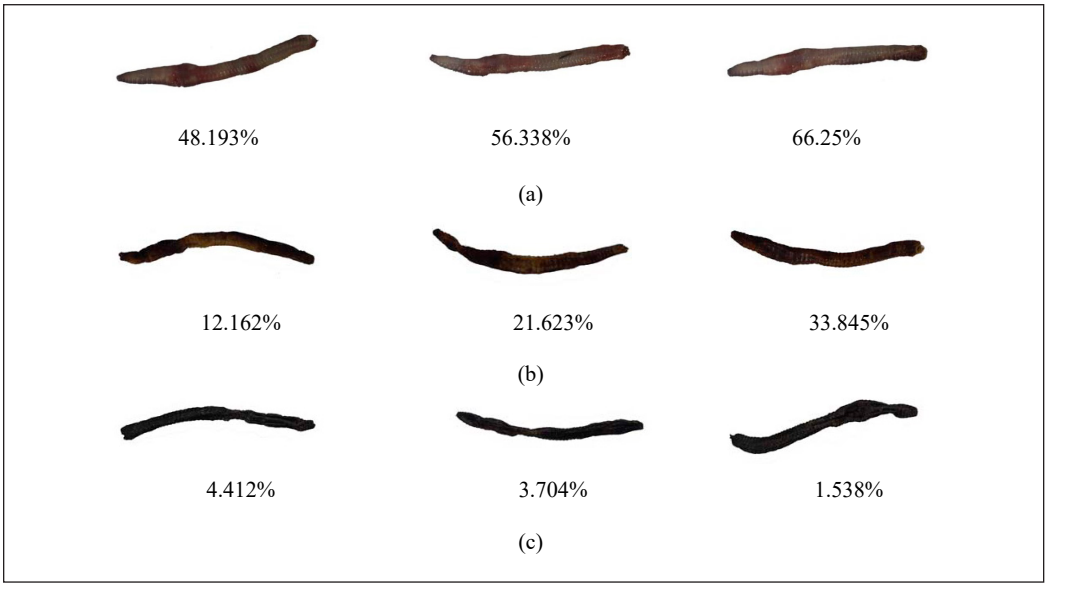

Figure 2. The appearance of dried earthworms in three types of moisture content categories: (a) Wet (moisture content >40%); (b) Semi-dry (moisture content 40%–12%); (c) Dry (moisture content <12%)

time was short, and the products could not be processed into flour. In the dry class, dried earthworms can be stored for a long time and can be processed into flour (Hamdan et al., 2021). The calculation of moisture content in this study used a wet basis (Antia et al., 2021; Chukwunonye et al., 2016).

Three independent drying runs were performed. Each run used 50 worm pieces placed on a perforated tray, with a total of 9 drying repetitions, resulting in 450 images being obtained. Images and masses were recorded simultaneously every 15 min for 2–3 hours at a temperature of 60 ºC. Immediately after each image capture, the tray was removed, weighed to obtain wet-basis mass, and returned to the dryer; thus, the gravimetric reference corresponds one-to-one with each image. Drying continued until equilibrium mass (< 12 % wb) was reached, followed by a 4 h post-dry at 105 °C to determine residual moisture for calibration.

Feature Selection

The image dimensions were changed to 451 × 300 pixels in BMP format. The extracted features were texture features and color features. Texture features are extracted using gray-level co-occurrence matrices (GLCM), with texture parameters such as contrast, correlation, and energy. This research also used color parameters, which were red-green-blue (RGB) and hue-saturation-value (HSV). The next process was feature selection, which functioned to reduce irrelevant data so that the identification process would be effective and efficient, resulting in higher accuracy. The Waikato Environment for Knowledge Analysis (WEKA)

toolkit (version 3.9.6; Hall et al., 2009) was employed. Four evaluators (Correlation, Gain Ratio, Relief F, and One-R) were combined with the Ranker search method to score and order features; the top-ranked subsets were forwarded to the classifiers. Image data generated by feature selection was then used as ANN input. In the learning process using an ANN, digital images were divided into two groups: 60% of the data were used in the training process (270 images), and 40% of the data were used in the validation process (180 images). ANN learning used back-propagation (Matlab, 2021a) with a goal MSE of 0.01, a learning rate of 0.1, a momentum of 0.5, and an epoch cap of 1000. This study used several variations of learning functions (traincgb, traincgf, traincgp, traingda, traingdm, traingdx, trainoss, trainr, trainrp, and trainscg) and activation functions (logsig, tansig, and purelin). The output variable was the moisture content of earthworms, consisting of three classes (wet, semi-dry, and dry). Sensitivity analysis was performed by varying the number of nodes (30 or 40), hidden layer (1 or 2), learning function variation, and activation function.

RESULTS AND DISCUSSIONS

Dried earthworms need about 2–3 hours at a temperature of 60 ºC to reach a moisture content below 12%. The average initial moisture content of dried earthworms was 79%. Then, in the first 15 minutes, it increased to 60.2% and continued to decrease by 21.1% at the 45th minute. At the 60th minute, the moisture content reached 13.6%. At 75 minutes, the average moisture content was 11.0%; at 90th minutes, the moisture content became 9.5%; and finally, at 105th and 120th minutes, the moisture content became 7.8% and 7.5%, respectively. The product experienced a reduction in moisture content to the equilibrium point, whereas in this study, at 120th minutes, there was no significant change in moisture content. Figure 2 shows the appearance of dried earthworms in three moisture content categories: dry, semi-dry, and wet. Earthworms with moisture content above 40% had brown skin color characteristics where the clitellum and segments of the earthworm can be seen, and the vessels inside the earthworm's body were also clearly visible. An example of an earthworm image at a moisture content above 40%, which was classified in the soak class, is shown in Figure 2a. Then, an example of a dried earthworm image from the first 15 minutes of drying is shown in Figure 2b. The dried earthworm in Figure 2b can be classified in the semi-dry class with a moisture content of 12%–40%. It had a dark brown color with a slightly faint clitellum, but the skin segments were still visible. The veins in the middle of the earthworm's body were still visible even though they were slightly blackened, approaching a brick-red color. An example of dried earthworms at 45th minutes of drying can be seen in Figure 2c. The dried earthworm in Figure 2c can be classified in the dry class. Dried earthworms in the dry class had a moisture content below 12% and had a characteristic dark brown color close to black. There were no reddish or brick-red marks. The part of the clitellum that was slightly wider becomes narrower. The black color of the earthworm's body was uneven, and there

were still brown parts. The line of the earthworm's veins was faint. The line of earthworm vessels was visible only in the brown part, while the black part at the head and bottom ends of the earthworm was not clearly visible.

Based on the drying data in Figure 3, the longer the drying time, the smaller the moisture content. The moisture content decreased significantly from 15 minutes to 120 minutes of drying, and the value equilibrated at 105 to 120 minutes of drying with a moisture content range of 2.5%–10%.

The results of feature selection are shown in Table 1. Feature selection uses WEKA software with several attributes, namely one ratio attribute, correlation attribute, relief F, and gain ratio attribute, with a ranker scoring method. Based on feature selection, image features were sorted starting from the largest weight. ANN modeling was performed based on the ranking of feature selection, as shown in Table 2 so that the mean squared error (MSE) training and validation MSE values were obtained. The lowest validation MSE value, based on the ANN modeling, was achieved for features ranked 1-8 when using the gain ratio attribute, with a training MSE value of 0.0683 and a validation MSE value of 0.087045. Therefore, the color and textural features used as input to the ANN modeling in this study were 8 image features: saturation, value, green, blue, hue, red, correlation, energy, and contrast.

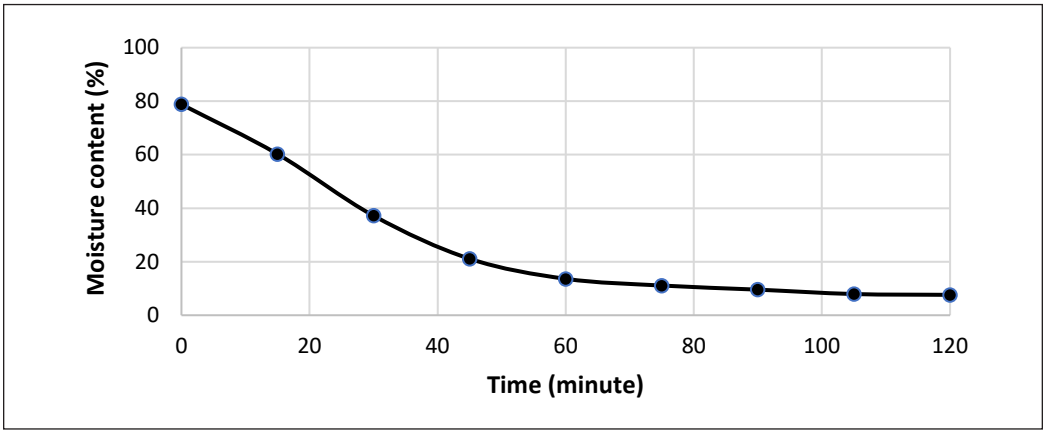

Figure 3. Relationship graph of moisture content to drying time

Table 1
Feature selection using WEKA

No	Attribute Evaluator	Search Method	Feature	Weight	Rank
1	Gain Ratio Attribute Evaluator	Ranker	Saturation	0.996	1
			Value	0.996	2
			Green	0.996	3
			Blue	0.996	4
			hue	0.996	5

Table 1 *(continue)*

No	Attribute Evaluator	Search Method	Feature	Weight	Rank
			Red	0.996	6
			Correlation	0.996	7
			Energy	0.996	8
			Contrast	0.994	9
2	One R Attribute Evaluator	Ranker	Energy	0.667	1
			Hue	0.667	2
			Green	0.667	3
			Blue	0.667	4
			Saturation	0.667	5
			Correlation	0.667	6
			Value	0.667	7
			Contrast	0.667	8
			Red	0.667	9
3	Correlation Attribute Evaluator	Ranker	Contrast	0.00465	1
			Energy	0.00461	2
			Red	0.0046	3
			Correlation	0.0046	4
			Hue	0.0046	5
			Value	0.00459	6
			Blue	0.00459	7
			Green	0.00459	8
			Saturation	0.00459	9
4	Relief F Attribute Evaluator	Ranker	Saturation	0.94	1
			Blue	0.94	2
			Value	0.94	3
			Green	0.94	4
			Correlation	0.94	5
			Hue	0.94	6
			Red	0.94	7
			Energy	0.94	8
			Contrast	0.94	9

Table 2
ANN modeling results with input from feature selection

No	Attribute Evaluator	Search Method	ANN Input	Training MSE	Validation MSE
1	Gain Ratio Attribute Evaluator	Ranker	feature rank 1–2	0.1900	0.20647
			feature rank 1–3	0.1233	0.1718
			feature rank 1–4	0.0700	0.11165
			feature rank 1–5	0.0850	0.13269
			feature rank 1–6	0.0933	0.099578
			feature rank 1–7	0.0733	0.13527

Table 2 *(continue)*

No	Attribute Evaluator	Search Method	ANN Input	Training MSE	Validation MSE
			feature rank 1–8	**0.0683**	**0.087045**
			feature rank 1–9	0.0950	0.14473
2	One R Attribute Evaluator	Ranker	feature rank 1–2	0.3100	0.41313
			feature rank 1–3	0.2000	0.3358
			feature rank 1–4	0.1050	0.13558
			feature rank 1–5	0.0767	0.13222
			feature rank 1–6	0.0950	0.10087
			feature rank 1–7	0.0633	0.11232
			feature rank 1–8	0.1033	0.10517
			feature rank 1–9	0.0783	0.14958
3	Correlation Attribute Evaluator	Ranker	feature rank 1–2	0.3367	0.38067
			feature rank 1–3	0.3150	0.43197
			feature rank 1–4	0.3117	0.37057
			feature rank 1–5	0.2317	0.36141
			feature rank 1–6	0.2600	0.28416
			feature rank 1–7	0.1083	0.14317
			feature rank 1–8	0.0800	0.098798
			feature rank 1–9	0.0700	0.15072
4	Relief F Attribute Evaluator	Ranker	feature rank 1–2	0.1767	0.16878
			feature rank 1–3	0.1500	0.21119
			feature rank 1–4	0.0817	0.10963
			feature rank 1–5	0.0883	0.13556
			feature rank 1–6	0.0883	0.11003
			feature rank 1–7	0.0917	0.13928
			feature rank 1–8	0.0583	0.08956
			feature rank 1–9	0.0950	0.13446

In industrial practice, the three moisture bands are intentionally broad; a worm batch needs only to fall below 12% wb to be safely milled into flour, while 40%–12% represents a still-pliable product used directly as feed. Thus, a precise percentage prediction is unnecessary; rapid band classification suffices to trigger dryer shut-off or progression to the next process stage, saving energy and preserving color. The small overlap observed in single-feature distributions (Figure 4) reflects natural color variability among individual worms but is readily resolved by the multivariate ANN. Based on the results, the standard deviation value in the dry classification was 0.080619, semi-dry 0.112439, and wet 0.074115. The average saturation value in the dry classification was 0.26, semi-dry 0.19, and wet 0.24, indicating that the saturation value in the dry classification was greater when compared to the semi-dry and wet classifications. Value is part of the HSV color that describes the proportion of color brightness levels.

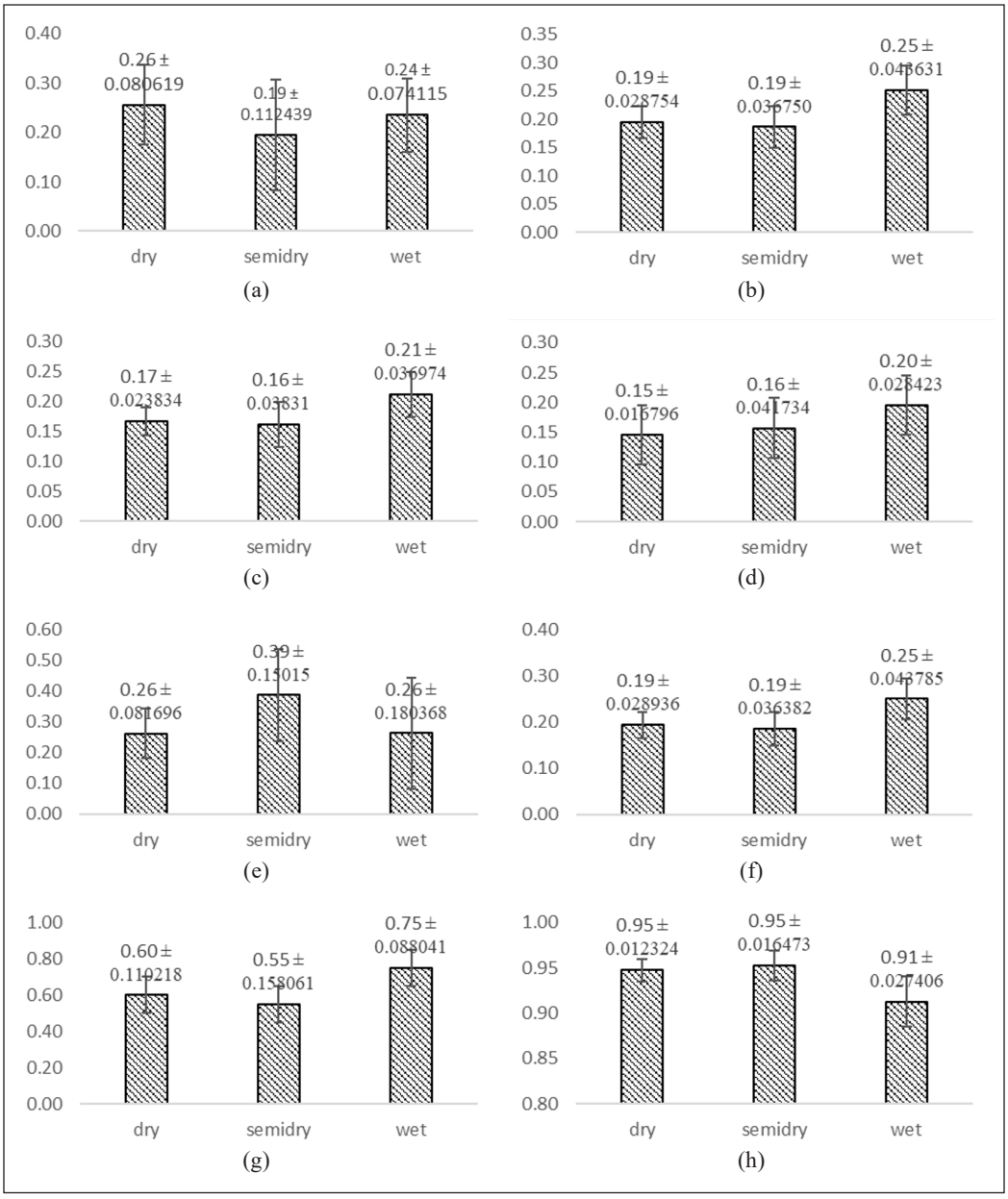

Figure 4. Relationship between moisture content and image features: (a) normalized saturation; (b) normalized value; (c) normalized green; (d) normalized blue; (e) normalized hue; (f) normalized red; (g) normalized correlation; and (h) normalized energy

The standard deviation value in the dry classification was 0.028754, semi-dry 0.036750, and wet 0.043631. The average value in the dry classification was 0.19, semi-dry 0.19, and wet 0.25, indicating that the value in the dry and semi-dry classifications was smaller when compared to the wet classification. Green is part of the RGB color space, which shows the

greenness of the object. The standard deviation value in the dry classification was 0.023834, semi-dry 0.03831, and wet 0.036974. The average green value in the dry classification was 0.17, semi-dry 0.16, and wet 0.21, indicating that the green value in the dry and semi-dry classifications was smaller when compared to the wet classification. Blue is part of the RGB color space, which shows the blueness of the object. The standard deviation value in the dry classification was 0.016796, semi-dry 0.041734, and wet 0.028432.

The average value of blue in the dry classification was 0.15, semi-dry 0.16, and wet 0.20, indicating that the blue value in the dry and semi-dry classifications was smaller when compared to the wet classification. Hue is part of HSV, which is defined as the color reflected or transmitted by the object. The standard deviation value in the dry classification was 0.081696, semi-dry 0.15015, and wet 0.180368. The average hue value in the dry classification was 0.26, semi-dry 0.39, and wet 0.26, indicating that the hue value in the dry and semi-dry classifications was close to 1 because in this classification, visually, the color of dry worms was dark brown, close to black. Red is part of the RGB color space, which shows the level of redness of the object.

Based on the research results, the standard deviation value in the dry classification was 0.028936, semi-dry 0.036382, and wet 0.043785. The average red value in the dry classification was 0.19, semi-dry 0.19, and wet 0.25, indicating that the red value in the dry and semi-dry classifications was smaller when compared to the wet classification. Correlation is part of textural analysis to measure how correlated pixels are with other pixels in the whole image. The standard deviation value in the dry classification was 0.110218, semi-dry 0.158061, and wet 0.088041. The average correlation value in the dry classification was 0.60, semi-dry 0.55, and wet 0.75. The energy feature is part of the textural analysis to measure the level of texture uniformity or repetition of pixel pairs. The standard deviation value in the dry classification was 0.012324, semi-dry 0.016473, and wet 0.027406. The average energy value in the dry classification was 0.95, semi-dry 0.95, and wet 0.91. However, from the eight graphs, single individual features cannot be used for classifying dry earthworm moisture content because, based on the standard deviation data, there is still an overlap between one class and another. So, the use of ANN models involving multiple variables is needed for moisture content classification. The use of multiple variables as input to the ANN model can improve classification performance.

Sensitivity analysis in ANN was used to select the right hyperparameter so that the ANN model could be optimized with high accuracy. Table 3 shows the results of trial and error on the learning function. The learning functions used were traincgb, traincgf, traincgp, traind, trainda, traingdm, traingdx, trainlm, trainnoss, trainrp, and trainscg. This study uses variations of hidden layers 30 and 40 at a learning rate parameter of 0.1, momentum of 0.5, maximum epoch of 1000, and error tolerance of 0.01. Based on the results, the lowest validation MSE value was trainlm of 0.087045 with a training MSE value of 0.0683, R

training of 0.95023, and R validation of 0.92417. Table 4 shows the activation functions used in this study, i.e., tansig, logsig, and purelin. The lowest validation MSE result was obtained when using the logsig activation function in the hidden layer and purelin in the output layer. MSE validation was 0.087045, MSE training was 0.0683, R validation was 0.92417, and R training was 0.95023.

Table 5 shows the trial and error on ANN structure using a learning rate of 0.1 and momentum of 0.5. Trials and errors were conducted to find the optimal hidden neuron

Table 3
Trial and error on learning function

No	Learning function	R Training	R Validation	MSE Training	MSE Validation
1	Traincgb *(Conjugate Gradient BP with Powell – Beale Restart)*	0.91743	0.90795	0.1017	0.10472
2	Traincgf *(Conjugate BP with Fletcher Reeves Update)*	0.8564	0.83575	0.1950	0.18009
3	Traincgp *(Conjugate Gradient BP with Polak Ribiere Update)*	0.90475	0.8984	0.1233	0.11395
4	Traingd (*Gradient Descent BP*)	0.17559	0.26246	1.2483	1.6844
5	Traingda (*Gradient Descent with Adaptive Learning Rate BP*)	0.70683	0.72575	0.3250	0.28115
6	Traingdm (*Gradient Descent with momentum Adaptive Learning*)	0.88174	0.86137	0.1633	0.15542
7	Traingdx (*Gradient Descent with momentum Adaptive Learning*)	0.74743	0.74934	0.2983	0.26591
8	Trainlm **(***Lavenberg Marquadt BP***)**	**0.95023**	**0.92417**	**0.0683**	**0.087045**
9	Trainoss (*One Step Secant BP*)	0.87884	0.85749	0.1717	0.15822
10	Trainrp (*Resilient BP*)	0.93682	0.91723	0.0817	0.093759
11	Trainscg Scaled (*Conjugate Gradient BP*)	0.84967	0.82758	0.2133	0.18772

Table 4
Trial and error on the activation function

Learning function	Activation function			R Training	R Validation	MSE Training	MSE Validation
	Hidden layer 1	Hidden layer 2	Hidden layer 3				
Trainlm	Tansig	Tansig	Purelin	0.94796	0.91402	0.0667	0.097982
	Tansig	Tansig	Tansig	0.95957	0.91153	0.0683	0.10217
	Tansig	Tansig	Logsig	0.83925	0.78914	0.2933	0.31569
	Logsig	**Logsig**	**Purelin**	**0.95023**	**0.92417**	**0.0683**	**0.087045**
	Logsig	Logsig	Tansig	0.95392	0.9244	0.0750	0.088424
	Logsig	Logsig	Logsig	0.83641	0.8202	0.3017	0.30992

Table 5
Trial and error on ANN structure

ANN Structure	R Training	R Validation	MSE Training	MSE Validation
8-30-1	0.9549	0.92766	0.0733	0.097926
8-40-1	0.94893	0.92355	0.0733	0.091087
8-30-30-1	0.95081	0.91226	0.0833	0.11343
8-30-40-1	0.94522	0.8721	0.0800	0.14774
8-40-40-1	0.95294	0.90299	0.0700	0.12699
8-30-2	0.94985	0.92423	0.0683	0.096321
8-40-2	0.95438	0.90485	0.0767	0.11266
8-30-30-2	0.93096	0.90348	0.1017	0.12542
8-30-40-2	0.95933	0.87961	0.0683	0.1414
8-40-40-2	0.91691	0.91563	0.1117	0.11479
8-30-3	0.9432	0.89883	0.0833	0.11639
8-40-3	**0.95309**	**0.92962**	**0.0733**	**0.086058**
8-30-30-3	0.93983	0.9223	0.0750	0.10842
8-30-40-3	0.95205	0.92244	0.0717	0.099762
8-40-40-3	0.95512	0.9121	0.0617	0.11349

and hidden neuron parameters. The smallest validation MSE value was 0.086058, the training MSE was 0.0733, the training R-value was 0.95309, and the validation R was 0.92962. The gap between training (0.073) and validation (0.086) MSE is modest (≈ 0.013). This difference stems mainly from a slight class imbalance in the validation set, not from over-fitting. The learning performance graph for ANN modeling is shown in Figure 5. Based on the graph, the error value decreases as the epoch value increases. Epoch stops at 19 with a validation MSE of 0.086058. The training correlation coefficient value was 0.95309, and the validation correlation coefficient value was 0.92962, as shown in Figure 6. The best ANN architecture model recommended in this study is one with 8 inputs, 40 nodes in the hidden layer, and 3 outputs (8-40-3), as shown in Figure 7. The input layer consists of 8 features: saturation, value, green, blue, hue, red, correlation, and energy. The 3 outputs were levels of dry earthworm moisture content, namely dry, semi-dry, and wet.

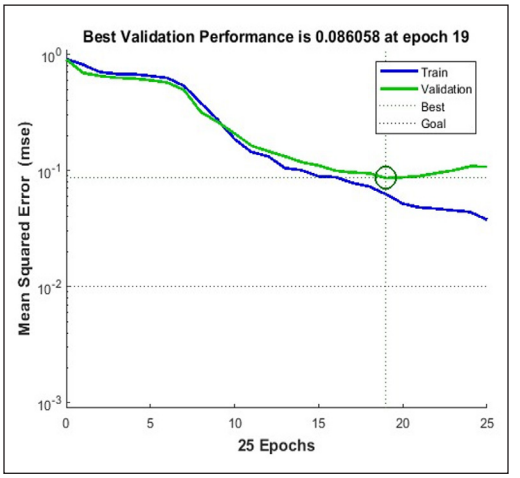

Figure 5. Best training and validation performance of the ANN model

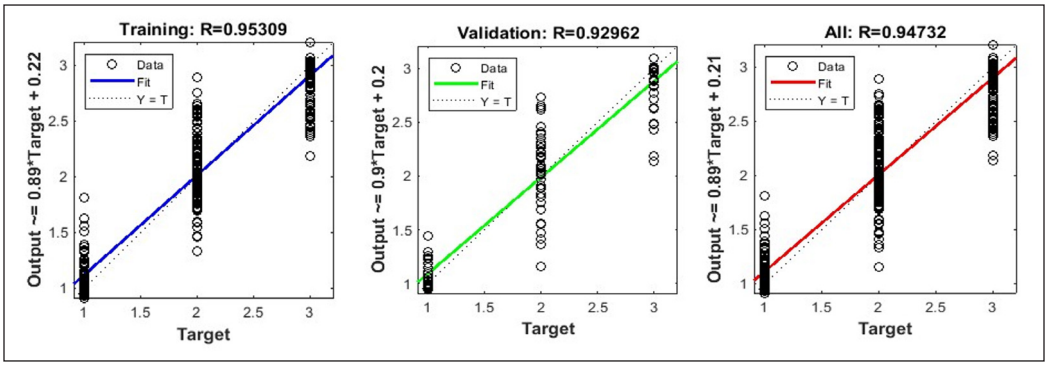

Figure 6. The correlation coefficient between the target and predicted data

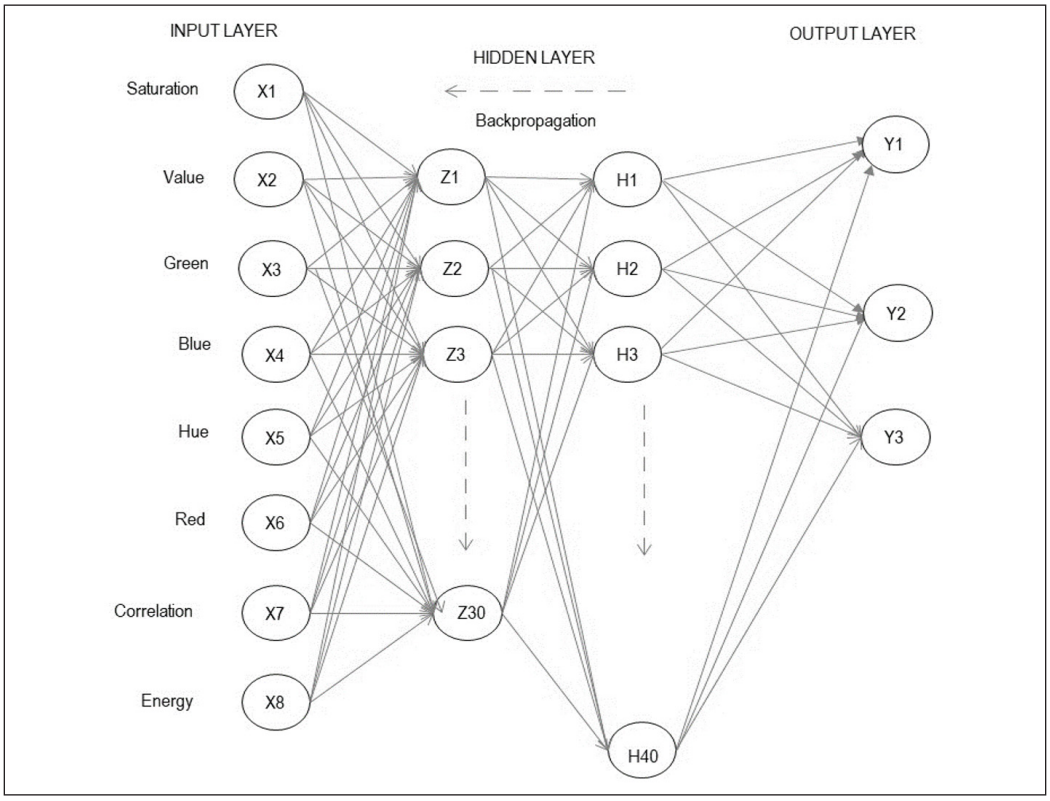

Figure 7. ANN structure for dry earthworm classification

The vision-ANN system can be embedded in line with low-cost cameras and a microcontroller running the 8-40-3 network (≈ 2 kB weight matrix), enabling real-time moisture feedback without destructive sampling. Future studies should extend the approach to other edible insect species and explore hyperspectral imaging to tighten the semi-dry band for premium products.

CONCLUSION

This study demonstrates that a compact machine-vision platform, coupled with supervised learning, can provide rapid, non-destructive moisture control during *Eudrilus eugeniae* drying. After WEKA-based feature ranking, eight color/texture descriptors (S, V, G, B, H, R, correlation, energy) were retained and fed to an 8-40-3 feed-forward ANN, with MSE training of 0.0733 and MSE validation of 0.086058 (R = 0.95309 and 0.92962, respectively). The three moisture bands used (>40%, 40%–12%, <12% wb) match industrial decision points, allowing the classifier to trigger dryer shut-off or downstream processing in real time. This avoids the 3-h gravimetric assay and minimizes energy use and color darkening. Because the final network contains only ~2 kB of weight, it can be embedded in low-cost edge hardware. Future work should extend the model to other edible insect species, explore hyperspectral or NIR imaging to refine the semi-dry band for premium feed products and integrate the vision sensor with closed-loop heater control to create a fully automated, quality-driven drying line.

ACKNOWLEDGEMENTS

The authors wish to acknowledge support from the Department of Biosystems Engineering, Faculty of Agricultural Technology, University of Brawijaya, for the assistance given during the research. This study was funded by the Faculty of Agricultural Technology, University of Brawijaya, and the Ministry of Research, Technology, and Higher Education of the Republic of Indonesia.

REFERENCES

Antia, O., Olosunde, W.A., & Antia, E.O. (2021). Application of basic drying theory to determine drying mass constants of selected seafoods. *Global Journal of Engineering and Technology Advances*, *7*(1), 137-143. https://doi.org/10.30574/gjeta.2021.7.1.0062

Antonova, E., Titor, I., Pashkova, I., & Stom, D. (2021). Vermiculture as a source of animal protein. *Journal of FARBA*, *254*, Article 8006. https://doi.org/10.1051/e3sconf/202125408006

Azmi, N., Hashim, F., Hashim, D., Halimoon, N., & Majid, N. (2014). Anti-elastase, anti-tyrosinase and matrix metalloproteinase-1 inhibitory activity of earthworm extracts as potential new anti-aging agent. *Asian Pacific Journal of Tropical Biomedicine*, *4*(1), 248-352. https://doi.org/10.12980/APJTB.4.2014C1166

Carneiro, J., Nogueira, R., Martins, M., Valladao, D., & Pires, E. (2018). The oven-drying method for determination of water content in Brazil nut. *Bioscience Journal, 34*(3), 595-602.

Chukwunonye, C., Naemeka, N., Chijioke, O., & Obiora, N. (2016). Thin layer drying modelling for some selected Nigerian produce: A review. *American Journal of Food Science and Nutrition Research*, *3*(1), 1-15.

Damayanti, R., Rachma, N., Al Riza, D. F., & Hendrawan, Y. (2021). The prediction of chlorophyll content in african leaves (Vernonia amygdalina del.) using flatbed scanner and optimised artificial neural network. *Pertanika Journal of Science & Technology*, *29*(4), 2509-2530. https://doi.org/10.47836/pjst.29.4.15

Deepika, B., Leela, V., & Valavan, S. (2018). Nutritional analysis of earthworm meal (Eudrilus eugeniae). *International Journal of Chemical Studies*, *6*(6), 1536-1539.

Fortu Jr, A. F., Lozada, E. P., Peralta, E. K., & Suministrado, D. C. (2019). Drying kinetics and anticoagulant activity of microwave-vacuum, dehumidified-air and freeze-dried African night crawler (Eudrilus eugeniae kinberg). *IOP Conference Series: Earth and Environmental Science*, *542*(1), Article 012004. https://doi.org/10.1088/1755-1315/542/1/012004

Gunya, B., Masika, P. J., & Muchenje, V. (2016). Nutrient composition and fatty acid profiles of oven-dried and freeze-dried earthworm Eisenia foetida. *Journal of Food and Nutrition Research*, *4*(6), 343-348.

Hall, M., Frank, E., Holmes, G., Pfahringer, B., Reutemann, P., & Witten, I. H. (2009). The WEKA data mining software: An update. *SIGKDD Explorations, 11*(1), 10–18. https://doi.org/10.1145/1656274.1656278

Hamdan, M., Sulaiman, N., Amin, N., & Adam, F. (2021). Moisture content and mechanical properties reduction of hard capsule upon prolong drying process. *IOP Conference Series: Materials Science and Engineering*, *1092*(1), Article 012057. https://doi.org/10.1088/1757-899X/1092/1/012057

Hendrawan, Y., Amini, A., Maharani, D. M., & Sutan, S. M. (2019). Intelligent non-invasive sensing method in identifying coconut (Coco nucifera var. Ebunea) ripeness using computer vision and artificial neural network. *Pertanika Journal of Science & Technology*, *27*(3), 1317-1339.

Hendrawan, Y., Widyaningtyas, S., & Sucipto, S. (2019). Computer vision for purity, phenol, and pH detection of Luwak coffee green bean. *Telkomnika*, *7*(6), 3073-3085. http://doi.org/10.12928/telkomnika.v17i6.12689

Hendrawan, Y., Hawa, L. C., & Damayanti, R., (2018). Fish swarm intelligent to optimize real time monitoring of chips drying using machine vision. *IOP Conference Series: Earth and Environmental Science*, *141*(1), Article 012020. https://doi.org/10.1088/1755-1315/131/1/012020

Hendrawan, Y., Perkasa, T. E., Prasetyo, J., Al-Riza, D. F., Damayanti, R., Hermanto, M. B., & Sandra, S. (2023). Moringa leaf chlorophyll content measurement system based on optimized artificial neural network. *Advances in Food Science, Sustainable Agriculture and Agroindustrial Engineering*, *Special Issue*, 1-10.

Kröncke, N., Grebenteuch, S., Keil, C., Demtroder, S., Kroh, L., Thünemann, A., Benning, R., & Haase, H. (2019). Effect of different drying methods on nutrient quality of the yellow mealworm (Tenebrio molitor L.). *Insects, 10*(4), Article 84. https://doi.org/10.3390/insects10040084

Letner, A., & Kajtar, L. (2018). Thermal environment assessment of gas stove surroundings. *Slovak Journal of Civil Engineering*, *26*(4), 26-31. https://doi.org/10.2478/sjce-2018-0025

Mohanta, K. N., Subramanian, S., & Sidweerayya, V. (2016). Potential of earthworm (Eisenia foetida) as dietary protein source for rohu (Labeo rohita) advanced fry. *Cogent Food & Agriculture*, *2*(1), Article 1138594. https://doi.org/10.1080/23311932.2016.1138594

Musyoka, S., Liti, D., Ogello, E., & Waidbacher, H. (2019). Utilization of the earthworm, Eisenia fetida (Savigny, 1826) as an alternative protein source in fish feeds processing: A review. *Aquaculture Research, 50*(9), 2301-2315. https://doi.org/10.1111/are.14091

Prilianti, K. R., Anam, S., Brotosudarmo, T., & Suryanto, A. (2021). Non-destructive photosynthetic pigments prediction using multispectral imagery and 2D-CNN. *International Journal of Computing*, *20*(3), 391-399.

Rohmatulloh, B., Lee, M. N., Alatiffa, R. M., Megatama, R. P., Napitupulu, R. A. C., Hendrawan, Y., & Lutfi, M. (2022). Non-destructive prediction of piperine in Javanese chilli (Piper retrofractum vahl) based on color and texture analysis using artificial neural network. *IOP Conference Series: Earth and Environmental Science*, *1083*(1), Article 012040. https://doi.org/10.1088/1755-1315/1083/1/012040

Sandra, S., Hendrawan, Y., Damayanti, R., & Perdana, L. P. R. (2021). Analysis of cassava chip image characterization during drying process. *IOP Conference Series: Earth and Environmental Science*, *924*(1), Article 012016. https://doi.org/10.1088/1755-1315/924/1/012016

Sivasubramaniam, S. (2021). The earthworm eudrilus eugeniae: A model organism for regenerative biology. *HSOA Journal of Genetics & Genomic Science*, *6*, Article 023. https://doi.org/10.24966/GGS-2485/100023

Sun, Z. (2015). Earthworm as a biopharmaceutical: From traditional to precise. *European Journal of Biomedical Research, 1*(2), 28-35.

Suryana, A. L., Rosiana, N. M., & Olivia, Z. (2022). Effect of drying method on the chemical properties of local soy flour. *IOP Conference Series: Earth and Environmental Science*, *980*, Article 12030. https://doi.org/10.1088/1755-1315/980/1/012030

Uyeh, D. D., Kim, J., Lohumi, S., Park, T., Cho, B. K., Woo, S., Lee, W. S., & Ha, Y. (2021). Rapid and nondestructive monitoring of moisture content in livestock feed using a global hyperspectral model. *Animals*, *11*(5), Article 1299. https://doi.org/10.3390/ani11051299

Wu, J., Ren, Z., Zhang, C., Motelica-Heino, M., Deng, T., Wang, H., & Dai, J. (2019). Effects of soil acid stress on the survival, growth, reproduction, antioxidant enzyme activities, and protein contents in earthworm (Eisenia fetida). *Environmental Science and Pollution Research*, *27*(27), 33419–33428. https://doi.org/10.1007/s11356-019-04643-y

Zambrano, M. V., Dutta, B., Mercer, D. G., Heather, M. L., & Touchie, M. F. (2019). Assessment of moisture content measurement methods of dried food products in small-scale operations in developing countries: A review. *Trends in Food Science*, *88*(5), 484-496. https://doi.org/10.1016/j.tifs.2019.04.006

Pertanika J. Sci. & Technol. 33 (S5): 59 - 74 (2025)

PERTANIKA JOURNALS

SCIENCE & TECHNOLOGY

Journal homepage: http://www.pertanika.upm.edu.my/

Liquid Biphasic Flotation System (LBFS) for Separation of Protein from *Azolla pinnata*

Kiishhen Kobbin[1], Angela Paul Peter[3], Mohd Zuhair Mohd Nor[1]* and Pau Loke Show[2]

[1]Department of Process and Food Engineering, Faculty of Engineering, Universiti Putra Malaysia, 43400 UPM Serdang, Selangor, Malaysia.
[2]Department of Chemical Engineering, Khalifa University, P.O. Box 127788, Abu Dhabi, United Arab Emirates
[3]School of Engineering, Taylor's University Lakeside Campus, 47500 Subang Jaya, Selangor, Malaysia

ABSTRACT

The demand for plant-based protein has surged as consumers nowadays are highly conscious about their daily intake; thus, this has driven extensive research on plant-based protein. Industries are now focusing on minimal operational costs while being environmentally friendly. This project specifically targets the extraction of protein from *Azolla pinnata* using a liquid biphasic flotation system (LBFS). LBFS is a promising extraction method incorporating microbubbles to enhance protein separation efficiency in liquid-liquid extraction. The LBFS processing parameters are the type of solvent (ethanol and 2-propanol), solvent concentration (75-100%), salt concentration (200-500 g/L), biomass load (100-400 mg), and flotation time (5-15 min). The study's findings revealed that 2-propanol, with its polarity, yielded the highest protein recovery and separation efficiency. Increasing the solvent concentration led to a higher yield of extracted protein due to the greater number of hydroxyl groups per unit volume. Higher salt concentrations aid the separation process by enhancing hydrophobic contact between the protein and water. A higher biomass load resulted in greater protein recovery, while a longer flotation duration improved protein extraction due to lower particle surface tension. However, vigorous flotation conditions could lead to protein degradation. Based on the study's optimisation, the LBFS conditions that yielded the best results were 80% 2-propanol solvent, 400 g/L salt concentration, 300 mg biomass load, and a flotation time of 10 min. These conditions resulted in a protein yield recovery of 78.19% ±4.31 and a protein separation efficiency of

ARTICLE INFO

Article history:
Received: 13 February 2024
Accepted: 28 May 2025
Published: 10 July 2025

DOI: https://doi.org/10.47836/pjst.33.S5.04

E-mail address:
kiishhen@gmail.com (Kiishhen Kobbin)
angela.peter@taylors.edu.my (Angela Paul Peter)
zuhair@upm.edu.my (Mohd Zuhair Mohd Nor)
pauloke.show@ku.ac.ae (Pau Loke Show)
*Corresponding author

e-ISSN: 2231-8526

79.39% ±2.80. This method provides a high protein yield recovery and separation efficiency for the extraction of biomolecules.

Keywords: Azolla pinnata, liquid biphasic flotation system, liquid-liquid extraction, plant-based protein, protein separation.

INTRODUCTION

Azolla pinnata, a free-floating fern from the *Azollaceae* family, is a rich source of protein that contains practically all essential amino acids, along with numerous important minerals (Cherryl et al., 2014). Figure 1 shows the image of an *Azolla pinnata* plant. It is commonly used as a feed ingredient in the poultry industry due to its high protein content of 25%–30% and its ease of cultivation (Swain et al., 2022). Plant-derived proteins are currently undergoing extensive research, as consumers nowadays are highly health-conscious about their daily intake. The growing global demand for plant-based protein is driven by the increasing number of people who are more mindful of their health in the post-COVID-19 pandemic. According to the World Health Organization (WHO), cardiovascular disease accounts for 31% of deaths worldwide. To reduce the number of deaths caused by this disease, an alternative protein source is necessary, and plant-based protein is an optimal choice, as it contains lower levels of saturated fatty acids compared to animal-based protein (Zhubi-Bakija et al., 2021). Moreover, *Azolla pinnata* contains up to 18 amino acids, of which glutamic acid makes up to 12.6% and glutamic acid is known to reduce the risk of cardiovascular diseases by lowering blood pressure, thus reducing the risk factors (Refaey et al., 2023).

Plant-based protein sources that are readily available in the market include soybean, quinoa, chickpea, rice, beans, and chia seeds (Darmalinggam & Kaliannan, 2020). In Malaysia, up to 90% of soybeans are imported from various countries to obtain plant-based protein (AgFlow, 2023). The abundant protein content found in *Azolla pinnata* presents a promising alternative source of protein for various industries, including the food and pharmaceutical sectors. It can be utilised to develop vaccines and produce plant-based, protein-based foods. Malaysia, being a tropical country with ample resources of *Azolla pinnata*, has

Figure 1. Shows the leaves of an *Azolla pinnata* plant

the potential to produce plant-based protein domestically instead of relying on imports, thus contributing to the country's economic development. Besides that, *Azolla pinnata* is able to grow in nitrogen-depleted areas, and it is also an effective nitrogen fixer due to the symbiont Anabaena azollae, which is present within the leaf cavities of the *Azolla pinnata* (Kaur et al., 2018).

Several widely used protein extraction processes include alkaline extraction-isoelectric precipitation, salt extraction-dialysis, membrane extraction, ultrasonic, and chromatography (Stone et al., 2015). The challenges encountered in the conventional extraction process are achieving high yield efficiency and managing the associated costs. Recent studies have demonstrated the promising nature of liquid-liquid extraction methods in achieving high yields at a cost-effective rate. This includes a novel technology known as the liquid biphasic flotation system (LBFS), which offers several advantages in solving complex processes, reducing time consumption, and minimising energy input during the extraction process. LBFS is a developing and rapid extraction process characterised by high-yield efficiency and cost-effectiveness (Saw et al., 2020). Its purification and separation capabilities are excellent due to low interfacial tension, which prevents the denaturation of biological activities (Asenjo & Andrews, 2012). Previous studies have reported successful protein extraction using liquid biphasic systems from *Persicaria tenulla* leaf (Saw et al., 2020), microalgae (Sankaran et al., 2018), and *Chlorella vulgaris* (Koyande et al., 2019). However, no documentation exists regarding using the same extraction process for separating proteins from *Azolla pinnata*. Therefore, this study aims to optimise selected processing factors of the liquid biphasic flotation system (LBFS) to recover protein from *Azolla pinnata*.

MATERIALS AND METHODS

Materials

Ammonium sulphate ($(NH_4)_2SO_4$), 2-propanol (C_3H_8O), ethanol (C_2H_6O), Bradford reagent and a disposable 2.5 mL cuvette were purchased from R&M Chemicals (Selangor, Malaysia).

Sample Preparation

The matured *Azolla pinnata* plant in the cultivation tank was harvested. The plant is then dried in an oven at 40 °C overnight because the protein found in *Azolla pinnata* denatures at higher temperatures, and studies have shown that *Azolla pinnata* protein hydrolysates (AFPHs) are still present at a maximum temperature of 70 °C (Qoms et al., 2024). The dried plant is then ground and sieved to obtain uniform particle size. An airtight container was used to prevent air and moisture from clumping the powder, which can also cause chemical reactions that can cause degradation.

Liquid Biphasic Flotation System

The experiment began with the preparation of the chemical; for this research, ammonium sulphate and 2-propanol were used. These solvents were chosen due to the ability of the solvent to form separation phases, which aids in the extraction process based on the compounds' polarity (Cumplido et al., 2018). The initial state of the experiment was conducted with the preparation of 250 g/L of ammonium sulphate, which was dissolved with 20 mL of distilled water, 10 mL of 100% 2-propanol, and 300 mg of *Azolla pinnata* powder. This formulation was based on our preliminary experiments.

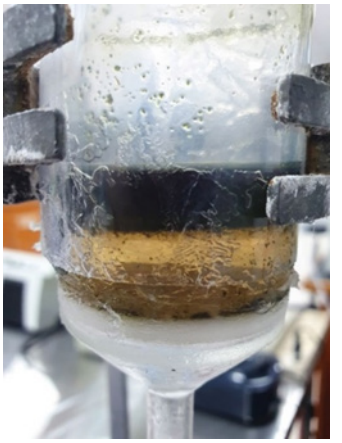

Figure 2. The separation layer of the solvent and salt solution of the liquid biphasic flotation system

First, the dissolved salt solution was poured into the sintered glass tube, followed by the solvent. Then, the Azolla pinnata powder was added last to the sintered glass tube. The sintered glass tube aids the mixture and separation of the solution as air passes through the sintered disk with G4 porosity ranging from 5 to 15 µm. After the mixture had settled, the air pump was turned on for 10 minutes for flotation to occur. Once the air pump was turned off, the separation layer could be seen instantaneously, as shown in Figure 2. The top layer and bottom layer would then be pipetted into separate 15 mL centrifuge tubes, and the volumes would be recorded. The separated layers were analysed further for the protein content.

Protein Assay

The concentration of protein obtained was determined through the Bradford reagent method (Saw et al., 2020). The Bradford method is a rapid, simple and refined approach that precisely measures the protein concentration (Kielkopf et al., 2020). Within a cuvette, 0.25 mL of the extracted protein sample was mixed with 2.5 mL of the Bradford reagent. The mixture was then stirred. After 10 min of homogenisation, the absorbance reading was recorded using the UV-Vis spectrophotometer set at 595 nm. The obtained absorbance reading was then converted to a protein concentration using a standard calibration curve established using a standard protein, specifically bovine serum albumin (BSA). This curve determined the relationship between the absorbance reading and the protein concentration. The findings were reported using a mean value calculated from measurements replicated four times (Saw et al., 2020).

Determination of Separation Efficiency and Recovery Yield

The percentage of protein that was successfully extracted in the solvent phase is referred to as the separation efficiency (E) of the top phase. The derived estimated efficiency before and after flotation of the process between the protein concentration of the bottom phase and the top phase was analysed using Equation 1.

$$E = \left(\frac{C_B - C_{Bi}}{C_{Bi}}\right) \times 100\% \quad [1]$$

where C_B stands for the concentration of protein in the bottom phase after flotation, and C_{Bi} stands for the concentration of protein in the bottom phase before flotation. The E value gives an indication of the amount of protein that has been effectively extracted from the alcohol-rich top phase (Saw et al., 2020).

The application of Equation 2 was used to determine the overall recovery yield (R) of protein. C_T resembles the protein concentration that is recovered in the top phase, whereas V_T volume is in the top phase. The recovery yield (R) was calculated by comparing the quantity that was acquired with the theoretical amount of protein contained in mg. This is done based on the protein concentration obtained from the top phase (Saw et al., 2020).

$$R(\%) = (C_T \, x \, V_T) / \, (Protein \; content \; based \; on \; proximate \; analysis) \times 100\% \quad [2]$$

Statistical Analysis

All measurements were performed in triplicate, and statistical analysis was conducted using Minitab version 18.1. A one-factor analysis of variance (ANOVA) was carried out using the Tukey LSD (least significant difference) method to compare the treatments. It is to assess any significant differences ($p<0.05$), and the results are displayed as mean ± standard error.

RESULT AND DISCUSSION

Proximate Analysis of *Azolla pinnata* Powder

The *Azolla pinnata* powder sample was subjected to proximate analysis, which yielded various data points, as shown in Table 1. The moisture content of the *Azolla pinnata* powder is 10.9%; this could be due to the nature of the plant, as it is grown in the water surrounding area; thus, moisture can still be retained in the cell wall of the plant, although the plant has been dried at 40 °C overnight. The fibrous properties of the *Azolla pinnata* plant, which have 27.5%, make it prone to the retention of moisture. The ash content of *Azolla pinnata* powder was 16.2%, followed by the total fat, 4.9%, protein, 26.1%, and carbohydrate, 41.9%, which contributes to 316 kcal of energy. The proximate analysis is

based on 100 g of *Azolla pinnata* powder. The data obtained are similar to those from the proximate analysis of *Azolla pinnata*, which was used as a feed supplement for poultry (Kumar et al., 2018).

Table 1
Proximate analysis of Azolla pinnata *powder*

Analysis	**Amount Per 100g of *Azolla pinnata* Powder**
Total Ash	16.2%
Moisture	10.9%
Total Fat	4.9%
Protein	26.1%
Carbohydrate	41.9%
Energy	316kcal
Crude Fiber	27.5%

The most important component that is focused on in the study is protein. The amount of protein available in the *Azolla pinnata* powder is 26.1% per 100 g of sample, which is slightly higher than the 22.25% reported by Kumar et al. (2018). The difference in protein content could be due to the different environments and cultivation practices (Hertzler et al., 2020). It may also be due to variations in the drying process, as the protein is sensitive to heat. The protein content of *Azolla pinnata* is still not as high as the protein content of soybean, which is reported to be 45 g of protein per 100 g of sample (Kakati et al., 2024). Nevertheless, the cultivation period of *Azolla pinnata* is significantly shorter, with only 14 days (Utomo et al., 2019), compared to soybean, which will take up to 70 to 80 days to be harvested (Idaryani et al., 2021). A shorter cultivation time leads to lower operating costs, making Azolla pinnata a promising alternative for high-protein-based products that can replace soybeans. To facilitate this, the subsequent sections will discuss the protein extraction of *Azolla pinnata*, particularly using the liquid biphasic flotation system (LBFS).

Type of Solvent

Figure 3 displays the LBFS yield recovery and separation efficiency of two types of solvents, ethanol and 2-propanol, for extracting protein from *Azolla pinnata*. A solvent is an essential chemical in this study since it extracts soluble compounds during the LBFS process and creates the separation later with an aqueous salt solution. The finding indicates that 2-propanol has a higher recovery yield of 78.19% ±3.74 of protein and separation efficiency of 79.39% ±2.16 compared to ethanol, with 42.66% ±4.65 recovery yield and 76.53% ±2.84 separation efficiency, respectively.

This might be due to a better solubility characteristic offered by 2-propanol, particularly for extracting protein from *Azolla pinnata* (Jouyban et al., 2018). The polarity of solvents

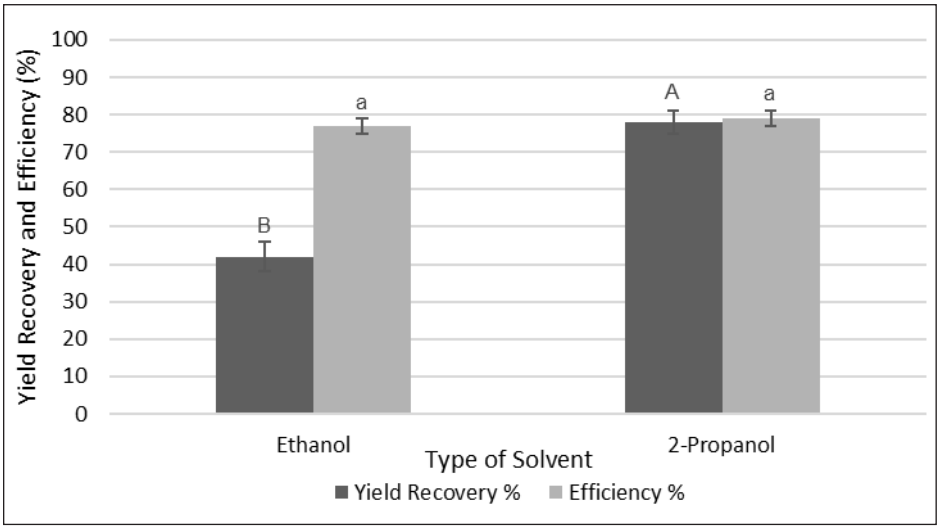

Figure 3. Effect of the type of alcohol on the yield recovery and separation efficiency of protein from *Azolla pinnata* during the LBFS process. (The alphabetical indication of capital and lower letters states the yield recovery and efficiency indicate the significantly different means of $p \leq 0.05$)

could also affect the extraction of the compounds, including protein (Susanto et al., 2018). A solvent is an important element in the LBFS for the formation of the separation layer to aid the extraction process of the solvent-soluble compounds. Besides that, 2-propanol has a higher hydrophobicity than ethanol, which is less soluble in water and provides better protein precipitation, allowing for better protein recovery (Chow et al., 2023). Hence, 2-propanol has been chosen as the solvent for the LBFS for the subsequent extraction processes in this study. The study was performed using 250 g/L of ammonium sulphate, and 100% propanol was chosen for the following parameters.

Concentration of Solvent

As shown in Figure 4, the effect of solvent concentration on the yield recovery and separation efficiency of the protein from Azolla pinnata during the LBFS process is illustrated. The solvent concentration (2-propanol) ranged from 75% to 100% with a 5% variation. Distilled water was used to lower the concentration of the solvent. Based on our preliminary findings, the solvent with a concentration of less than 75% was unable to form a visible two-phase layer, which might be due to high dilution that reduces the solvent's solubility capability. A low concentration of alcohol can result in weak ionic and van der Waals interactions, which could not be strong enough to attract biomolecules to the upper phase and vice versa (Aron et al., 2022)

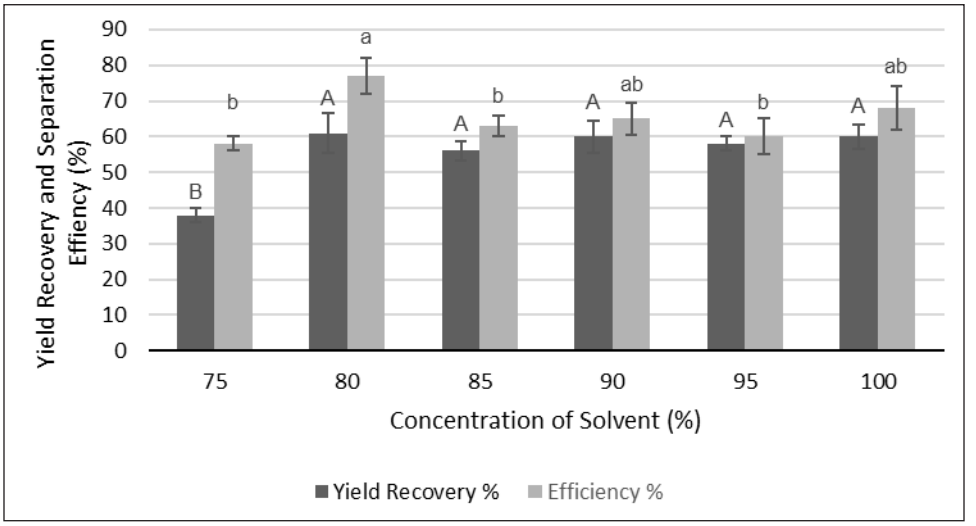

Figure 4. Effect of concentration of solvent on the yield recovery and separation efficiency of protein from *Azolla pinnata* during the LBFS process. (The alphabetical indication of capital and lower letters states the yield recovery, and efficiency indicates the significantly different means of $p \leq 0.05$)

Based on Figure 4, the yield recovery and protein separation efficiency are relatively constant throughout the entire range of 2-propanol concentrations except at 75%. It can be seen that 75% of concentration has the lowest recovery yield; this could be due to the polarity of the solvent; when it is too diluted, the polarity reduces, which also decreases the hydrophobicity, thus reducing the solubility as protein with polar amino acids tend to be more soluble in polar solvent (Madeira et al., 2024). Higher solvent concentration contains a greater number of hydroxyl groups per unit volume; hence, it has the potential to attract a greater number of biomolecules (Aron et al., 2022). The concentration of solvent at 80% resulted in the highest yield recovery of 60.76% ±5.57 and protein separation efficiency of 76.19% ±5.18. This might be due to the availability of the biomolecules in the sample, as a higher solvent concentration of more than 80% did not result in any further increment. Hence, an 80% solvent concentration is chosen for further optimisation in this study.

Concentration of Salt

Figure 5 depicts the influence of salt concentration on LBFS yield recovery and protein separation efficiency from *Azolla pinnata*. The concentration of salt is another factor that should be focused on in the liquid biphasic flotation system, as it affects the salting-out effect to separate water-miscible organic solvents in the liquid biphasic flotation system. The study on the effect of salt concentration was initiated with a constant concentration of solvent, which was set to 80%, and the amount of *Azolla pinnata* powder sample that was used was 300mg for each concentration. Based on Figure 5, as the concentration of salt

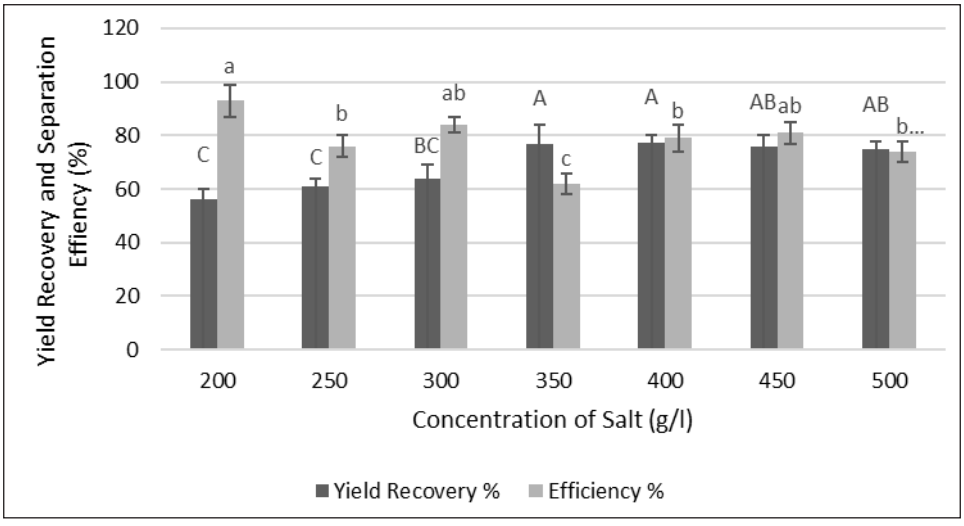

Figure 5. Effect of concentration of salt on the yield recovery and separation efficiency of protein from *Azolla pinnata* during the LBFS process. (The alphabetical indication of capital and lower letters states the yield recovery, and efficiency indicates the significantly different means of $p \leq 0.05$)

increased, so did the yield recovery of protein. The two-phase separation layer formed by this liquid-liquid separation process is also known as salt-induced phase separation (Majors, 2009). Because salt is present in the solution, the surface tension of the water will be altered, consequently increasing the hydrophobic contact between the protein and the water. The nature of the targeted protein will determine whether the protein remains in the aqueous phase after this alteration or moves into the solvent phase (Saw et al., 2020). Raj et al. (2023) studied the deconstruction of microalgae biomass and reported that when the phase molecules interact beyond a critical concentration, the attraction between the molecules and the phase components determines the selective extraction of specific biomolecular compounds. Although the recovery rate for concentrations of salt above 350 g/L to 500 g/L was relatively similar, 400 g/L of salt concentration showed the highest protein recovery of 78.19% ±2.50 with a separation efficiency of 79.39% ±5.73.

In Figure 5, the separation efficiency between different salt concentrations did not follow a consistent trend. At a 300 g/L salt concentration, the efficiency dropped drastically due to the high amount of undissolved salt in the solution, resulting in a salt precipitate that affected the extraction process. Besides, our preliminary findings also found that salt concentration below 200 g/L did not manage to produce the separation layer, as the polarity of the solution was too low to produce the separation layer (Asenjo & Andrews, 2012).

The salting-out effect can help us establish the upper boundary of salt concentration for the LBFS since different proteins salt out at different salt concentrations (Saw et al., 2020). A study conducted on the purification of amylase from sweet potato slurry through

a liquid biphasic system reported that a better purification factor can be achieved due to a better partition coefficient when the salt concentration is higher in the system (Yusree et al., 2022). Furthermore, another study on the extraction of protein from *Moringa oleifera* further describes that a higher concentration of salt is able to yield better protein extraction; however, excessively high salt concentration can also denature the protein, thus reducing the protein recovery (Illingworth et al., 2022). This study chose 400 g/L of salt solution as the optimised salt concentration for the LBFS of protein from *Azolla pinnata*.

Load of Biomass

The effect of biomass load on the LBFS yield recovery and separation efficiency of protein from *Azolla pinnata* is displayed in Figure 6. The load of *Azolla pinnata* powder used for the liquid biphasic flotation system can also influence the protein recovery. The sample that was experimented with in this study ranged from 200 mg to 350 mg. Due to the unique partition behaviour of the target protein, raising the concentration of protein sources can substantially affect the performance of phase separation (Chew et al., 2019). For this study, the concentration of solvent and salt was kept constant, whereby the concentration of solvent was 80%, and the concentration of salt was 400 g/L with a flotation time of 10 min.

Based on Figure 6, generally, the increment of the *Azolla pinnata* powder sample load increased the efficiency of the separation as well as the yield recovery of the protein. The highest yield recovery protein was obtained at 300 mg sample load with 78.19% ±8.17, with a protein separation efficiency of 79.39% ±5.61. This indicates that 300 mg of *Azolla*

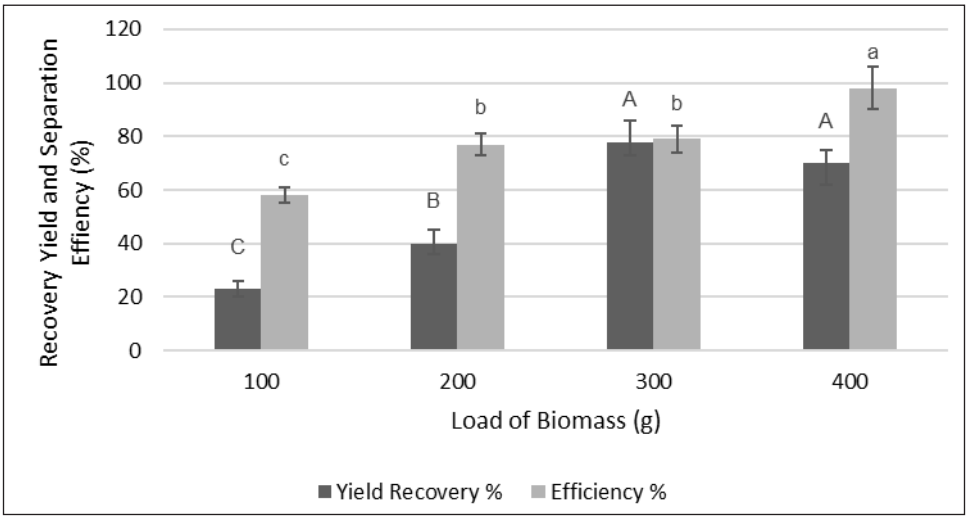

Figure 6. Effect of a load of biomass on the yield recovery and separation efficiency of protein from *Azolla pinnata* during the LBFS process. The alphabetical indication of capital and lower letters states the yield recovery, and efficiency indicates the significant difference ($p \leq 0.05$)

pinnata powder is the optimum amount needed to achieve the highest yield recovery and be as efficient as the rest of the sample sizes in this study. It can also be seen that as a load of biomass increases, the yield recovery of protein decreases; a similar trend was also noticed by a study of extraction protein from *Persiscaria tenulla,* and it was deduced that due to the high amount of biomass was present in the system, the increase of contaminant and impurities increases in the system as well which therefore reduces the performance of the LBFS separation (Saw et al., 2020). A study by Idowu et al. (2024) on protein extraction from *P. palmata* found that protein yield varies depending on the biomass-to-solvent ratio, which directly affects extraction efficiency. Therefore, optimising this ratio is essential to achieving a high protein recovery yield.

The data obtained from this study opposed the study conducted on the protein extraction from *Persicaria tenulla* leaf, which found that at 100 mg to 400 mg, it shows a downward trend of protein recovery (Saw et al., 2020). As for *Azolla pinnata* powder, it indicates an upward trend in protein recovery as the biomass load increases from 100 mg to 300 mg; however, once the load exceeds 300 mg, the protein recovery rate decreases. The difference in findings might be due to the availability of the biomolecules contained in the sample, whereby *Azolla pinnata* powder contains a higher amount of biomolecules, which portrays higher protein yield recovery (Saw et al., 2020). Moreover, Awad et al. (2021) stated that increasing the surface area and contact between the biomass and solvent enhances the yield and concentration of the active compound in the extract. However, an excessive biomass load can reduce protein recovery efficiency. Since 300 mg of *Azolla pinnata* powder sample load produces the highest yield of protein, it was chosen as the optimised condition for the LBFS extraction of protein from *Azolla pinnata*.

Flotation Time

Figure 7 displays the effect of floating time variation on the LBFS yield recovery and protein separation efficiency from *Azolla pinnata*. Flotation time is the period during which microbubbles are introduced into the liquid biphasic flotation system. The microbubbles aid the LBFS in separating the important compounds, which in this case are the proteins. The microbubbles reduce the surface tension of the particles during the process, which helps prevent the deterioration of the protein, as it is the main composition aimed at being extracted. The duration of the flotation process affects the final product, affecting the area of the air-water interface generated per unit volume of aqueous solution over time (Saw et al., 2020).

The study was initiated with the concentration of solvent and salt being kept constant at 80% solvent concentration and 400 g/L salt concentration, with a 300 mg sample load, as optimised in the previous sections. The flotation system was compared with flotation times of 5 to 15 minutes. Based on Figure 7, a longer flotation time resulted in a higher

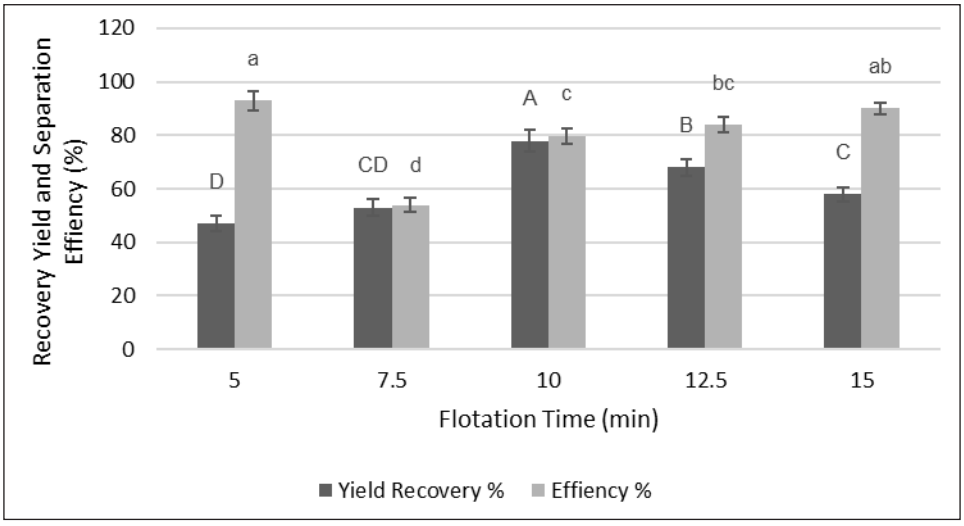

Figure 7. Effect of flotation time on the yield recovery and separation efficiency of protein from *Azolla pinnata* during the LBFS process. (The alphabetical indication of capital and lower letters states the yield recovery, and efficiency indicates the significantly different means of $p \leq 0.05$)

protein recovery yield and efficiency, with the optimised condition obtained after 10 min of flotation time (78.19% ±4.31 yield recovery and 79.39% ±2.80 separation efficiency). A decrease in yield and efficiency was observed when the flotation time exceeded 10 min, likely due to protein denaturation caused by prolonged exposure to vigorous flotation conditions. Besides, from an operational point of view, the process should be performed as quickly as possible to reduce operating costs. All in all, 10 min would be the optimum choice, as it yields the highest protein recovery and protein separation efficiency.

A study by Koyande et al. (2019) on protein extraction from *Chlorella vulgaris* suggests that a high biomass load can reduce the efficiency of flotation systems. This occurs because the increased biomass load raises the viscosity of the mixture, making it more difficult for microbubbles to form. As a result, both yield recovery and separation efficiency are impaired. Another study on the recovery of protein from dairy milk waste products states that the increase in flotation time exceeding 10 minutes reduces the protein recovery yield. This is because molecules that are not proteins are being blown to the top phase, causing the total concentration of proteins at the top phase to decrease (Tham et al., 2019).

CONCLUSION

This study evaluated the potential of a liquid biphasic flotation system as a liquid-liquid extraction method to extract protein from *Azolla pinnata* powder. According to the results of this research, it is possible to achieve a high rate of protein recovery and separation

efficiency by employing the LBFS method. The parameters used for this system have to be optimised to achieve the highest protein recovery and separation efficiency. The optimised parameter can produce a separation layer as the polarity of the solvent and salt can produce the top and bottom layers to separate the protein. The optimised value is 80% concentration of 2-propanol, 400 g/L concentration of ammonium sulphate, 300 mg of *Azolla pinnata* powder and 10 min of flotation time, which results in 78.19% ±4.31 protein yield recovery and 79.39% ±2.80 protein separation efficiency. Upscaling the process can further improve protein recovery and separation efficiency. Thus, the liquid biphasic flotation system is a promising technology for extracting plant-based protein, which can benefit both the food industry and the pharmaceutical industry.

ACKNOWLEDGEMENT

The authors thank the Ministry of Higher Education Malaysia and Universiti Putra Malaysia for sponsoring this work under UPM Putra Grant: GP-IPS/2023/9769500.

REFERENCES

AgFlow. (2023, January 13). Malaysia is doing intercontinental soybean oil business- AgFlow. *Agricultural Markets News*. https://www.agflow.com/agricultural-markets-news/malaysia-is-doing-intercontinental-soybean-oil-business/

Aron, N. S. M., Chew, K. W., Ang, W. L., Ratchahat, S., Rinklebe, J., & Show, P. L. (2022). Recovery of microalgae biodiesel using liquid biphasic flotation system. *Fuel, 317*, Article 123368. https://doi.org/10.1016/j.fuel.2022.123368

Asenjo, J. A., & Andrews, B. A. (2012). Aqueous two-phase systems for protein separation: Phase separation and applications. *Journal of Chromatography A*, *1238*, 1–10. https://doi.org/10.1016/J.CHROMA.2012.03.049

Awad, A. M., Kumar, P., Ismail-Fitry, M. R., Jusoh, S., Aziz, M. F. A., & Sazili, A. Q. (2021). Green extraction of bioactive compounds from plant biomass and their application in meat as natural antioxidant. *Antioxidants*, *10*(9), Article 1465. https://doi.org/10.3390/ANTIOX10091465

Cherryl, D. M., Prasad, R. M. V., Jagadeeswararao, S., Jayalaxmi, P., & Kumar, S. D. (2014). A study on the nutritive value of Azolla pinnata. *Livestock Research International, 2*(1), 13-15.

Chew, K. W., Chia, S. R., Krishnamoorthy, R., Tao, Y., Chu, D. T., & Show, P. L. (2019). Liquid biphasic flotation for the purification of C-phycocyanin from *Spirulina platensis* microalga. *Bioresource Technology, 288*, Article 121519. https://doi.org/10.1016/J.BIORTECH.2019.121519

Chow, Y. H., Poh, C. T., Kee, P. E., Ng, H. S., Lan, J., & Yoon, L. W. (2023). Application of alcohol-salt aqueous biphasic system for the recovery of ectoine. *Processes*, *11*(9), Article 2560. https://doi.org/10.3390/PR11092560

Cumplido, M. P., Cháfer, A., de la Torre, J., & Montón, J. B. (2018). Study of separation of water + 2-propanol mixture using different ionic liquids: 1-Butyl-3-methylimidazolium bis(trifluoromethylsulfonyl)

imide or 1-butyl-1-methylpyrrolidinium bis(trifluoromethylsulfonyl)imide. *The Journal of Chemical Thermodynamics, 116*, 32-41. https://doi.org/10.1016/J.JCT.2017.08.020

Darmalinggam, D., & Kaliannan, M. (2020). Economic growth in the Malaysian vegetarian market potential: Internalized dimension of motivation. *International Journal of Social Economics, 47*(9), 1181–1202. https://doi.org/10.1108/IJSE-04-2020-0190

Hertzler, S. R., Lieblein-Boff, J. C., Weiler, M., & Allgeier, C. (2020). Plant proteins: Assessing their nutritional quality and effects on health and physical function. *Nutrients, 12*(12), Article 3704. https://doi.org/10.3390/NU12123704

Idaryani, Rauf, A. W., Fattah, A., & Suriany. (2021). Effect of harvest time on soybean seed quality of detap-1 variety. *IOP Conference Series: Earth and Environmental Science*, *828*(1), Article 012027. https://doi.org/10.1088/1755-1315/828/1/012027

Idowu, A. T., Amigo-Benavent, M., & FitzGerald, R. J. (2024). Impact of alkaline solution, carbohydrase and biomass: Solvent on extraction efficiency, and protein and amino acid profiles of *Palmaria palmata* protein extracts. *Food and Bioproducts Processing*, *148*, 285-297. https://doi.org/10.1016/J.FBP.2024.09.017

Illingworth, K. A., Lee, Y. Y., & Siow, L. F. (2022). The effect of isolation techniques on the physicochemical properties of *Moringa oleifera* protein isolates. *Food Chemistry Advances, 1*, Article 100029. https://doi.org/10.1016/J.FOCHA.2022.100029

Jouyban, A., Nozohouri, S., & Martinez, F. (2018). Solubility of celecoxib in {2-propanol (1) + water (2)} mixtures at various temperatures: Experimental data and thermodynamic analysis. *Journal of Molecular Liquids, 254*, 1–7. https://doi.org/10.1016/j.molliq.2018.01.033

Kakati, J. P., Fallen, B., Armstrong, P., Yan, S., Bridges, W., & Narayanan, S. (2024). High-protein soybean lines with stable seed protein content under heat and drought stresses. *Journal of Agriculture and Food Research*, *18*, Article 101469. https://doi.org/10.1016/j.jafr.2024.101469

Kaur, M., Kumar, M., Sachdeva, S., & Puri, S. K. (2018). Aquatic weeds as the next generation feedstock for sustainable bioenergy production. *Bioresource Technology, 251*, 390–402. https://doi.org/10.1016/j.biortech.2017.11.082

Kielkopf, C. L., Bauer, W., & Urbatsch, I. L. (2020). Bradford assay for determining protein concentration. *Cold Spring Harbor Protocols, 2020*(4), pdb-prot102269 https://doi.org/10.1101/PDB.PROT102269

Koyande, A. K., Chew, K. W., Lim, J. W., Lee, S. Y., Lam, M. K., & Show, P. L. (2019). Optimization of protein extraction from *Chlorella Vulgaris* via novel sugaring-out assisted liquid biphasic electric flotation system. *Engineering in Life Sciences, 19*(12), 968–977. https://doi.org/10.1002/ELSC.201900068

Kumar, M., Dhuria, R. K., Jain, D., Sharma, T., Nehra, R., & Prajapat, U. K. (2018). A nutritional evaluation of Azolla (*Azolla pinnata*) as feed supplement. *Veterinary Practitioner, 19*(1), 132–133.

Madeira, P. P., Todorov, G., Uversky, V. N., & Zaslavsky, B. Y. (2024). Solvent polarity and hydrophobicity of solutes are two sides of the same coin. *Biochemical and Biophysical Research Communications, 701,* Article 149600. https://doi.org/10.1016/j.bbrc.2024.149600

Majors, R. (2009). Salting-out liquid-liquid extraction (SALLE). *LCGC North America*, *27*(7), 526-533.

Qoms, M. S., Arulrajah, B., Ibadullah, W. Z. W., Ramli, N. S., Chau, D. M., Sarbini, S. R., & Saari, N. (2024). Performance of *Azolla pinnata* fern protein hydrolysates as an emulsifier and nutraceutical ingredient in an O/W emulsion system and their effect on human gut microbiota and mammalian cells. *Food & Function, 15*(12), 6578-6596. https://doi.org/10.1039/D4FO00377B

Raj, T., Morya, R., Chandrasekhar, K., Kumar, D., Soam, S., Kumar, R., Patel, A. K., & Kim, S. H. (2023). Microalgae biomass deconstruction using green solvents: Challenges and future opportunities. *Bioresource Technology*. *369*, Article 128429. https://doi.org/10.1016/j.biortech.2022.128429

Refaey, M. M., Mehrim, A. I., Zenhom, O. A., Areda, H. A., Ragaza, J. A., & Hassaan, M. S. (2023). Fresh azolla, *Azolla pinnata* as a complementary feed for O*reochromis niloticus*: Growth, digestive enzymes, intestinal morphology, physiological responses, and flesh quality. *Aquaculture Nutrition*, *2023*(1), Article 1403704. https://doi.org/10.1155/2023/1403704

Sankaran, R., Show, P. L., Cheng, Y. S., Tao, Y., Ao, X., Nguyen, T. D. P., & Quyen, D. V. (2018). Integration process for protein extraction from microalgae using liquid biphasic electric flotation (LBEF) system. *Molecular Biotechnology, 60*, 749-761. https://doi.org/10.1007/S12033-018-0111-6

Saw, H. S., Sankaran, R., Khoo, K. S., Chew, K. W., Phong, W. N., Tang, M. S. Y., Lim, S. S., Zaid, H. F. M., Naushad, M., & Show, P. L. (2020). Application of a liquid biphasic flotation (LBF) system for protein extraction from *Persiscaria tenulla* leaf. *Processes, 8*(2), Article 247. https://doi.org/10.3390/pr8020247

Stone, A. K., Karalash, A., Tyler, R. T., Warkentin, T. D., & Nickerson, M. T. (2015). Functional attributes of pea protein isolates prepared using different extraction methods and cultivars. *Food Research International, 76*, 31–38. https://doi.org/10.1016/j.foodres.2014.11.017

Susanto, D. F., Hapsari, S., Trilutfiani, Z., Borhet, A., Aparamarta, H. W., Widjaja, A., & Gunawan, S. (2018). Effect of solvent polarity levels on separation of xanthone and coumarin from *Calophyllum inophyllum* leaves extract. *IOP Conference Series: Materials Science and Engineering, 334*(1), Article 012071. https://doi.org/10.1088/1757-899X/334/1/012071

Swain, B. K., Naik, P. K., & Beura, C. K. (2022). Nutritive value of azolla as poultry feed-a review. *Indian Journal of Animal Nutrition, 39*(1), 1–11. https://doi.org/10.5958/2231-6744.2022.00001.9

Tham, P. E., Ng, Y. J., Sankaran, R., Khoo, K. S., Chew, K. W., Yap, Y. J., Malahubban, M., Zakry, F. A. A., & Show, P. L. (2019). Recovery of protein from dairy milk waste product using alcohol-salt liquid biphasic flotation. *Processes*, *7*(12), Article 875. https://doi.org/10.3390/PR7120875

Utomo, R., Noviandi, C. T., Umami, N., & Permadi, A. (2019). Effect of composted animal manure as fertilizer on productivity of *Azolla pinnata* grown in earthen ponds. *Journal of Biological Sciences Original Research Paper*, *19*(4), 232-236. https://doi.org/10.3844/ojbsci.2019.232.236

Yusree, F. I. F. M., Peter, A. P., Zulkifli, N. A. binti, Nor, M. Z. M., Basri, M. S. M., Mokhtar, M. N., Awasthi, M. K., & Show, P. L. (2022). Towards green recovery of β-amylase from slurry of sweet potato (*Ipomoea batatas*) of VitAto variety via liquid biphasic system. *Sustainable Chemistry and Pharmacy, 25,* Article 100579. https://doi.org/10.1016/J.SCP.2021.100579

Zhubi-Bakija, F., Bajraktari, G., Bytyçi, I., Mikhailidis, D. P., Henein, M. Y., Latkovskis, G., Rexhaj, Z., Zhubi, E., Banach, M., Alnouri, F., Amar, F., Atanasov, A. G., Bartlomiejczyk, M. A., Bjelakovic, B., Bruckert, E., Cafferata, A., Ceska, R., Cicero, A. F. G., Collet, X., … Zirlik, A. (2021). The impact of

type of dietary protein, animal versus vegetable, in modifying cardiometabolic risk factors: A position paper from the international lipid expert panel (ILEP). *Clinical Nutrition, 40*(1), 255–276. https://doi.org/10.1016/j.clnu.2020.05.017

Pertanika J. Sci. & Technol. 33 (S5): 75 - 107 (2025)

PERTANIKA JOURNALS

SCIENCE & TECHNOLOGY

Journal homepage: http://www.pertanika.upm.edu.my/

Effect of Composite Technologies on the Mechanical Properties and Biodegradability of Agricultural Polymeric Materials

Nor Syahidah Md Sam[1,2]*, Ganisan Krishnen[2], Norfhairna Baharulrazi[1], Luqman Chuah Abdullah[3] and Rohah Abdul Majid[1]

[1]Faculty of Chemical and Energy Engineering, Universiti Teknologi Malaysia, 81310 UTM Skudai, Johor, Malaysia

[2]Soil Science, Water and Fertilizer Research Centre, Malaysian Agricultural Research and Development Institute (MARDI), MARDI Headquarters, 43400 Serdang, Malaysia

[3]Department of Chemical and Environmental Engineering, Faculty of Engineering, Universiti Putra Malaysia, 43400 UPM Serdang, Selangor, Malaysia

ABSTRACT

Polymeric materials are widely applied in agriculture for purposes such as weed control, nutrient delivery, and the controlled release of pesticides and herbicides. However, their environmental impact, particularly from synthetic polymers like polyethylene and polystyrene, stems from their resistance to degradation. With an estimated 80% of global plastic waste accumulating in ecosystems or landfills, the development of biodegradable alternatives has become a critical concern. This has led to a growing demand for biodegradable polymers in applications such as plastic mulching and controlled-release systems, aiming to reduce pollution, support soil health and ease post-harvest residue management. This paper provides an overview of recent developments in biodegradable polymer composites, with a focus on how composite technologies enhance both the mechanical performance and biodegradability of these materials. It also provides an overview of the growing recognition of polymer composites for their role in improving the efficiency and precision of nutrient, pesticide, and herbicide delivery to plants, minimizing environmental losses and enhancing resource use. The discussion emphasizes the need for biodegradable polymers to meet functional criteria similar to synthetic plastics, such as adequate tensile strength and elongation while remaining capable of degrading under agricultural conditions. The integration of fillers, reinforcements, and polymer blends has shown promise in improving durability during

ARTICLE INFO

Article history:
Received: 13 February 2024
Accepted: 28 May 2025
Published: 10 July 2025

DOI: https://doi.org/10.47836/pjst.33.S5.05

E-mail address:
nor86@graduate.utm.my (Nor Syahidah Md Sam)
ganisan@mardi.gov.my (Ganisan Krishnen)
norfhairna@utm.my (Norfhairna Baharulrazi)
chuah@upm.edu.my (Luqman Chuah Abdullah)
r-rohah@utm.my (Rohah Abdul Majid)
*Corresponding author

e-ISSN: 2231-8526

use and facilitating breakdown afterward. Such dual performance is vital for sustainable agricultural systems. This review aims to offer insights into the role of composite technologies in advancing biodegradable polymer materials for agriculture, supporting both efficient input delivery and long-term environmental compatibility.

Keywords: Biodegradable polymer, controlled release system, degradation

INTRODUCTION

Polymeric materials are frequently utilized in agriculture for weed control, controlled release of agricultural active agents such as herbicides and pesticides, and controlled release of fertilizers (Sikder et al., 2021). The use of synthetic polymers, such as polystyrene, polyvinyl chloride, and polyethylene, has an environmental impact due to their delayed or non-degradable nature (Kiselev et al., 2021). According to Geyer et al. (2017), a significant amount of plastic waste, approximately 80%, is currently estimated to be present in natural ecosystems or landfills. As a result, it is critical to convert it to a biodegradable polymer that can biodegrade in the soil. They must exhibit adequate mechanical properties to withstand agricultural operations while degrading within a defined timeframe to release environmentally safe byproducts, such as CO_2 and H_2O. For instance, in agricultural mulches, the degradation period should align with crop cycles, and the byproducts must not hinder soil health.

Aside from biodegradability, the mechanical properties of the manufactured biodegradable polymers must meet synthetic polymer standards. For example, the tensile characteristics and elongation at the break of mulching are critical in ensuring that the plastic is not torn or broken during mulching preparation (Merino et al., 2022). Other than that, controlled-release fertilizers (CRFs) allow nutrients to be released gradually or in stages, which can be optimized to coincide with the timing of nutrient requirements during crop growth, potentially saving labor costs (Vejan et al., 2021). Therefore, researchers and industry players have extensively researched the use of fillers, reinforcements, or other polymers to improve the characteristics and biodegradability of agricultural polymeric materials.

Fitriani et al. (2025) developed a hybrid biodegradable film composed of whey protein isolate, polyvinyl alcohol, and cellulose nanocrystals derived from pineapple crown leaves, utilizing optimal concentrations determined in prior research. The results demonstrate that incorporating PVA and CNC into the WPI matrix enhances the mechanical, physicochemical, morphological, and thermal properties of the resulting hybrid film. PBAT/PLA-PPC-PTLA ternary blend polymer composites, incorporating polybutylene adipate-co-terephthalate, polylactic acid, polypropylene carbonate, and a lactic acid-isopropyl carbonate copolymer, have shown promise in recent studies for agricultural applications.

These composites exhibit improved tensile strength and water vapor barrier properties, along with a comparable biodegradation rate (Guo et al., 2024).

The present review aims to look into various fillers or reinforcement agents utilized in the production of biodegradable polymer composites and their influence on the mechanical characteristics and biodegradability of polymeric materials. The discussion will also encompass polymer composites and their function in regulating the release of pesticides, herbicides, and nutrients. We believe that this brief overview provides a vital insight into the importance of polymeric composites in improving the mechanical characteristics, release characteristics and biodegradability of polymers while being ecologically benign.

BIODEGRADATION

The definition of biodegradation varies depending on the specific domain of application of the polymers, whether it be in the biomedical or natural environment. Numerous discrete definitions have been formally established, as per the historical records of standard-setting entities and their corresponding interests. According to the definition provided by Albertsson and Karlsson (2002), biodegradation is a phenomenon that entails the enzymatic and/or chemical breakdown of living organisms and their excretions. It is imperative to take into account abiotic reactions, including photodegradation, hydrolysis, and oxidation, as they have the potential to alter the polymer before, during, or instead of biodegradation as a result of environmental influences. The process of polymer biodegradation is characterized by the degradation of its chemical and physical properties, resulting in a reduction in its molecular mass and the production of low-molecular-weight products, such as CO_2, CH_4, and H_2O. This process is facilitated by microorganisms in both aerobic and anaerobic conditions, as well as abiotic chemical reactions such as photodegradation, hydrolysis, and oxidation (Luckachan & Pillai, 2011).

Several biopolymers have been designed to be biodegradable in soil, landfills, or composting facilities. The process of material degradation is dependent on the existence of specific microorganisms. The requirement of indigenous soil microorganisms and moisture is commonly essential, thereby enhancing the appeal of microbially degraded plastics (Kasirajan & Ngouajio, 2012).

Biodegradation Process

Biodegradation is the only degradation mechanism that is capable of completely removing a polymer or its breakdown byproducts from the environment. The process of biodegradation occurs in a dual-phase manner. The initial step involves the depolymerization of the macromolecules, resulting in the formation of shorter chains (Figure 1). Typically, this particular stage takes place extracellularly owing to the considerable size of the polymer chain and the insolubility of numerous polymers. Polymeric chain cleavage is attributed to

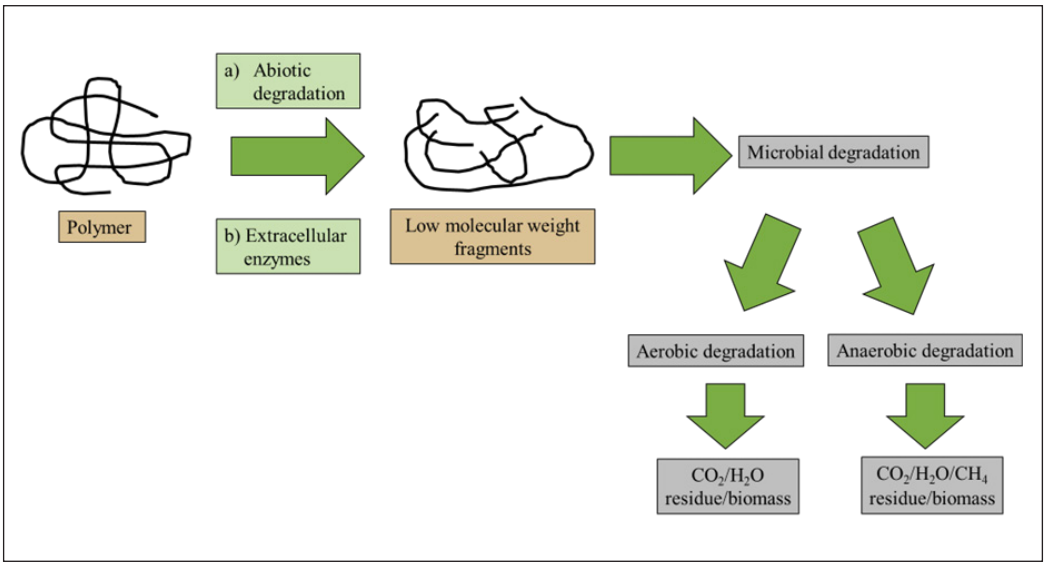

Figure 1. A diagrammatic illustration of biodegradation's chemistry (Luckachan & Pillai, 2011)

extracellular enzymes, including endo- and exo-enzymes, as well as abiotic reactions. In this phase, there is an increase in the contact area between the polymer and the microorganism (Luckachan & Pillai, 2011)

The subsequent stage relates to mineralization. Upon reaching a diminutive size, oligomeric fragments undergo cellular transportation and subsequent bioassimilation by microorganisms, ultimately leading to mineralization. Biodegradation occurs under distinct conditions, depending on the presence or absence of oxygen: aerobic biodegradation occurs in the presence of oxygen, while anaerobic biodegradation occurs in the absence of oxygen. Complete biodegradation or mineralization is achieved when there is no residual matter left, signifying that the initial product has been fully transformed into gaseous byproducts and salts.

The presence of weak links within a chain can facilitate attacks by specific microorganisms. The major chains of polyolefin and vinyl groups include carbon atoms, making them resistant to breakdown and biodegradation. Biodegradable polyesters such as poly(hydroxyalkanoates), adipate/terephthalate, and polylactic acid are hydrolyzed due to ester linkages. Hydrolysis non-specifically cleaves the primary polymer chain, reducing molecular weight. Smaller molecules are more vulnerable to enzymatic processes, accelerating biodegradation. Thus, chemical composition determines a polymer's biodegradability and erosion process (Kasirajan & Ngouajio, 2012). Some polymers and their biodegradability are presented in Table 1.

Table 1
Polymers and their biodegradability

Polymer	Biodegradability	Notes	References
Low-density polyethylene (LDPE)	No	Commercially available mulch	Hussain & Hamid, 2003
Linear low-density polyethylene (LLDPE)	No	Commercially available mulch	Espi, 2006
Ethylene-vinyl acetate (EVA)	No	Commercially available mulch	Espi, 2006
Ethylene butyl acrylate (EBA)	No	Commercially available mulch	Espi, 2006
Blends of LDPE, or LLDPE, with EVA	No	Commercially available mulch	Amin, 2001
Poly(butylene adipate-co-terephthalate)	Yes	60% after 45 days.	Kijchavengkul et al., 2008
PBAT			Kijchavengkul et al., 2008
Cellulose		100% after 45 days	
Polylactide or polylactic acid (PLA) with spinach stem	Yes	38% after 6 months	Merino et al., 2022
Polyhydroxybutyrate (PHB)	Yes	62% after 6 weeks	Altaee et al., 2016
Copolymer of PCL and starch	Yes	88% after 44 days under aerobic conditions	Cho et al., 2011
Ramie and cotton fiber/starch film	Yes	53.7% after 30 days	Tan et al., 2016
Ramie and cotton fiber/ polyvinyl alcohol film	Yes	79.2% after 45 days	Tan et al., 2016
Ramie and cotton fiber/ polyacrylate	Yes	16.0% after 30 days	Tan et al., 2016

COMPOSITE MATERIAL

Composite materials are assemblies of two or more materials that result in a final product with properties that surpass those of individual constituent materials (Hsissou et al., 2019; Khalil et al., 2012). These materials consist of a matrix that contains embedded materials, maintaining the cohesion and orientation of the load. The matrix can transmit stresses to the load, exhibiting high degrees of heterogeneity and often possessing anisotropic properties. Composite materials can be categorized into organic, mineral, and metallic categories based on the matrix nature (Hsissou et al., 2021). Organic composites include cardboard, reinforced plastics, and laminated tires. Mineral composites include carbon-carbon composites, concrete, and ceramic composites. Metallic composites are composed of aluminum/boron fibers and aluminum/carbon fibers. The final category comprises

metallic composites, which are composed of aluminum/boron and aluminum/carbon fibers (Hsissou et al., 2021). Composite materials have a significant impact on various fields of application, including packaging, biomedicine, lightweight structures, civil engineering, thermomechanical components, and the automotive, aviation, sports, and aerospace industries. The matrix nature, charge shape and proportion, interface quality, and production process all impact the properties of composite materials.

Biodegradable Polymers Composites

The development of composites and nanocomposites has revolutionized materials science, with biodegradable polymer matrices being crucial for their advancement (Bortolin et al., 2013; Giroto et al., 2014). Natural fiber eco-composites are a rapidly emerging product, and renewable, biodegradable polymers such as cellulosic plastics, corn-based plastics, and polyhydroxyalkanoates can be utilized in nanocomposites for various applications (Kiselev et al., 2021; Stasi et al., 2020) . These nanocomposites will exhibit enhanced strength, stiffness, toughness, reduced permeability, reduced thermal expansion, and elevated heat deflection temperature. Green, lightweight nanocomposite materials are expected to supplant conventional petroleum-based composites.

The incorporation of biodegradable natural fibers as reinforcement in natural polymer composites represents a new development. The use of natural polymer-based packaging materials is limited due to their low mechanical properties and low water resistance. However, these inherent shortcomings can be addressed by utilizing nanocomposite technology. For example, the packaging properties of natural biopolymer-layered silicate nanocomposites are significantly enhanced owing to their uniform dispersion at the nanometer scale. The mentioned improvements pertain to enhanced modulus and strength, reduced gas permeability, and improved water resistance (Rhim & Ng, 2007).

Polymer composites play a vital role in enhancing the mechanical properties and biodegradability of materials used in agriculture. Several approaches utilize natural fillers and synthetic polymers to achieve this. Polyvinyl alcohol composites, for example, are created through casting methods, incorporating fillers like starch (Wang et al., 2017) and natural fibers derived from agricultural waste such as sugarcane bagasse, apple pomace, and orange peels (Chiellini et al., 2001) and cellulose nanocrystals derived from pineapple crown leaves (Fitriani et al., 2025). Similarly, poly(butylene succinate) composites are manufactured using hot-pressing techniques with starch as a filler, resulting in biodegradable materials (Flores et al., 2009).

Further innovations include mango seed starch matrices reinforced with kraft pulp microfibrillated cellulose for enhanced performance and chemically modified maize starch combined with a lignin filler to improve structural integrity (Patil & Netravali, 2016; Spiridon et al., 2011). Thermoplastic maize starch composites utilize carbon ash

from agricultural waste, thereby expanding their applications in sustainable materials (Stasi et al., 2020). Tapioca starch/PBS composites are reinforced with empty fruit bunch fibers, providing an eco-friendly option (Ayu et al., 2020). Polylactic acid composites are developed with fillers like Osage orange wood fibers, processed into films with varying fiber sizes and weights, and also with vegetable wastes such as spinach stems, tomato pomace, and cocoa shells, blended with epoxidized soybean oil methyl ester for enhanced properties (Finkenstadt & Tisserat, 2010; Merino et al., 2022). Furthermore, polyvinyl alcohol/starch composites incorporate halloysite nanotubes for improved functionality in specific agricultural applications (Zeng et al., 2019). Controlled-release fertilizer coatings are manufactured using various polymer matrices, including polyurethane and starch-based composites, combined with fillers like montmorillonite, bentonite, cellulose, and chitosan to enhance efficiency and sustainability (Liao et al., 2021). These diverse polymer composites demonstrate the innovative use of fillers to meet the demands of modern agriculture while promoting environmental responsibility. Through various production methods, they contribute to advancements in mulches, controlled-release herbicides and pesticides, and other biodegradable agricultural products.

Clay

Polymer nanocomposites are created through the use of intercalation chemistry involving layered inorganic solids. These solids may include graphite, clay minerals, transition metal dichalcogenides, metal phosphates, phosphonates, and layered double hydroxides. The unique structure and characteristics of clay minerals, such as montmorillonite, hectorite, and saponite, have led to their widespread use. Minerals can be classified into three distinct groups, namely the 2:1 type, the 1:1 type, and the layered silicic acids. The 2:1 clay belongs to the smectite family and is composed of thin plates that are only a few nanometers thick. These plates are made up of sheets of aluminum octahedrons that are sandwiched between two sheets of silicon tetrahedrons. The neutralization of the van der Waals gap is achieved by the exchangeable metal cations present due to the arrangement of layers. The 1:1 type is composed of alternating layers of aluminum octahedrons and silicon tetrahedrons. The bonding between the layers is maintained by hydrogen bonding (Zeng et al., 2005).

Layered silicic acids are composed of silicon tetrahedron sheets with varying layer thicknesses, with a fundamental architecture consisting of stratified silicate frameworks and intercalated hydrated alkali metal cations. The presence of silanol groups within the interlayer regions facilitates organic modification through the grafting of functional groups onto the regions (Zeng et al., 2005).

The presence of clay minerals is crucial in polymer nanocomposites owing to their intricate intercalation chemistry, remarkable strength and stiffness, and the aspect ratio of individual platelets. Due to their distinctive layered structure and remarkable intercalation capabilities, they can undergo chemical modification to achieve compatibility with polymers

(Figure 3). Modifications such as organic surface treatments (e.g., with organic cations or silanes) enhance their compatibility with polymer matrices. These modifications enable improved dispersion and mechanical properties, particularly tensile strength and stiffness. For example, montmorillonite (MMT) nanocomposites have been used in agricultural mulches and controlled-release fertilizers, offering both enhanced tensile properties and slower nutrient release (Wang et al., 2017). A simple diagram illustrating the layered structure of clay minerals and their cation exchange process is included in Figure 2 to aid comprehension.

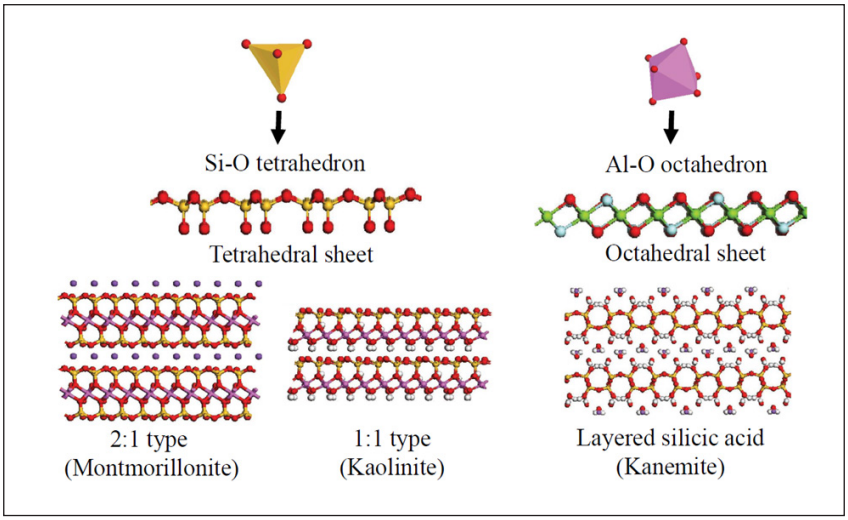

Figure 2. The structure of montmorillonite, kaolinite, and kanemite clay minerals. Combinations of tetrahedral and octahedral sheets, whose fundamental elements are typically Si-O octahedron, are used to construct them (Zeng et al., 2005)

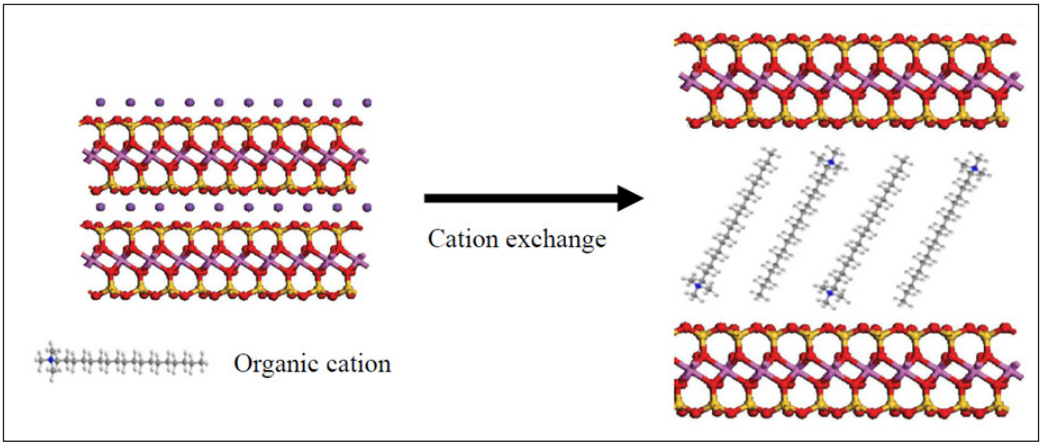

Figure 3. Schematic illustration of organo-modification of montmorillonite by organic cation

Smectite clays, such as MMT and hectorite, have the ability to undergo exfoliation or delamination, resulting in the formation of nanometer platelets. These platelets have a thickness of 1 nm, a surface area of 700 to 800 m^2/g and an aspect ratio ranging from 100 to 1500. Platelets exhibit exceptional strength and rigidity, rendering them rigid inorganic polymers (Zeng et al., 2005).

Organic Fillers

Organic fillers are composed of organic substances, including cellulose fibers, wood flour, fruit bark flour, vegetable fibers, and starches. The utilization of cellulose fillers is common in thermosetting resins such as aminoplasts and phenoplasts. This is primarily due to their low density and low cost. The addition of wood flour to a material can improve its impact resistance, shrinkage, and dimensional stability. On the other hand, fruit bark flour is commonly incorporated into thermoplastic matrices such as ABS and polypropylene. Cellulose is the primary component of vegetable fibers, which exhibit high mechanical strength and low density. Starches are a type of carbohydrate that is present in plants. They come in different sizes and configurations and are utilized as fillers in plastics to regulate their biodegradability (Hsissou et al., 2021).

Natural fibers have been used in composites since the 1970s, with cellulose fiber-reinforced polymer composites gaining interest in various industries. These composites exhibit high specific tensile strength and stiffness, making them lightweight alternatives to traditional reinforcements, such as glass fibers. They are less hazardous to handle and require less energy during processing. Natural fibers sequester carbon dioxide during growth and are biodegradable. However, due to different growing conditions, natural fibers often show a large scatter of properties compared to industrially made glass fibers. Strong quality management and extreme care are necessary for reliable and reproducible results (Huber et al., 2012).

Cellulose

Cellulose is a versatile biopolymer with numerous applications, including reinforcing components in biocomposites and as a renewable and biodegradable raw material. It is composed of d-anhydroglucopyranose units $(C_6H_{11})_5$/IUPAC, which are glucose units assembled into groups of two called "cellobiose" units. Cellulose microfibrils, found in plants' secondary cell walls, exhibit crystalline, paracrystalline, and amorphous regions. The degree of polymerization (DP) of cellulose varies depending on the source, with wood fibers having a higher degree of polymerization (300) and plant fibers and bacterial cellulose having a higher degree of polymerization (10,000). Cellulose microfibrils can be classified as nanomaterials due to their lateral dimensions of 5–50 nm. The mechanical properties of cellulose compete well with other engineering materials like aluminum and

glass fibers, with the specific stiffness of native cellulose being among the highest among all natural materials (Huber et al., 2012).

Halloysite Nanotubes

Halloysite nanotubes (HNTs) have garnered significant interest from the scientific community, both experimentally and theoretically, in recent times (Liu et al., 2014; Yuan et al., 2012, 2015). HNTs are a multilayered nanotubular structure with a structural formula of $Al_2(OH)_4Si_2O_5.nH_2O$ (Figure 4). They belong to the kaolin group of natural aluminum silicate minerals and have a range of dimensions, including 0.5–2 μm lengths and occasionally exceeding 30 um. HNTs are used as adsorbent materials for the controlled release of active molecules due to their biocompatibility and tubular structure (Huang et al., 2017; Zeng et al., 2019).

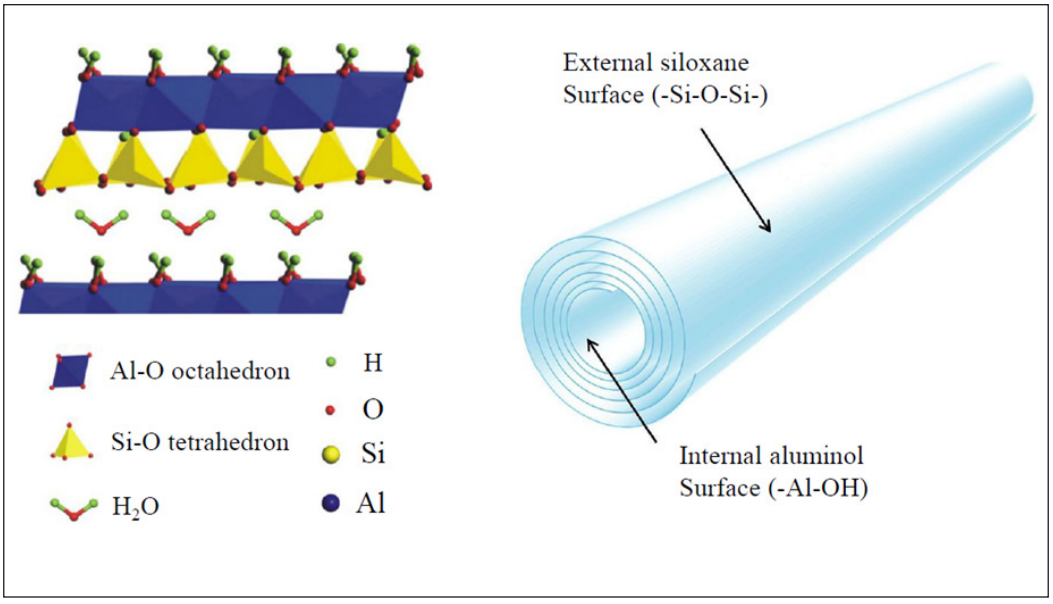

Figure 4. Structure and chemistry of halloysite nanotubes

BIODEGRADABLE COMPOSITES FOR CONTROLLED-RELEASE HERBICIDES AND PESTICIDES

Agrochemicals, such as fertilizers, herbicides, and pesticides, are essential for modern agriculture but often have unfavorable environmental consequences, such as bioaccumulation within the food web and pollution of ecosystems. Integrating functional polymers with agrochemicals can achieve the controlled release of active ingredients over extended periods, thereby minimizing the risk of environmental contamination.

This approach can mitigate degradation, evaporation, and washout processes, increasing efficacy while decreasing environmental toxicity. The optimal delivery systems for sustainable agriculture should ensure regulated release, protection from deteriorating factors, reduced cytotoxicity, and prolonged durability of nanocarriers. These features minimize pesticide application and treatment frequency, extending the validity period. (Sikder et al., 2021).

The addition of fillers and enforcement agents, such as bentonite clay, montmorillonite, and kaolinite, has enhanced the nutrient-release properties of the agricultural active agent. Nisar et al. (2009) developed coatings composed of polymers and clay that incorporate azadirachtin A to preserve the quality of soybean seeds during storage. The carriers employed in the study included ethyl cellulose, methylcellulose, gum acacia, gum tragacanth, rosin, hydroxyethyl cellulose, polyethyl methacrylate, polyethylene glycol, polyvinyl chloride, polyvinyl pyrrolidone, polyvinyl acetate, Agrimer VA 6 polymers, and bentonite clay. The study found that azadirachtin-A has a 50% discharge duration of 8.02 to 21.36 hours in aqueous solutions. The half-life of the substance in seed coats ranged from 4.37 to 11.22 months, while in azadirachtin-A WP, it was 3.45 months. The coats functioned as a barrier against moisture, decreasing azadirachtin A degradation and hindering fungi growth. Polyvinyl acetate, polyethyl methacrylate, and polyvinyl pyrrolidone showed higher superiority. The study found a significant positive association between azadirachtin A and seed germination and vigor, while a negative correlation was observed between azadirachtin A and moisture content.

Additionally, Kumar et al. (2010) conducted a study on the development of controlled-release formulations for the insecticide cartap hydrochloride. This was achieved through the utilization of commercially available materials such as carboxymethyl cellulose and polyvinylchloride (emulsion and suspension), in combination with clays such as kaolinite, bentonite, and fuller's earth. The formulation consisting of sodium carboxymethyl cellulose, cartap hydrochloride, and kaolinite exhibited exceptional efficacy (3.33%) in managing rice leaf folders in rice (Oryza sativa L.) cultivated in open fields.

Giroto et al. (2014) developed a host system consisting of starch gel, a biodegradable polymer, and montmorillonite clay (MMT) for slow-release delivery of hydrophobic herbicides. The nanocomposite structure regulates the release of the active compound by imposing diffusional barriers. The nanocomposites retained more herbicide than pure samples, indicating a cooperative or synergistic effect between the constituents. Biodegradation tests showed extended biodegradation periods for the nanocomposite compared to pure materials. The release behavior was governed by the interaction between the constituents, even at extremely high concentrations of the herbicide. The

study examined the impact of MMT incorporation on the biodegradation of starch gel and ametryne. The initial period showed similar degradation extension across various samples, but a noticeable contrast was observed after a 20-day composting period. The biodegradation of ametryne and starch was hindered by the addition of MMT, as evidenced by higher levels of CO_2 evolution in the absence of MMT compared to the levels in the St/MMT 1:1, 1:1:2, 1:2:3, and 1:4:5 Amet nanocomposites. This occurrence can be attributed to a possible van der Waals interaction between starch and ametryne, as well as clay and ametryne, as evidenced by FTIR findings.

Li et al. (2011) studied the efficacy of an amphiphilic chitosan-poly(lactide) graft copolymer, where poly(lactide) was grafted onto the water-soluble chitosan to improve insecticide loading. The submicron nanoparticles, which were formed by the amphiphilic polymer, exhibited the ability to encapsulate imidacloprid and provide a sustained release profile. In a subsequent study, the identical nanocarrier was employed as a delivery system for fungicide, specifically flusilazole, which was incorporated into the polymeric micelles using a modified nanoprecipitation technique (Mei et al., 2014). According to the authors' report, the mechanism of flusilazole release involved diffusion through the polymer matrix. Additionally, the utilization of nanoparticles was found to be effective in augmenting the activity of flusilazole by facilitating improved penetration through grape leaves.

Another key factor in the design of controlled-release formulations is the consideration of the mechanical properties and biodegradability of the delivery system. Mechanical properties, such as tensile strength, flexibility, and durability, play a crucial role in the controlled release of active ingredients, ensuring that the formulation can withstand the stresses encountered during application and storage and release the compounds at the desired rate and location. Biodegradability, on the other hand, is essential for minimizing the environmental impact of the delivery system, as it allows the formulation to degrade over time, reducing the persistence of the active ingredients in the environment (Dhaliwal, 2018).

The importance of mechanical properties and biodegradability in the development of controlled-release formulations for pesticides and herbicides cannot be overstated. By considering these factors, researchers can develop innovative solutions that mitigate the environmental impact of these chemicals while maintaining their efficacy, ultimately contributing to more sustainable agricultural practices.

Wang and his coworkers have prepared a controlled-release pesticide using a polyvinyl alcohol starch composite with sodium montmorillonite and alginate crosslinked structures (Wang et al., 2017). The herbicide 2,4-dichlorophenoxyacetic acid (2,4-D) as

a model drug was incorporated into sodium montmorillonite (Na-MMT) and an alginate ion-crosslinking structure. The result showed that the incorporation of Na-MMT and alginate ion crosslinking structure into the composite polymer significantly reduces the release rate of the model drug. In addition, it was able to sustain the release of the model drug for an extended duration. Experiments involving diffusion through the soil layer revealed that both composite polymers possessed excellent release characteristics. After eight irrigations, the total quantity of leached herbicide 2,4-D decreased from 100% to 57.6%. Additionally, the film exhibited advantageous thermal and mechanical properties, and it is anticipated to have applications in agriculture and other disciplines.

Zeng et al. (2019) have utilized Halloysite nanotubes (HNTs) to load the botanical herbicide that is an active ingredient of Eupatorium adenophora Spreng (AIEAS). Furthermore, the AIEAS-loaded HNTs were incorporated into poly(vinyl alcohol)/starch composites (PVA/ST) to prepare a dual delivery system for AIEAS. The AIEAS that were loaded in HNTs exhibited a significantly reduced release rate when passing through the soil layer of PVT/ST film, in comparison to the AIEAS that were not bound to HNTs. Following ten cycles of immersion in water, the PVA/ST film containing HNTs-AIEAS exhibited a total release quantity of AIEAS of merely 31.7%, in contrast to the PVA/ST film containing free AIEAS, which demonstrated a release quantity of 61.3%. Tensile tests were conducted to evaluate the stability of the leached film. The results indicated that the tensile strength of both PVA/ST/AIEAS and PVA/ST/HNTs-AIEAS films decreases continuously as the leaching number increases.

Kiselev et al. (2021) have developed environmentally friendly slow-release pesticide formulations using a biodegradable matrix made of poly-3-hydroxybutyrate and natural materials like peat, clay, and wood flour. These formulations have been infused with various pesticides, such as metribuzin, tribenuron-methyl, fenoxaprop-P-ethyl, azoxystrobin, epoxiconazole, and tebuconazole. Research shows that these formulations have sustained efficacy for up to 90 days. Polyhydroxyalkanoates (PHA) have gained interest as a promising material for drug delivery systems. The degradation rate is correlated with the physical form and the concentration of the active ingredient. Tablets with 10% metribuzin experienced a degradation period lasting over 60 days, with microparticles showing the highest rate of degradation. Fillers are incorporated to minimize costs and impact the hydrophilic-hydrophobic equilibrium and relaxation mechanisms within the polymer matrix, affecting the active substance's outflow kinetics and contributing to formulation degradation. Table 2 presents the properties of biodegradable composites used for the controlled release of herbicides and pesticides.

Table 2
Properties of biodegradable composites for controlled release herbicides and pesticides

Filler	Matrix	Agrochemicals	Properties	References
Bentonite clay	Gum acacia, gum tragacanth, rosin, ethyl cellulose, hydroxyethyl cellulose, Polyethylene methacrylate, methylcellulose, Polyvinyl acetate, Polyvinyl pyrrolidone	Azadirachtin-A	The duration of 50% discharge of azadirachtin-A into aqueous solution varied between 8.02–21.36 h. The half-life of the substance in the seed coats varies between 4.37–11.22 months. Polyethyl methacrylate, polyvinyl acetate, and polyvinyl pyrrolidone exhibited a higher degree of superiority compared to the remaining polymers	Nisar et al., 2009
Bentonite, kaolinite, fuller's earth	Polyvinyl chloride, carboxymethyl cellulose	Insecticide-Cartap hydrochloride	Catrap hydrochloride, sodium carboxymethyl cellulose and kaolinite exhibited exceptional efficacy (3.33%) in managing rice leaf folder in rice cultivated in open fields	Kumar et al., 2010
Sodium montmorillonite and alginate	Polyvinyl alcohol/starch composite	2,4-Dichlorophenoxyacetic acid	The release rate was reduced, maintaining the release of herbicide for a longer period. Possesses good mechanical and thermal properties	Wang et al., 2017
Montmorillonite (MMT)	Starch gel	Amethyne	Nanocomposites retained more herbicide than the pure samples. MMT addition retarded the starch and ametryne biodegradation.	Giroto et al., 2014
Chitosan	Polylactide	Imidacloprid	The submicron particles can prolong the pesticide release time owing to the amphiphilic structure of the copolymer	Li et al., 2011
Halloysite nanotubes	Polyvinyl alcohol/starch composites	Botanical herbicide -active ingredient of Eupatorium adenophora Spreng (AIEAS)	The AIEAS loaded in HNTs showed much slower release from PVT/ST film through the soil layer than free AIEAS. The tensile strength of the composite is higher than that of the non-composite polymers	Zeng et al., 2019
Peat, clay, wood flour	Poly-3-hydroxybutyrate	Metribuzin, tribenuron-methyl, fenoxaprop-P-ethyl, azoxystrobin, epoxiconazole, tebuconazole	Fillers reduce pesticide formulation costs by affecting hydrophilic-hydrophobic balance and relaxation processes, affecting active substance outflow and causing degradation	Kiselev et al., 2021

BIODEGRADABLE COMPOSITES FOR MULCHES

Plastic mulch, first discovered in the 1950s (Kasirajan & Ngouajio, 2012), increases soil temperature and alters crop microclimate (Tarara, 2000), protecting crops from weather, insects, and birds. It has been used in agriculture since its development in developed countries and is now spreading to developing countries. It has led to significant yield increases in vegetable production, particularly for tomatoes, peppers, eggplants, watermelons, muskmelons, cucumbers, and squash. Reflective mulch has been found to increase soluble solids content, total phenolics, flavonoids, and anthocyanins in Ontario wine grapes (Coventry et al., 2005), increase soluble solids in plums (Kim et al., 2008), and alter the anthocyanins content in butterbean (Kasperbauer & Loughrin, 2004). Strawberries ripened over red plastic mulch have higher aroma and flavor compounds.

Plastic mulches offer varying levels of weed control depending on the amount of light allowed through the mulch. Studies show that weed appearance decreases by 64-98% during the growth season. Additionally, reflective plastic mulch can protect crops against insect pests and diseases, similar to imidacloprid treatment. However, interference with visual cues by insects can cause increased attraction or repulsion to plastic mulched fields and crops.

Mulch films made from petroleum-based plastics, such as polyethylene, pose significant waste disposal issues and environmental pollution (Kasirajan & Ngouajio, 2012). The growing production of commercial polymers, particularly in agriculture and packaging, has raised concerns about long-term environmental accumulation and pollution (Albertsson et al., 1987). The removal of plastic is time-consuming (about 16 h/ha) and requires manual labor (Kasirajan & Ngouajio, 2012), with residual film in the field potentially affecting crop root development. The lack of biodegradability of these polymers has raised concerns about the long-term environmental effects of these plastics (Albertsson et al., 1987).

The incorporation of fillers into biodegradable matrices as a non-continuous phase has been observed to result in the formation of a complex structure, as reported by Khalil et al. (2019). According to Fowler et al. (2006), the combination of reinforcements and matrix yields a biomaterial that exhibits enhanced properties when compared to those of the individual components. In recent years, there has been a growing interest among the scientific community in biodegradable thermoplastics as a means to attain the parameters of polyethylene (PE) mulch films through the use of bio-composite materials (Sander, 2019).

According to Briassoulis (2006), biodegradable mulch films (BDMs) should exhibit suitable mechanical properties at the installation stage, such as tensile strength and elongation at break. Additionally, these mechanical properties should be maintained throughout the useful lifespan of the biodegradable mulches. Lastly, BDMs must be completely biodegradable in the soil before the commencement of the next crop season. The property of water vapor permeability (WVP) is crucial for mulching applications,

especially in dry regions, in addition to mechanical characteristics and biodegradability. Obtaining a comparable PE water vapor barrier value is imperative.

After reinforcements have been added, the material's strength and durability may be gauged by testing its mechanical characteristics. It is essential for mulching applications that bio-composites keep their shape under certain pressures and can still spread out and cover the soil (Yang et al., 2020). Three characteristics commonly reported and/or tested to provide insight into the mechanical properties of bio-based materials are tensile strength, elongation at break, and Young's modulus. All of them feature the following information: The tensile strength may be used to determine the durability of a material, while the elongation at break can reveal its pliability, elasticity, and ductility, and Young's modulus can reveal its rigidity (Khalil et al., 2019).

According to Merino et al. (2018), starch is one of the most commonly utilized agro-polymers for the production of cost-effective and biodegradable thermoplastic films. Starch-based biodegradable mulch films can be utilized in two distinct ways: either as a biodegradable reinforcement or as a biodegradable matrix. This polysaccharide serves as the fundamental component for both applications.

Starch was used as an organic filler in poly(vinyl alcohol) (PVA) films by Chiellini et al. (2001) and poly(butylene succinate) (PBS) films by Flores et al. (2009). Chiellini et al. (2001) made PVA-based bio-composite films from starch and sugarcane, apple and orange waste and apple fibers. These authors cast biodegradable films and examined the mechanical characteristics of starch content from 0 to 25% wt%. By adding 25% wt% starch content to PVA/orange and PVA/apple pomace fiber bio-composites, elongation at break values drop from 105.4 and 149.7% without filler to 29.6 and 65%, respectively. Tensile strength improved somewhat for PVA/sugarcane bagasse fibers with 25 wt% starch, which doubled their tensile strength values.

Flores and colleagues created bio-composite films using PBS and starch filler through a hot-pressing technique (Flores et al., 2009). The mechanical characteristics of the composite films were analyzed while altering the starch content, which included concentrations of 0, 20, 40, and 60 weight percent. The authors have reported a decrease in tensile strength values with an increase in starch content (0 wt% and 60 wt%), from 37.2 MPa to 5.7 MPa. A minor improvement in elongation at break was observed upon the integration of a decreased quantity of starch. Nevertheless, this particular parameter exhibited a decline upon the inclusion of contents exceeding 20% weight.

Both studies found that adding organic fillers enhances tensile strength qualities till a specific weight content due to the homogeneous dispersion of starch fillers into PBS and PVA and the matrix. According to their findings, the incorporation of plasticizers resulted in a rise in the elongation at break values in comparison to films that were not plasticized. However, the authors observed significant reductions in tensile strength. Plasticized and

suitable biopolymers are needed to employ starch as a biodegradable matrix (Briassoulis, 2004). Starch matrix-based biodegradable mulch films with organic reinforcements had superior mechanical characteristics compared to those of the polysaccharide matrix alone (Khalil et al., 2019).

Patil and Netravali (2016) introduced Kraft pulp microfibrillated cellulose into a mango seed starch matrix. In the production of biodegradable films, an environmentally friendly cross-linker was employed. To enhance the interfacial bonding in bio-composites, the chemical similarity between the matrix and fillers was utilized. Microfibrillated cellulose in mango seed starch matrix increased tensile strength and Young's modulus. Fillers loaded from 0% to 40% enhanced Young's modulus from 1.347 to 2.407 GPa. Patil and Netravali (2016) found that bio-composite films with informed filler dispersion and cellulose reinforcement had outstanding mechanical characteristics.

Spiridon et al. (2011) used maize starch as a matrix and microparticles from chemically modified starch as reinforcements to create bio-composite films. They added boost and beech lignin to chemically modified corn starch and starch microparticles. Lignin lowered Young's modulus and elongation at break but enhanced tensile strength. When compared to the original films, starch-beech and starch-boost lignin bio-composites have a higher degree of rigidity. Tensile strength rose by over 47% and 21%, Young's modulus fell by 8% and 31%, and elongation at break decreased by almost 39% and 30%. The explanation for this mechanical behavior was that strong intermolecular hydrogen bonds between the lignin and the starch caused the generation of compact structures.

In addition, Stasi et al. (2020) employed carbon ashes sourced from agricultural waste rich in lignocellulose to augment the mechanical characteristics of the thermoplastic maize starch matrix. The present study investigated the impact of carbon ashes on the mechanical behavior of thermoplastic maize starch. The findings revealed that the incorporation of carbon ashes resulted in a 15% rise in Young's modulus, a decline in elongation at break from 0.66 to 0.33, and a 14% reduction in the value of tensile strength.

The study conducted by Ayu et al. (2020) investigated the utilization of modified tapioca starch and polybutylene succinate (PBS) as a biodegradable matrix for bio-composite films. The said matrix was reinforced with empty fruit bunch fibers. In this study, biodegradable films were created using a consistent combination of PBS and modified tapioca starch. The volume fractions of fibers were altered to observe their effects. The incorporation of higher amounts of empty fruit bunch fiber content resulted in a notable decrease in both Young's modulus and tensile strength values, with reductions of 28% and 37%, respectively, observed at a fiber content of 50 wt%. The authors elucidated the matrix and fiber interactions through the lens of inadequate interfacial adhesion, disparities in functional groups, and non-uniform filler dispersion.

The study conducted by Finkenstadt and Tisserat (2010) aimed to assess the properties of biocomposite films of poly(lactic acid) (PLA) containing Osage orange wood fibers with varying particle sizes and weight percentages of 0, 10, and 25 wt%. Overall, the utilization of PLA/Osage orange wood fibers in the production of biodegradable mulch films resulted in marginal enhancements in terms of Young's modulus values at 25 wt% in comparison to pure PLA. In contrast, the elongation at break and tensile strength values exhibited a decrease when Osage wood fibers with a size of 400 nm and a weight percentage of 25 were employed; specifically, the elongation at break decreased from 18.7% to 8%, and the tensile strength decreased from 57.3 MPa to 36.6 MPa.

Merino and Alvarez (2020) investigated the use of natural seaweed microparticles as fillers in a thermoplastic starch blend matrix for the production of biodegradable mulch films. The incorporation of a low filler content resulted in enhancements in elongation at break, while the bio-composites Young's modulus increased. The addition of 10 weight percent of filler resulted in a decrease in the value of Young's modulus. According to the authors, the trend observed in Young's modulus can be attributed to the favorable adhesion and chemical compatibility between the matrix and seaweed microparticles. Discontinuities may arise at elevated levels of filler content, and the elongation during break behavior can also be impacted. Table 3 summarizes the mechanical properties of biodegradable composites used in mulches.

A novel agricultural mulch film, which is extremely stretchy, biodegradable, and entirely biobased, has been developed by Merino et al. (2022) at a price comparable to LDPE (Figure 5). They combine amorphous polylactic acid (PLA), 10 wt% epoxidized soybean oil methyl ester (ESOME), and inedible vegetable leftovers as fillers at various ratios to create composite materials for biodegradable mulches. The biodegradability of the films was found to be greatly impacted by the type of vegetable waste used as a filler. For instance, following 6 months of a soil burial experiment, PLA composites' biodegradability in soil rose from 0 to 38 wt% when films made with 20 wt% of spinach stems were used. The results also demonstrated that, depending on the type and quantity of vegetable waste added, proper PLA plasticization and vegetable waste addition can produce mulching-ready film with tensile strengths in the 10–24 MPa range and elongation at break values up to 460%.

The biodegradability of polysaccharides can be attributed to the presence of numerous hydrophilic polar functional groups in their polymeric chain. The biodegradability of polysaccharides in composite materials is altered when they are used as fillers or in the matrix. This affects the biodegradability of bio-composite films, which is influenced by factors such as chemical structure (Garrison et al., 2016), crosslinking density (Garrison et al., 2016), the nature of the components, and soil conditions.

Table 3
The mechanical properties of biodegradable composites for mulches

Filler	Matrix	Properties	References
Starch and sugarcane, apple fibers and orange waste	Polyvinyl alcohol	By adding 25% wt% starch content to PVA/orange and PVA/apple pomace fiber bio-composites, elongation at break values drop from 105.4% and 149.7% without filler to 29.6% and 65%, respectively. Tensile strength improved somewhat for PVA/sugarcane bagasse fibers with 25 wt% starch, which doubled their tensile strength values.	Chiellini et al., 2001
Starch	Poly(butylene succinate) (PBS)	Increasing starch content led to a decrease in tensile strength values from 37.2 MPa to 5.7 MPa, with a minor improvement in elongation at break but a decline in the parameter with higher starch content.	Flores et al., 2009
Kraft pulp microfibrillated cellulose	Mango seed starch matrix	Microfibrillated cellulose in mango seed starch matrix increased tensile strength and Young's modulus. Fillers loaded from 0% to 40% enhanced Young's modulus from 1.347 to 2.407 GPa.	Patil & Netravali, 2016
Microparticles from chemically modified starch	Maize starch	Tensile strength rose by over 47% and 21%, Young's modulus fell by 8% and 31%, and elongation at break decreased by almost 39% and 30%.	Spiridon et al., 2011
Agricultural waste carbon ashes	Maize starch	The addition of carbon ashes led to a 15% increase in Young's modulus, a decrease in elongation at break from 0.66 to 0.33, and a 14% reduction in tensile strength.	Stasi et al., 2020
Empty fruit bunch fibers	Tapioca starch and polybutylene succinate (PBS)	The addition of empty fruit bunch fiber significantly reduced Young's modulus and tensile strength values by 28% and 37% at a fiber content of 50 wt%.	Ayu et al., 2020

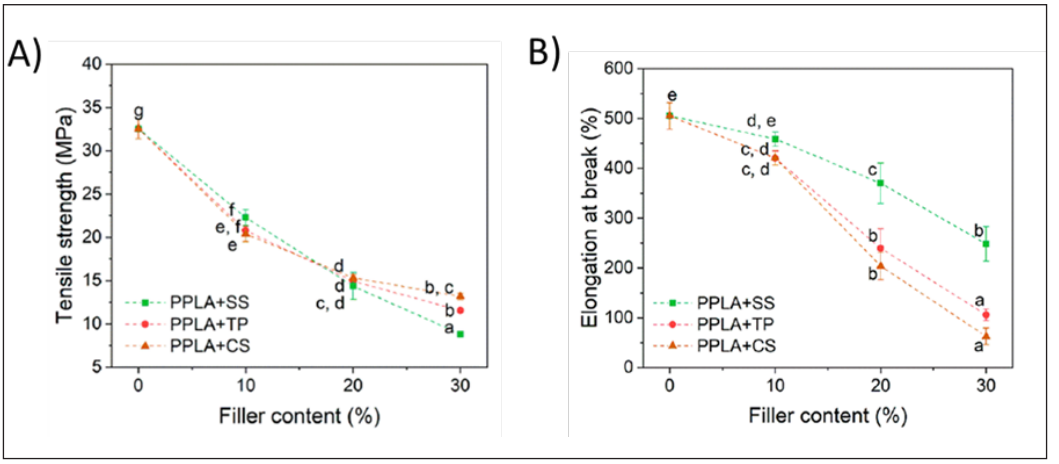

Figure 5. A) Tensile strength (MPa) and B) Elongation at break (%) of PPLA and its composites with 10, 20, and 30 wt% spinach stems (SS), tomato pomace (TP), or cocoa shells (CS). PPLA is the plasticized PLA with 10 wt% ESOME (Merino et al., 2022)

In the past, initial investigations into the biodegradability of biocomposite-based biodegradable mulch films centered on the assessment of mineralization tests conducted by soil microorganisms. Corti et al. (2002), Imam et al. (2005), and Chiellini et al. (2008) are examples of cases that have been studied. The authors incorporated blended polysaccharides or polysaccharide fillers into their research to augment the rate of biodegradability of PVA. Polyvinyl alcohol (PVA) is a vinyl polymer that comprises oxidizable functional groups within its polymeric chain. According to Briassoulis' (2004) report, secondary alcohol peroxidases isolated from soil have demonstrated the ability to effectively biodegrade PVA, indicating its high biodegradability.

The research carried out by Corti et al. (2002) sought to examine the influence of incorporating sugar cane bagasse, a naturally occurring filler, into the PVA matrix on the biodegradability of biocomposites. According to the authors' study, after an incubation period of 160 days, the mineralization of PVA containing 50 wt% sugar cane achieved a plateau of around 23.7%. The incorporation of a hydrophilic organic filler into the PVA matrix is responsible for the significant two-fold increase in mineralization of PVA film shown by the aforementioned value.

Imam et al. (2005) fabricated bio-composites utilizing PVA and PVA with lignocellulosic fibers that were strengthened with maize starch. The researchers then conducted a comparative analysis of the biodegradability of these composites over a 120-day period while they were exposed to prevailing environmental conditions in the soil. Following 90 days, the bio-composite films exhibited a notable decrease in both their dimensions and overall mass. In relation to the PVA composite filled with corn starch, it was observed that the film experienced a weight loss of around 51% from its original weight. Conversely, the

PVA/lignocellulosic fiber film filled with corn starch exhibited a weight reduction of 41%. One possible explanation for the discrepancy between the bio-composite films is that the PVA/lignocellulosic film, which features stronger crosslinking, degrades at a slower rate.

In contemporary times, there has been a growing interest in exploring alternative biopolymers as matrices or reinforcements to assess their biodegradability. Examples of such biopolymers include kenaf fibers (Pua et al., 2013), PBAT (Wang et al., 2015), chitosan (Arrieta et al., 2016), cotton fibers (Tan et al., 2016) and carnauba wax (Oliveira et al., 2019).

Pua et al. (2013) created citric acid and NaOH-modified kenaf/PVA composite films with different fiber concentrations. The weight of these bio-composite films was measured 15 days before and after a soil burial test to determine their biodegradability. The films became fragile, brittle, and weightless after being buried in the soil. Fiber loading worsened citric acid and NaOH-modified kenaf with PVA films. PVA film without fibers lost less weight (1.6%) than kenaf PVA bio-composites after 15 days. The biggest weight loss was 8.9% with 15 wt% citric acid-modified kenaf with PVA, followed by 7.73% with 5 wt% NaOH. The significant degradability of kenaf fibers is explained by the fact that all samples lost more weight than the pristine PVA film.

Moreover, Tan et al. (2016) fabricated mulch films composed of biodegradable polymers and natural fibers, as reported in their study. The biodegradable composites were made of cotton fiber combined with starch and cotton fiber combined with PVA, with a loading of biodegradable polymer equal to 16 wt%. The process of biodegradation was examined through laboratory and field-based soil burial tests. After 45 days, the cotton fiber/PVA composite exhibited a weight loss of approximately 54% due to biodegradation. The findings of both laboratory and field tests suggest that cotton fiber with starch has the potential to serve as a viable option for crops with abbreviated growth cycles, owing to its rapid rate of decomposition in soil.

The impact of incorporating small quantities of chitosan on the disintegration characteristic of the PLA/PHB matrix was investigated by Arrieta et al. (2016). The study examined three distinct biocomposites with the aim of producing electrospun mats that are both flexible and degradable, utilizing PLA-PHB as the base material. The biocomposites were composed of varying amounts of chitosan, specifically 0, 1, and 5 wt%. The researchers investigated the biodegradability of the films under composting conditions at a laboratory scale over 37 days. Their findings indicated that all biocomposite films underwent disintegration. The researchers arrived at the conclusion that the incorporation of chitosan, an organic filler, led to an augmentation in the rate of disintegration.

The addition of polysaccharide fillers has been observed to enhance the biodegradation rates of PVA-based mulches. According to Imam et al. (2005), mulch films that were fortified with 20% starch demonstrated a biodegradation rate of almost 50% after three

months. Similarly, Chiellini et al. (2008) found that mulches composed of PVA as a matrix and green algae with corn starch as fillers also exhibited a biodegradation rate of nearly 50%. Regrettably, all of the PVA mulch films under investigation failed to attain complete biodegradation. The biodegradation rates of PBAT-based mulches are affected differently by the inclusion of polysaccharides. According to a study conducted by Wang et al. (2015), there is a positive correlation between the starch content of mulches and their weight loss. Conversely, Oliveira et al. (2019) found that mulches with a 5% sugar cane content retained more weight than those with a 2.5% content. However, this trend was altered upon the inclusion of carnauba wax.

In summary, based on the findings, it appears crucial and obligatory to adhere to crop schedules. To adhere to the process of biodegradation, it is possible to alter the biodegradability rates of polysaccharide-based biodegradable mulch film by incorporating organic fillers and/or additives. It is recommended that endeavors be undertaken to conduct biodegradation analyses that compare various biocomposite biodegradable mulch films featuring distinct organic filler contents over an extended period.

BIODEGRADABLE COMPOSITES FOR CONTROLLED-RELEASE FERTILIZER

The implementation of controlled-release fertilizer in agricultural settings has emerged as a viable strategy for promoting long-term sustainability and safeguarding the environment. According to Liu et al. (2020), controlled-release fertilizers offer a regulated supply of nutrients to plants for a predetermined duration, thereby minimizing the loss of fertilizers into the soil. The utilization of controlled-release fertilizers (CRFs) has been the subject of significant research efforts aimed at delivering nutrients to the intended target in a more secure, cost-effective, and efficient manner. CRFs are designed to release nutrients at a desired concentration level and rate, thereby prolonging their availability in the soil. The application of this technique results in an enhancement of nutrient use efficiency (NUE) due to reduced frequency of dosing, as well as a decrease in environmental hazards by mitigating the rate of nutrient removal from the soil through precipitation or irrigation, as noted by Lawrencia et al. (2021). In contemporary times, the academic community has directed its attention towards composite technologies as a means to enhance the properties of controlled-release fertilizers. The term "composite material" refers to a combination of two or more materials that results in a final product possessing properties that surpass those of the individual constituent materials. In contemporary discourse, composite materials are frequently referred to as reinforcement arrangements or fillers that are incorporated within a matrix. According to Hsissou et al. (2021), the matrix is responsible for maintaining the coherence and alignment of the load.

The use of modern adsorbents, such as bentonite nanoclays, montmorillonite (MMT), zeolite, and halloysite, is prevalent in the production of coating materials. This is because of their exceptional cation exchange properties, as noted by Dubey and Mailapalli (2019). The use of nonionic polymers to modify the surface of clays like bentonite and MMT has become a popular method for enhancing the properties of polymers. This is due to the unique characteristics of these clays, including their mechanical and thermal properties, as well as their ability to absorb water. This information is supported by a study conducted by Zhao et al. (2018). The cost-effective and eco-friendly Montmorillonite (MMT) is a type of nanomaterial. According to Abdel-Wahhab et al. (2015), MMT is classified as a 2:1 type silicate within the structural family. This type of silicate consists of a layer of aluminum oxide dioctahedral that is situated between two layers of silicon oxytetrahedron.

Several investigations have been conducted using bentonite and montmorillonite as additives in polymer coatings to regulate the release of fertilizers (Bortolin et al., 2013; Liao et al., 2021; Sarkar et al., 2021; Ying et al., 2012; Zhao et al., 2018). Zhao et al. (2018) conducted a study wherein bentonite was subjected to modification through intercalation of polyethylene glycol within the interlayer space. The modified bentonite was then utilized in the preparation of polyurethane using in-situ polymerization with bentonite/isocyanate and soybean oil-based polyols. The resulting polyurethane was utilized as a coating for urea granules to reduce the rate of nitrogen release. Compared to pure PU, there has been a 27.5% increase in tensile strength and a 68% increase in breaking elongation. The coated PU-5%-bentonite composites exhibited a release duration of 74 days, as per the findings. Sarkar et al. (2021) developed biodegradable encapsulating films by blending clay and polymeric materials (starch/PVA). The clay used in the study was obtained from economically viable bentonite fractions. The encapsulating films were utilized for the production of diammonium phosphate (DAP) that was encapsulated within the CPSBs. The findings indicate that an increase in bentonite content (0–20 wt%) led to a reduction in both porosity and water absorption. The Korsmeyer-Peppas model was found to be a suitable fit for the release of nitrogen (N) and phosphorus (P) data obtained from the fertilizer. An increased proportion of bentonite in the composition of controlled-release fertilizers has been found to enhance structural stability and decrease the release of nitrogen and phosphorus from diammonium phosphate.

The study conducted by Ying et al. (2012) involved modifying urea-formaldehyde (UF) resins with montmorillonite (MMT) to create coating materials for controlled-release fertilizers. The addition of MMT to UF resins results in improved mechanical properties. The addition of 3% MMT to modified UF resin results in a significant increase in shear strength, with a nearly 20% improvement observed. The maximum shear strength is achieved under these conditions. The study reveals that the urea permeation rate of UF resin membranes that have been modified is inversely proportional to the thickness of

the membrane, while it is directly proportional to the content of MMT. Qu et al. (2015) conducted a study on the modification of urea-formaldehyde (UF) resins using soy protein isolates (HSPI) through copolymerization. The researchers aimed to investigate the impact of HSPI on the biodegradability of UF resins. According to Qu et al. (2015), the addition of HSPI with a lower hydrolysis degree to the system resulted in an accelerated rate of degradation.

Liao et al. (2021) incorporated MMT into a coating made of starch-based polyurethane (SPU) to enhance the regulation of nutrient release. The utilization of dodecyl dihydroxyethyl methyl ammonium chloride (DDMAC) as a cation exchange agent has been implemented to alter the properties of MMT. This modification is anticipated to enhance the hydrophobicity and dispersibility of MMT in SPU. The findings indicate that the dispersion of MMT particles within the SPU matrix was effective, resulting in an SPU/MMT composite coating that exhibited a denser and more resilient morphology with reduced visible porosity in comparison to SPU coatings. The increase in MMT content to 3% resulted in a prolonged duration of 49 days for the release of 75% nitrogen, which is significantly longer than the 14 days observed with SPU coating.

Wu et al. (2007) have prepared the encapsulation of Phosphate-solubilizing bacteria (PSB) cells in biodegradable capsules using PCL as the core matrix material and clay and starch as fillers to modify their physical properties, including permeability, biodegradability, and mechanical strength. Capsules are formulated to address challenges encountered in the practical application of bacterial cells as fertilizers. The system is designed to safeguard the cells while also enabling their gradual release into the soil in a manageable fashion. The findings indicate that PSB effectively decomposed all the cell-encapsulated capsules composed of PCL and PCL composites, leading to a sustained release of cells. The biodegradability of the capsules was observed to increase with the inclusion of starch, while the composites blended with clay exhibited lower biodegradability. The quantity and velocity of cell discharge from capsules made of PCL and encapsulated in cells were found to be directly proportional to the level of biodegradability and inversely proportional to the reduction in mechanical strength. However, the manner in which cells were released exhibited a high degree of similarity across all varieties of capsules.

In a study conducted by Harmaen et al. (2015), a slow-release fertilizer was created through the utilization of the extrusion technique. This was achieved by blending granular NPK fertilizer and empty fruit bunch (EFB) fibers. The thermal stability of BpF (bioplastic fertilizer) composites was found to be enhanced by the synergistic effect of PLA and EFB fibers. A homogenous blend of BpF was observed through the use of a scanning electron microscope (SEM). The biodegradation process resulted in a greater percentage of weight loss for fertilizers containing PLA and EFB fibers, primarily attributed to the inclusion of EFB fibers. Specifically, the weight loss percentages were 64.3% and 76.3%, respectively. In the course of the soil burial experiment, the fertilizer exhibited swelling and subsequently

permeated the tea bag. The degradation and solubility of fertilizer were impacted by factors such as temperature, moisture content, and soil water content.

Melaj et al. (2019) developed biodegradable polymer blends based on hydroxypropyl methylcellulose (HPMC) and chitosan to improve mechanical properties for coating tablets and granules. HMPC film has short soil durability, disappearing within 8 days. Chitosan films have more permanence, lasting 85 days in soil. The addition of chitosan to HPMC results in a longer-lasting film with a durability of 78 days, as compared to HPMC alone. Samples tested under conditions of higher relative humidity (76% RH) exhibited a decrease in Young's Modulus and resistance, whereas there was an increase in elongation at break. This may be due to synergistic or cumulative effects of plasticizers like glycerol, a low-molecular-weight, hygroscopic plasticizer that adds water to the polymer matrix.

In accordance with Ge et al. (2002) and Majeed et al. (2014), the incorporation of additives such as cellulose, starch and lignin has been found to improve the biodegradability of both natural and synthetic PC-CRFs. The biodegradability of synthetic materials was enhanced in mixed blends of starch/polysulfone (Tomaszewska & Jarosiewicz, 2004), starch/polyvinyl alcohol (PVA) (Han et al., 2009), starch/polyurethane (PU) (Ge et al., 2002) and ethyl cellulose (EC)/poly(3-hydroxybutyrate) PHB (Costa et al., 2013). Peng and Chen (2011) reported that the incorporation of lignin in a PU-based hydrogel resulted in an improvement in biodegradability. Conversely, the addition of PU chains to a lignin-based hydrogel was found to enhance its strength for coating ammonium sulfate. Singh and Sharma (2007) reported a degradation rate of 37% in polystyrene-g-starch samples after 160 days of incubation with soil media. The duration for which nutrients are released by fertilizers coated with lignin, cellulose, or starch is relatively brief, typically less than 30 days, as reported by Jamnongkan and Kaewpirom (2010) and Mulder et al. (2011). Polymer blends and composites derived from both natural and synthetic sources exhibit distinct differences in their biodegradation, which can be attributed to variations in microbial susceptibility, novel chemical linkages, and structural configuration.

THE CORRELATION EFFECT OF BIODEGRADABLE POLYMER COMPOSITES ON MECHANICAL AND BIODEGRADABLE PROPERTIES IN AGRICULTURAL APPLICATIONS

Biodegradable polymer composites have garnered significant attention in recent years due to their potential for sustainable and eco-friendly applications, particularly in the agricultural sector. These materials offer a promising solution to the environmental challenges posed by conventional petroleum-based plastics, which can have a detrimental impact on the environment (Chiellini et al., 2008).

The correlation between the mechanical and biodegradable properties of these composites is crucial, as it determines their suitability for various agricultural applications.

Nanofiller-reinforced biodegradable polymer composites, for instance, can exhibit enhanced mechanical properties while maintaining their biodegradability, making them suitable for use in mulches, controlled-release herbicides and pesticides, and controlled-release fertilizers (Sun et al., 2018).

Mulches, which are often used in agriculture to suppress weed growth, retain soil moisture, and moderate soil temperature, can benefit from the incorporation of biodegradable polymer composites. These composites can provide improved mechanical strength and durability, ensuring the mulch remains intact and effective for a longer period. Furthermore, the biodegradable nature of the composites ensures that they can eventually break down in the soil, minimizing environmental impact.

Controlled-release herbicides and pesticides are another area where biodegradable polymer composites can have a significant impact. These composites can be designed to gradually release the active ingredients, reducing the need for frequent application and minimizing the risk of environmental contamination. Similarly, controlled-release fertilizers can also be formulated using biodegradable polymer composites, allowing for a more efficient and sustainable delivery of nutrients to plants.

Recent studies have highlighted the potential of ternary blend system polybutylene adipate-co-terephthalate, polylactic acid, polypropylene carbonate and added lactic acid–isopropyl carbonate copolymer (PBAT/PLA-PPC-PTLA) polymer composites, to enhance the tensile strength, water vapor barrier properties and comparable biodegradation rate, making them suitable for a wide range of agricultural applications (Guo et al., 2024).

CONCLUSION

The incorporation of fillers, such as cellulose, agricultural waste, and diverse types of clay, has the potential to enhance the properties of biodegradable polymers that have been previously produced. The utilization of biodegradable polymers is advantageous for soil and microorganisms due to their capacity to mitigate the environmental impact of non-biodegradable plastics. Furthermore, the efficacy of these biodegradable polymers is comparable and commendable.

At the same time, it is imperative and mandatory to comply with crop schedules. In order to conform to the biodegradation process, it is feasible to modify the biodegradability rates of biodegradable mulch film through the integration of organic fillers and/or additives. It is advisable to initiate endeavors to carry out biodegradation assessments that juxtapose diverse bio-composite biodegradable mulch films that exhibit discrete organic filler concentrations for a prolonged duration. A thorough evaluation of fillers and matrices is imperative to satisfy the mechanical characteristics of plastic mulch and the controlled release requirements of herbicides, pesticides, and fertilizers.

Moreover, the correlation between the mechanical and biodegradable properties of polymer composites is crucial for their successful application in the agricultural sector. Biodegradable polymer composites, including nanofiller-reinforced systems, offer a sustainable solution for the development of mulches, controlled-release herbicides and pesticides, and controlled-release fertilizers, with the potential to address environmental concerns while maintaining the necessary functional properties.

ACKNOWLEDGEMENT

This work was funded by the Ministry of Higher Education under the Fundamental Research Grant Scheme (FRGS/1/2023/TK09/UTM/02/18).

REFERENCES

Abdel-Wahhab, M. A., El-Denshary, E. S., El-Nekeety, A. A., Abdel-Wahhab, K. G., Hamzawy, M. A., Elyamany, M. F., Hassan, N. S., Mannaa, F. A., Shaiea, M. N., & Gado, R. A. (2015). Efficacy of organo-modified nano montmorillonite to protect against the cumulative health risk of aflatoxin B 1 and ochratoxin A in Rats. *Soft Nanoscience Letters, 5*(2), Article 21. https://doi.org/10.4236/snl.2015.52004

Albertsson, A. C., Andersson, S. O., & Karlsson, S. (1987). The mechanism of biodegradation of polyethylene. *Polymer Degradation and Stability, 18*(1), 73-87. https://doi.org/10.1016/0141-3910(87)90084-X

Altaee, N., El-Hiti, G. A., Fahdil, A., Sudesh, K., & Yousif, E. (2016). Biodegradation of different formulations of polyhydroxybutyrate films in soil. *SpringerPlus, 5*(1), Article 762. https://doi.org/10.1186/s40064-016-2480-2

Amin, A. R. (2001). LDPE/EPDM multilayer films containing recycled LDPE for greenhouse applications. *Journal of Polymers and the Environment, 9*(1), 25-30. https://doi.org/10.1023/A:1016040403779

Arrieta, M. P., López, J., López, D., Kenny, J. M., & Peponi, L. (2016). Effect of chitosan and catechin addition on the structural, thermal, mechanical and disintegration properties of plasticized electrospun PLA-PHB biocomposites. *Polymer Degradation and Stability, 132*, 145-156. /https://doi.org/10.1016/j.polymdegradstab.2016.02.027

Ayu, R. S., Khalina, A., Harmaen, A. S., Zaman, K., Mohd Nurrazi, N., Isma, T., & Lee, C. H. (2020). Effect of empty fruit brunch reinforcement in polybutylene-Succinate/modified tapioca starch blend for agricultural mulch films. *Scientific Reports, 10*(1), Article 1166. https://doi.org/10.1038/s41598-020-58278-y

Bortolin, A., Aouada, F. A., Mattoso, L. H. C., & Ribeiro, C. (2013). Nanocomposite PAAm/methyl cellulose/montmorillonite hydrogel: Evidence of synergistic effects for the slow release of fertilizers. *Journal of Agricultural and Food Chemistry, 61*(31), 7431-7439. https://doi.org/10.1021/jf401273n

Briassoulis, D. (2004). An overview on the mechanical behaviour of biodegradable agricultural films. *Journal of Polymers and the Environment, 12*(2), 65-81. https://doi.org/10.1023/B:JOOE.0000010052.86786.ef

Briassoulis, D. (2006). Mechanical behaviour of biodegradable agricultural films under real field conditions. *Polymer Degradation and Stability, 91*(6), 1256-1272. https://doi.org/10.1016/j.polymdegradstab.2005.09.016

Chiellini, E., Cinelli, P., Ilieva, V. I., & Martera, M. (2008). Biodegradable thermoplastic composites based on polyvinyl alcohol and algae. *Biomacromolecules, 9*(3), 1007-1013. https://doi.org/10.1021/bm701041e

Chiellini, E., Cinelli, P., Imam, S. H., & Mao, L. (2001). Composite films based on poly(vinylalcohol) and lignocellulosic fibers. In E. Chiellini, H. Gil, G. Braunegg, J. Buchert, P. Gatenholm & M. Zee (Eds.) *Biorelated polymers: Sustainable polymer science and technology* (pp. 87-100). Springer. https://doi.org/10.1007/978-1-4757-3374-7_8

Cho, H. S., Moon, H. S., Kim, M., Nam, K., & Kim, J. Y. (2011). Biodegradability and biodegradation rate of poly(caprolactone)-starch blend and poly(butylene succinate) biodegradable polymer under aerobic and anaerobic environment. *Waste Management, 31*(3), 475-480. https://doi.org/10.1016/j.wasman.2010.10.029

Corti, A., Cinelli, P., D'Antone, S., Kenawy, E.-R., & Solaro, R. (2002). Biodegradation of poly(vinyl alcohol) in soil environment: Influence of natural organic fillers and structural parameters. *Macromolecular Chemistry and Physics, 203*(10-11), 1526-1531. https://doi.org/10.1002/1521-3935(200207)203:10/11<1526::AID-MACP1526>3.0.CO;2-R

Costa, M. M., Cabral-Albuquerque, E. C., Alves, T. L., Pinto, J. C., & Fialho, R. L. (2013). Use of polyhydroxybutyrate and ethyl cellulose for coating of urea granules. *Journal of Agricultureal and Food Chemistry, 61*(42), 9984-9991. https://doi.org/10.1021/jf401185y

Coventry, J. M., Fisher, K. H., Strommer, J. N., & Reynolds, A. G. (2005). Reflective mulch to enhance berry quality in ontario wine grapes. *ISHS Acta Hortic. 689*, 95-102 https://doi.org/10.17660/ActaHortic.2005.689.7

Dhaliwal, K. (2018). Biodegradable polymers and their role in drug delivery systems. *Biomedical Journal of Scientific & Technical Research, 11*(1), 8315-8320. https://doi.org/10.26717/BJSTR.2018.11.002056

Dubey, A., & Mailapalli, D. R. (2019). Zeolite coated urea fertilizer using different binders: Fabrication, material properties and nitrogen release studies. *Environmental Technology & Innovation, 16*, Article 100452. https://doi.org/10.1016/j.eti.2019.100452

Espí, E., Salmerón, A., Fontecha, A., García, Y., & Real, A. I. (2006). Plastic films for agricultural applications. *Journal of Plastic Film & Sheeting*, *22*(2), 85-102. https://doi.org/10.1177/8756087906064220

Finkenstadt, V. L., & Tisserat, B. (2010). Poly (lactic acid) and osage orange wood fiber composites for agricultural mulch films. *Industrial Crops and Products, 31*(2), 316-320. https://doi.org/10.1016/j.indcrop.2009.11.012

Fitriani, F., Aprilia, S., Mahardika, M., Masruchin, N., & Rinaldi, W. (2025). Development of hybrid biodegradable polymer based on polyvinyl alcohol and whey protein isolate reinforced with cellulose nanocrystal from pineapple crown leaf. *Case Studies in Chemical and Environmental Engineering, 11*, Article 101061. https://doi.org/10.1016/j.cscee.2024.101061

Flores, E. D., Funabashi, M., & Kunioka, M. (2009). Mechanical properties and biomass carbon ratios of poly (butylene succinate) composites filled with starch and cellulose filler using furfural as plasticizer. *Journal of Applied Polymer Science, 112*(6), 3410-3417. https://doi.org/10.1002/app.29777

Fowler, P., Hughes, M., & Elias, R. (2006). Biocomposites: Technology, environmental credentials and market forces. *Journal of the Science of Food and Agriculture, 86*, 1781-1789. https://doi.org/10.1002/jsfa.2558

Garrison, T. F., Murawski, A., & Quirino, R. L. (2016). Bio-based polymers with potential for biodegradability. *Polymers, 8*(7), Article 262. https://doi.org/10.3390/polym8070262

Ge, J., Wu, R., Shi, X., Yu, H., Wang, M., & Li, W. (2002). Biodegradable polyurethane materials from bark and starch. II. Coating material for controlled-release fertilizer. *Journal of Applied Polymer Science, 86*(12), 2948-2952. https://doi.org/10.1002/app.11211

Geyer, R., Jambeck, J. R., & Law, K. L. (2017). Production, use, and fate of all plastics ever made. *Science Advances, 3*(7), Article e1700782. https://doi.org/10.1126/sciadv.1700782

Giroto, A. S., de Campos, A., Pereira, E. I., Cruz, C. C. T., Marconcini, J. M., & Ribeiro, C. (2014). Study of a nanocomposite starch–clay for slow-release of herbicides: Evidence of synergistic effects between the biodegradable matrix and exfoliated clay on herbicide release control. *Journal of Applied Polymer Science, 131*(23), Article 41188. https://doi.org/10.1002/app.41188

Guo, B., Zhu, L., He, X., Zhou, X., Dong, B., & Liu, J. (2024). Modified composite biodegradable mulch for crop growth and sustainable agriculture. *Polymers, 16*(9), Article 1295. https://doi.org/10.3390/polym16091295

Han, X., Chen, S., & Hu, X. (2009). Controlled-release fertilizer encapsulated by starch/polyvinyl alcohol coating. *Desalination, 240*(1), 21-26. https://doi.org/10.1016/j.desal.2008.01.047

Harmaen, A., Abdan, K., Hassan, M., Ibrahim, N., & Jawaid, M. (2015). Characterisation and biodegradation of poly (lactic acid) blended with oil palm biomass and fertiliser for bioplastic fertiliser composites. *BioResources, 11*(1), 2055-2070. https://doi.org/10.15376/biores.11.1.2055-2070

Hsissou, R., Seghiri, R., Benzekri, Z., Hilali, M., Rafik, M., & Elharfi, A. (2021). Polymer composite materials: A comprehensive review. *Composite Structures, 262*, Article 113640. https://doi.org/10.1016/j.compstruct.2021.113640

Huang, B., Liu, M., & Zhou, C. (2017). Cellulose–halloysite nanotube composite hydrogels for curcumin delivery. *Cellulose, 24*(7), 2861-2875. https://doi.org/10.1007/s10570-017-1316-8

Huber, T., Müssig, J., Curnow, O., Pang, S., Bickerton, S., & Staiger, M. P. (2012). A critical review of all-cellulose composites. *Journal of Materials Science, 47*(3), 1171-1186. https://doi.org/10.1007/s10853-011-5774-3

Hussain, I., & Hamid, H. (2003). Plastics in agriculture. In A. L. Andrady (Ed.) *Plastics and the environment* (pp. 185-209). Wiley. https://doi.org/10.1002/0471721557.ch5

Imam, S. H., Cinelli, P., Gordon, S. H., & Chiellini, E. (2005). Characterization of biodegradable composite films prepared from blends of poly (vinyl alcohol), cornstarch, and lignocellulosic fiber. *Journal of Polymers and the Environment, 13*(1), 47-55. https://doi.org/10.1007/s10924-004-1215-6

Jamnongkan, T., & Kaewpirom, S. (2010). Controlled-release fertilizer based on chitosan hydrogel: Phosphorus release kinetics. *Science Journal Ubon Ratchathani University, 1*(1), 43-50.

Kasirajan, S., & Ngouajio, M. (2012). Polyethylene and biodegradable mulches for agricultural applications: A review. *Agronomy for Sustainable Development, 32*(2), 501-529. https://doi.org/10.1007/s13593-011-0068-3

Kasperbauer, M. J., & Loughrin, J. (2004). Butterbean seed yield, color, and protein content are affected by photomorphogenesis. *Crop Science, 44*(6), 2123-2126. https://doi.org/10.2135/cropsci2004.2123

Khalil, H. P. S. A., Chong, E. W. N., Owolabi, F. A. T., Asniza, M., Tye, Y. Y., Rizal, S., Fazita, M. R N.., Haafiz, M. K. M., Nurmiati, Z., & Paridah, M. T. (2019). Enhancement of basic properties of polysaccharide-based composites with organic and inorganic fillers: A review. *Journal of Applied Polymer Science, 136*(12), Article 47251. https://doi.org/https://doi.org/10.1002/app.47251

Kijchavengkul, T., Auras, R., Rubino, M., Ngouajio, M., & Fernandez, R. T. (2008). Assessment of aliphatic-aromatic copolyester biodegradable mulch films. Part II: laboratory simulated conditions. *Chemosphere, 71*(9), 1607-1616. https://doi.org/10.1016/j.chemosphere.2008.01.037

Kim, E., Choi, D., & Jin, S. (2008). Effect of pre-harvest reflective mulch on growth and fruit quality of plum (Prunus domestica L.). *Acta Horticulturae*, *772,* 323-326. https://doi.org/10.17660/ActaHortic.2008.772.54

Kiselev, E. G., Zhila, N. O., & Volova, T. G. (2021). Biodegradable polymers – perspectives and applications in agriculture. *IOP Conference Series: Earth and Environmental Science, 689*(1), Article 012036. https://doi.org/10.1088/1755-1315/689/1/012036

Kumar, J., Shakil, N., Chander, S., Walia, S., Shukla, L., & Parmar, B. S. (2010). Field appraisal of controlled release formulations of cartap hydrochloride against rice leaf folder (Cnaphalocrocis medinalis). *Indian Journal of Agricultural Research, 80*(5), 405-408.

Lawrencia, D., Wong, S. K., Low, D. Y. S., Goh, B. H., Goh, J. K., Ruktanonchai, U. R., Soottitantawat, A., Lee, L. H., & Tang, S. Y. (2021). Controlled release fertilizers: A review on coating materials and mechanism of release. *Plants, 10*(2), Article 238. https://doi.org/10.3390/plants10020238

Li, M., Huang, Q., & Wu, Y. (2011). A novel chitosan-poly (lactide) copolymer and its submicron particles as imidacloprid carriers. *Pest Management Science, 67*(7), 831-836. https://doi.org/10.1002/ps.2120

Liao, Y., Liu, L., Wang, M., Li, L. X., Cao, B., Wang, H., & Huang, W. Q. (2021). Preparation and properties of starch-based polyurethane/montmorillonite composite coatings for controlled-release fertilizer. *Polymer Composites, 42*(5), 2293-2304. https://doi.org/10.1002/pc.25977

Liu, L., Ni, Y., Zhi, Y., Zhao, W., Pudukudy, M., Jia, Q., Shan, S., Zhang, K., & Li, X. (2020). Sustainable and biodegradable copolymers from SO_2 and Renewable eugenol: A novel urea fertilizer coating material with superio slow release performance. *Macromolecules, 53*(3), 936-945. https://doi.org/10.1021/acs.macromol.9b02202

Luckachan, G. E., & Pillai, C. K. S. (2011). Biodegradable polymers- A review on recent trends and emerging perspectives. *Journal of Polymers and the Environment, 19*(3), 637-676. https://doi.org/10.1007/s10924-011-0317-1

Majeed, Z., Ramli, N. K., Mansor, N., & Man, Z. (2014). Lignin loading effect on biodegradability and nitrogen release properties of urea modified tapioca starch in wet soil. *Key Engineering Materials, 594-595*, 798-802. https://doi.org/10.4028/www.scientific.net/KEM.594-595.798

Mei, X., Liang, Y., Zhang, T., Ning, J., & Wang, Z. (2014). An amphiphilic chitosan-Polylactide graft copolymer and its nanoparticles as fungicide carriers. *Advanced Materials Research, 1051*, 21-28. https://doi.org/10.4028/www.scientific.net/AMR.1051.21

Melaj, M. A., Daraio, M. E., & Vazquez, A. (2019). Controlled release on sand bed columns and biodegradability in soil of chitosan: Hydroxypropyl methylcellulose films. *Journal of Applied Polymer Science, 136*(20), Article 47532. https://doi.org/10.1002/app.47532

Merino, D., & Alvarez, V. A. (2020). Green microcomposites from renewable resources: Effect of seaweed (Undaria pinnatifida) as filler on corn starch–chitosan film properties. *Journal of Polymers and the Environment, 28*(2), 500-516. https://doi.org/10.1007/s10924-019-01622-9

Merino, D., Gutiérrez, T. J., Mansilla, A. Y., Casalongué, C. A., & Alvarez, V. A. (2018). Critical evaluation of starch-based antibacterial nanocomposites as agricultural mulch films: Study on their interactions with water and light. *ACS Sustainable Chemistry & Engineering, 6*(11), 15662-15672. https://doi.org/10.1021/acssuschemeng.8b04162

Merino, D., Zych, A., & Athanassiou, A. (2022). Biodegradable and biobased mulch films: Highly stretchable PLA composites with different industrial vegetable waste. *ACS Applied Materials & Interfaces, 14*(41), 46920-46931. https://doi.org/10.1021/acsami.2c10965

Mulder, W. J., Gosselink, R. J. A., Vingerhoeds, M. H., Harmsen, P. F. H., & Eastham, D. (2011). Lignin based controlled release coatings. *Industrial Crops and Products, 34*(1), 915-920. https://doi.org/10.1016/j.indcrop.2011.02.011

Nisar, K., Kumar, J., Kumar, M. A., Walia, S., Shakil, N. A., Parsad, R., & Parmar, B. S. (2009). Pesticidal seed coats based on azadirachtin-A: Release kinetics, storage life and performance. *Pest Management Science: Formerly Pesticide Science, 65*(2), 175-182. https://doi.org/10.1002/ps.1665

Oliveira, T., Mota, I., Mousinho, F., Barbosa, R., Carvalho, L., & Alves, T. (2019). Biodegradation of mulch films from poly(butylene adipate co-terephthalate), carnauba wax, and sugarcane residue. *Journal of Applied Polymer Science, 136*(47), 48240. https://doi.org/10.1002/app.48240

Patil, N. V., & Netravali, A. N. (2016). Microfibrillated cellulose-reinforced nonedible starch-based thermoset biocomposites. *Journal of Applied Polymer Science, 133*(45), Article 43803. https://doi.org/10.1002/app.43803

Peng, Z., & Chen, F. (2011). Synthesis and properties of lignin-based polyurethane hydrogels. *International Journal of Polymeric Materials and Polymeric Biomaterials, 60*(9), 674-683. https://doi.org/10.1080/00914037.2010.551353

Pua, F. L., Sapuan, S., Zainudin, E. S., & Adib, M. (2013). Effect of fibre surface modification on properties of kenaf/poly (vinyl alcohol) composite film. *Journal of Biobased Materials and Bioenergy, 7*, 95-101. https://doi.org/10.1166/jbmb.2012.1270

Qu, P., Huang, H., Wu, G., Sun, E., & Chang, Z. (2015). Hydrolyzed soy protein isolates modified urea–formaldehyde resins as adhesives and its biodegradability. *Journal of Adhesion Science and Technology, 29*(21), 2381-2398. https://doi.org/10.1080/01694243.2015.1067176

Rhim, J. W., & Ng, P. K. (2007). Natural biopolymer-based nanocomposite films for packaging applications. *Critical Reviews in Food Science and Nutrition, 47*(4), 411-433. https://doi.org/10.1080/10408390600846366

Sander, M. (2019). Biodegradation of polymeric mulch films in agricultural soils: Concepts, knowledge gaps, and future research directions. *Environmental Science & Technology, 53*(5), 2304-2315. https://doi.org/10.1021/acs.est.8b05208

Sarkar, A., Biswas, D. R., Datta, S. C., Dwivedi, B. S., Bhattacharyya, R., Kumar, R., Bandyopadhyay, K. K., Saha, M., Chawla, G., & Saha, J. K. (2021). Preparation of novel biodegradable starch/poly (vinyl

alcohol)/bentonite grafted polymeric films for fertilizer encapsulation. *Carbohydrate Polymers, 259*, Article 117679. https://doi.org/10.1016/j.carbpol.2021.117679

Sikder, A., Pearce, A. K., Parkinson, S. J., Napier, R., & O'Reilly, R. K. (2021). Recent trends in advanced polymer materials in agriculture related applications. *ACS Applied Polymer Materials, 3*(3), 1203-1217. https://doi.org/10.1021/acsapm.0c00982

Singh, B., & Sharma, N. (2007). Optimized synthesis and characterization of polystyrene graft copolymers and preliminary assessment of their biodegradability and application in water pollution alleviation technologies. *Polymer Degradation and Stability, 92*(5), 876-885. https://doi.org/10.1016/j.polymdegradstab.2007.01.019

Spiridon, I., Teaca, C. A., & Bodirlau, R. (2011). Preparation and characterization of adipic acid-modified starch microparticles/plasticized starch composite films reinforced by lignin. *Journal of Materials Science, 46*(10), 3241-3251. https://doi.org/10.1007/s10853-010-5210-0

Stasi, E., Giuri, A., Ferrari, F., Armenise, V., Colella, S., Listorti, A., Rizzo, A., Ferraris, E., & Corcione, C. E. (2020). Biodegradable carbon-based ashes/maize starch composite films for agricultural applications. *Polymers, 12*(3), Article 524. https://doi.org/10.3390/polym12030524

Sun, J., Shen, J., Chen, S., Cooper, M. A., Fu, H., Wu, D., & Yang, Z. (2018). Nanofiller reinforced biodegradable PLA/PHA composites: Current status and future trends. *Polymers, 10*(5), Article 505. https://doi.org/10.3390/polym10050505

Tan, Z., Yi, Y., Wang, H., Zhou, W., Yang, Y., & Wang, C. (2016). Physical and degradable properties of mulching films prepared from natural fibers and biodegradable polymers. *Applied Sciences, 6*(5), Article 147. https://doi.org/10.3390/app6050147

Tarara, J. (2000). Microclimate modification with plastic mulch. *HortScience, 35*(2), 169-180. https://doi.org/10.21273/HORTSCI.35.2.169

Tomaszewska, M., & Jarosiewicz, A. (2004). Polysulfone coating with starch addition in CRF formulation. *Desalination, 163*(1), 247-252. https://doi.org/10.1016/S0011-9164(04)90196-8

Vejan, P., Khadiran, T., Abdullah, R., & Ahmad, N. (2021). Controlled release fertilizer: A review on developments, applications and potential in agriculture. *Journal of Controlled Release, 339*, 321-334. https://doi.org/10.1016/j.jconrel.2021.10.003

Wang, H., Wei, D., Zheng, A., & Xiao, H. (2015). Soil burial biodegradation of antimicrobial biodegradable PBAT films. *Polymer Degradation and Stability, 116*, 14-22. https://doi.org/10.1016/j.polymdegradstab.2015.03.007

Wang, S., Jia, Z., Zhou, X., Zhou, D., Chen, M., Xie, D., Luo, Y., & Jia, D. (2017). Preparation of a biodegradable poly (vinyl alcohol)–starch composite film and its application in pesticide controlled release. *Journal of Applied Polymer Science, 134*(28), Article 45051. https://doi.org/10.1002/app.45051

Wu, K. J., Wu, C. S., & Chang, J. S. (2007). Biodegradability and mechanical properties of polycaprolactone composites encapsulating phosphate-solubilizing bacterium Bacillus sp. PG01. *Process Biochemistry, 42*(4), 669-675. https://doi.org/10.1016/j.procbio.2006.12.009

Yang, Y., Li, P., Jiao, J., Yang, Z., Lv, M., Li, Y., Zhou, C., Wang, C., He, Z., Liu, Y., & Song, S. (2020). Renewable sourced biodegradable mulches and their environment impact. *Scientia Horticulturae, 268*, Article 109375. https://doi.org/10.1016/j.scienta.2020.109375

Ying, Z. R., Liu, H. S., Yan, R., Yang, T. Y., & Dang, Z. M. (2012). Preparation and fertilizer-Permeation performance of urea-formaldehyde resins modified by montmorillonite. *Advanced Materials Research, 361*, 1441-1444. https://doi.org/10.4028/www.scientific.net/AMR.361-363.1441

Yuan, P., Tan, D., & Annabi-Bergaya, F. (2015). Properties and applications of halloysite nanotubes: Recent research advances and future prospects. *Applied Clay Science, 112*, 75-93. https://doi.org/10.1016/j.clay.2015.05.001

Zeng, Q. H., Yu, A. B., Lu, G. Q., & Paul, D. R. (2005). Clay-based polymer nanocomposites: Research and commercial development. *Journal of Nanoscience and Nanotechnology, 5*(10), 1574-1592. https://doi.org/10.1166/jnn.2005.411

Zeng, X., Zhong, B., Jia, Z., Zhang, Q., Chen, Y., & Jia, D. (2019). Halloysite nanotubes as nanocarriers for plant herbicide and its controlled release in biodegradable polymers composite film. *Applied Clay Science, 171*, 20-28. https://doi.org/10.1016/j.clay.2019.01.021

Zhao, M., Wang, Y., Liu, L., Liu, L., Chen, M., Zhang, C., & Lu, Q. (2018). Green coatings from renewable modified bentonite and vegetable oil based polyurethane for slow release fertilizers. *Polymer Composites, 39*(12), 4355-4363. https://doi.org/10.1002/pc.24519

Pertanika J. Sci. & Technol. 33 (S5): 109 - 119 (2025)

PERTANIKA JOURNALS

SCIENCE & TECHNOLOGY

Journal homepage: http://www.pertanika.upm.edu.my/

Pork Adulteration in Beef and Mutton Detection Using Visible Near-Infrared (Vis-NIR) Spectroscopy and Chemometrics

Rudiati Evi Masithoh[1]*, Aridatuz Zahroh[1], Muhammad Fahri Reza Pahlawan[2] and Laila Rahmawati[3]

[1]Department of Agricultural and Biosystems Engineering, Faculty of Agricultural Technology, Universitas Gadjah Mada, Jl. Flora No. 1 Bulaksumur, Yogyakarta 55281, Indonesia
[2]Department of Smart Agriculture Systems, College of Agricultural and Life Science, Chungnam National University, Daejeon 34134, Republic of Korea
[3]Research Center for Food Technology and Processing, National Research and Innovation Agency, Gunung Kidul, 55861 Yogyakarta, Indonesia

ABSTRACT

The addition of pork to beef and mutton is a potentially fraudulent practice. This study aims to detect adulteration of pork in beef and mutton using visible near-infrared (Vis-NIR) spectroscopy. Classification models for Beef+Pork and Mutton+Pork were developed using principal component analysis (PCA) and linear discriminant analysis (LDA). PCA demonstrated that respiratory pigments and the Soret band influenced the classification of meat based on Vis-NIR spectra. The most effective model was achieved by combining PCA with linear discriminant analysis (PCA-LDA), utilizing the original Vis-NIR spectra. The PCA-LDA model achieved a calibration accuracy of 99% for Beef+Pork and 82.4% for Mutton+Pork, with prediction accuracies of 91.3% and 73.7%, respectively. These results demonstrate that Vis-NIR spectroscopy can be utilized to authenticate minced meat, providing a promising approach for on-site screening or halal verification.

Keywords: Beef, food authentication, halal, mutton, PCA-LDA, pork, Vis-NIR

ARTICLE INFO

Article history:
Received: 13 February 2024
Accepted: 28 May 2025
Published: 10 July 2025

DOI: https://doi.org/10.47836/pjst.33.S5.06

E-mail address:
Evi@ugm.ac.id (Rudiati Evi Masithoh)
aridatuzzahroh@mail.ugm.ac.id (Aridatuz Zahroh)
mfrezap@mail.ugm.ac.id (Muhammad Fahri Reza Pahlawan)
laila.rahmawati53@gmail.com (Laila Rahmawati)
*Corresponding author

INTRODUCTION

Meat is one of the most widely traded processed foods, available in various forms, including cuts and minced meat. In minced form, meat is often prone to accidental or intentional mixing, as it is difficult to distinguish between different types of meat. Deliberately mixing two or more ingredients without the consumer's consent constitutes

e-ISSN: 2231-8526

adulteration. Such practices can be economically detrimental when low-quality products are sold as high-quality ones at inflated prices. The mixing of pork, beef, and mutton is a particular concern due to price discrepancies and religious dietary restrictions; pork consumption is prohibited for Muslims, and beef is forbidden for Hindus. Adulteration also poses health risks if the additives are allergens or have toxic effects (Kucharska-Ambrożej & Karpinska, 2019). Hence, a reliable method must be established to detect the presence of undeclared ingredients in minced meat.

Meat types can be differentiated through sensory evaluation of color, taste, or aroma. DNA analysis and PCR tests offer another approach (Hrbek et al., 2020; Hu et al., 2021). However, these chemical methods are expensive, time-consuming, and require expert handling. Moreover, PCR tests cannot quantify adulteration levels in meat (Mabood et al., 2020). Conversely, non-destructive methods using infrared (IR) spectroscopy have been employed to detect products with similar colors (Masithoh et al., 2020) and to identify adulteration (Nobari-Moghaddam et al., 2021). IR spectroscopy offers a rapid, accurate, inexpensive, and easy-to-use detection method.

The successful application of Fourier Transform IR (FTIR) and Visible Near-Infrared (Vis-NIR) spectroscopy in determining meat quality has been reported (Siddiqui et al., 2021; Zhang et al., 2022). Vis-NIR spectroscopy operates within the near-infrared and visible light spectrums (400–2500 nm). Vis-NIR spectra contain information about color pigments in the visible region and C-H-N-O molecules in the NIR region (Cortés et al., 2019). Meat spectra in the visible regions contain information related to myoglobin (Mb) (Cozzolino & Murray, 2004; Weng et al., 2020), while the NIR region provides information about protein and lipids (Barbin et al., 2013).

Spectroscopy and chemometrics are typically used together to extract relevant information from spectra and relate it to the target variable (Li et al., 2022). Chemometrics employs multivariate analysis techniques, such as partial least squares regression (PLSR) for prediction and principal component analysis (PCA) for classification. PCA and linear discriminant analysis (LDA) have been successfully used to discriminate between tea samples (Esteki et al., 2023) and coffee (Silva et al., 2021). Combining dimension reduction with PCA and classification using LDA has been shown to perform better for discrimination (Zhao et al., 2011). Therefore, this study aimed to use Vis-NIR spectroscopy (400–1000 nm) to detect pork adulteration in minced mutton and beef. A predictive model for quantifying pork adulteration levels in minced mutton and beef was developed using PCA and LDA.

MATERIALS AND METHODS

Samples

Beef, mutton, and pork samples were purchased from the local markets in Yogyakarta, Indonesia. The meat was refrigerated at 10 °C within 1 hour of collection to maintain

freshness. Each meat type was minced separately using a mince-machine. Minced pork was used as the adulterant, while minced beef and mutton were the adulterated meats. Eleven pork adulterant concentrations were prepared in beef and mutton: 0%, 10%, 20%, 30%, 40%, 50%, 60%, 70%, 80%, 90%, and 100%. For each concentration, 100 g mixtures of beef and pork (Beef+Pork) and mutton and pork (Mutton+Pork) were manually mixed for 20 minutes by two individuals to ensure homogeneity. All samples were stored at 10 °C until spectral acquisition to maintain sample freshness.

Spectra Acquisition

Reflectance spectra of visible near-infrared spectroscopy (Vis-NIRs) were obtained using a Vis-NIR spectrometer (Flame-T-VIS-NIR, Ocean Optics, 350-1000 nm). The system had a fiber optic reflection probe (QR400-7-Vis-NIR, Ocean Optics, USA) and a light source (tungsten halogen lamp, HL-2000-HP-FHSA, Ocean Optics, USA). Before spectra acquisition, the meat sample was removed from the refrigerator and cooled to room temperature. Each meat sample was divided into five small samples (each weighing approximately 20 g) and placed in an aluminum vial (7 cm diameter and 1 cm height) to ensure similar sample density. Twenty spectra were measured for each small sample.

Chemometrics Analysis

The reflectance spectra collected from Vis-NIR were imported into The Unscrambler®X software (CAMO, Oslo, Norway) for multivariate analysis, which contained independent variables (x-variables) and predictors (y-variables). The Vis-NIR spectra consisted of 3188 independent variables. Samples consisted of eleven variations of pork adulterant concentrations (0%, 10%, 20%, 30%, 40%, 50%, 60%, 70%, 80%, 90%, and 100%) and were grouped into five classes as the predictors (y-variables): Pure (100% beef or mutton), Low (10–30% pork), Medium (40–60% pork), High (70–90% pork), and Pork (100% pork).

Principal component analysis (PCA) was conducted to classify Beef+Pork and Mutton+Pork using Vis-NIR spectra. PCA is an unsupervised multivariate analysis used for dimension reduction, pattern analysis, important wavelength identification, and outlier selection. PCA-LDA was a well-justified choice for this study due to its ability to handle high-dimensional spectral data, classify categorical variables, and balance performance and computational efficiency well. The combination of PCA for dimension reduction and LDA for classification, along with appropriate preprocessing techniques, enabled the development of a robust and accurate model for detecting pork adulteration in beef and mutton. Using the PCA algorithm, the multivariate dimensions of the spectra are reduced into new variables, namely principal components (PCs). Pattern analysis was conducted based on the score plot, and essential wavelengths were identified based on the loading plot. Sample outliers were identified based on T2 and leverage. Eight hundred (800)

spectra of Vis-NIR were divided into a calibration and prediction set using the Kennard-Stone algorithm. The calibration set consisted of 500 spectra, while the prediction dataset consisted of 300 spectra.

PCA-LDA was used to build calibration models for predicting pork adulteration levels in beef and mutton. This supervised classification method is suitable for categorical variables, such as adulteration levels. Models were developed using spectra (x-variables) and adulteration levels (y-variables) from the calibration set. The development of the PCA-LDA model involves two essential steps. The first is the dimension reduction of multivariable spectra into 7 PCs using PCA. The second step uses the Quadratic method to construct an LDA model from the seven pre-built PCs. Model performance was evaluated using accuracy and misclassification rate using Equations 1 and 2. The ideal model has a high accuracy value and a low misclassification rate. Preprocessing techniques such as normalization and Savitzky-Golay first derivative were applied to the spectra.

$$Accuracy = \frac{n_{correct}}{n_{total}} \times 100\% \quad [1]$$

$$Misclassification\ rate\ = \frac{n_{false}}{n_{total}} \times 100\% = \ 100 - Accuracy \quad [2]$$

RESULTS AND DISCUSSION

Spectral Profiles of Pure and Pork-adulterated Samples Based on Vis-NIR Spectra

Figure 1 shows the profiles of minced pork, mutton, and beef developed using original Vis-NIR spectra. The overall spectral shapes and trends are similar, and the difference lies in the absorbance intensities, which distinguish the meat. The highest reflectance belongs to mutton, followed by pork and beef, while the highest absorbance belongs to beef, followed by pork and mutton. All pure meat spectra have similar patterns showing several peaks between 430 nm (hemoglobin pigments), 500–600 nm (respiratory pigments, and around 940–990 nm (related to OH and CH) (Ayaz et al., 2020; Peyvasteh et al., 2020).

Original Vis-NIR spectra of Beef+Pork and Mutton+Pork in various concentrations are shown in Figures 2a and 2b. Both figures exhibit similar trends, showing absorbance at 400-600 nm related to the Soret, oxymyoglobin, and myoglobin bands (Cozzolino & Murray, 2004). After being preprocessed using the Savitzky-Golay first derivative method, the spectra were altered, as shown in Figures 3a and 3b. The reflectance peaks are more distinct compared to the original spectra.

In the Vis-NIR region (400–600) nm, distinct respiratory pigment bands are related to meat myoglobin and heme absorption. This region (Figure 2a) shows the decrease in absorbance of those bands with the decrease of red pigments (Alamprese et al., 2013);

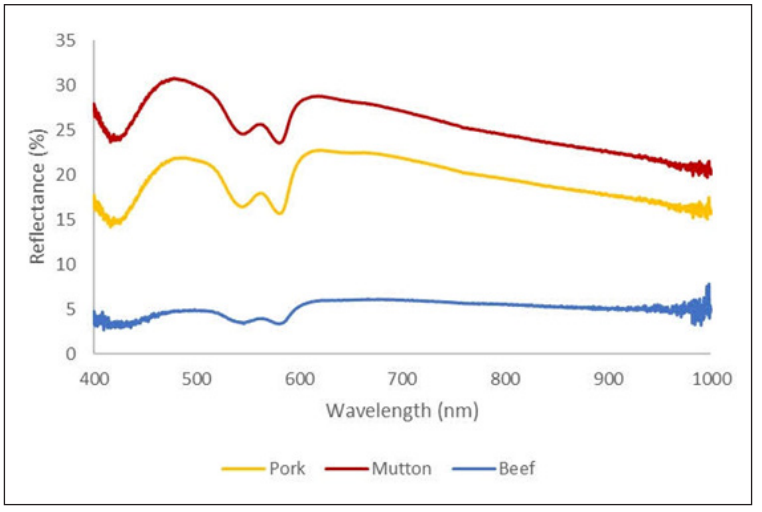

Figure 1. Original Vis-NIR spectra of pure minced pork, mutton, and beef

beef absorbances decrease if more pork concentration is added. More absorbances at 650 nm and 950–1000 nm are noticed for Beef+Pork than for Mutton+Pork. In Figure 2a, pure beef has no distinct absorbance, but a peak absorbance at 650 nm is observed after pork is added. The absorbance at 650 nm might be due to metmyoglobin (Bekhit et al., 2019) present in Beef+Pork. Peaks around 950–1000 nm correspond to O-H (Morsy & Sun, 2013) and are more distinct in Beef+Pork than Mutton+Pork, either for original spectra (Figure 2) or Savitzky-Golay first derivative spectra (Figure 3). These peaks are due to the higher average water content in beef compared to mutton and pork (Lee et al., 1995).

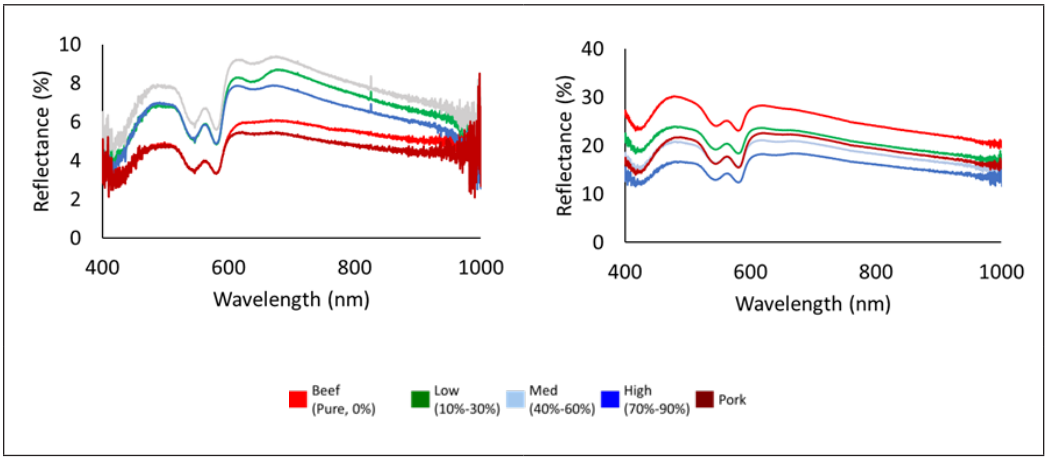

(a) (b)

Figure 2. Original Vis-NIR spectra of (a) Beef+Pork and (b) Mutton+Pork at varying pork concentrations

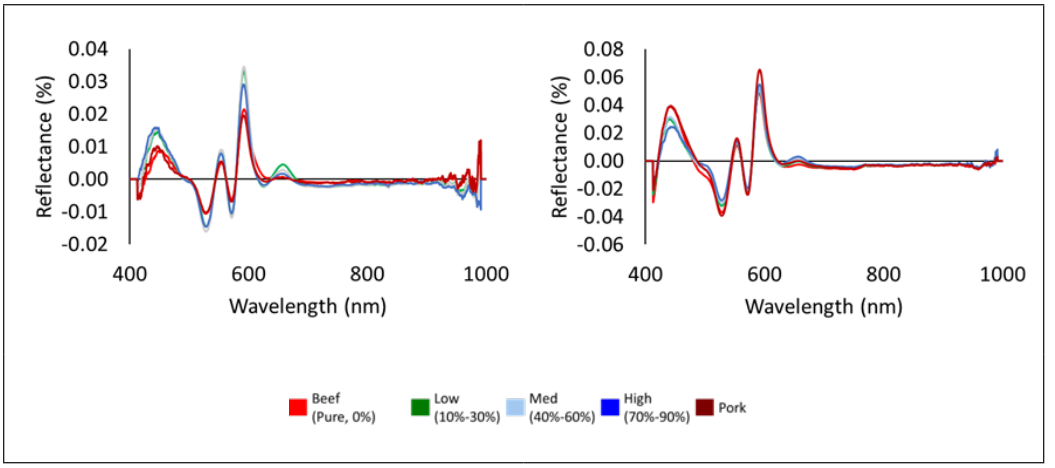

(a) (b)

Figure 3. Savitzky-Golay 1st derivative Vis-NIR spectra of (a) Beef+Pork and (b) Mutton+Pork at varying pork concentrations

Principal Component Analysis (PCA) of Vis-NIR Spectra

The PCA for beef adulterated with pork (Beef+Pork) using Vis-NIR spectra is shown in Figure 4. The total variance can be explained by 99% using the first three PCs, specifically PC-1 (96%), PC-2 (2%), and PC-3 (1%). The score plot of PC-2 vs. PC-3 effectively differentiated the meat samples into four distinct groups. Category I, the pure beef samples, are placed in the fourth quadrant of the graph. The combination samples of low and medium levels of adulteration (Category IV) are placed in the third quadrant of the graph. The highly contaminated samples (Category III) are in the second quadrant of the graph, while the pork samples (Category I) are in the first quadrant. The loading plot of PC-2 in Figure 2d shows that the Soret band influences PC-2 at around 400 nm and water content at around 975 nm (Alamprese et al., 2013; Weng et al., 2020). The PC-3 loading plot shows that the Soret band influences PC-3 at around 440 nm and respiratory pigments at 535–590 nm (Ayaz et al., 2020; Weng et al., 2020).

As shown in Figure 5, the PCA using Vis-NIR spectra was developed using raw spectra for mutton adulterated with pork (Mutton+Pork). The first 3 PCs explained 100% of the variance, namely PC-1: 99%, PC-2: 1%, and PC-3: 0%. The PC-1 has the highest explained variance. However, based on Figure 3a, PC-1 could not differentiate between Mutton+Pork samples. On the other hand, PC-2 and PC-3 could classify Mutton+Pork samples into four categories. The PC-2 could discriminate pork (Category IV) and highly adulterated beef (Category III) from pure mutton (Category I) and low and medium-adulterated mutton (Category II). Samples in Category IV and Category III have negative score values of PC-2, while samples in Category II and Category I have positive values of PC-2. The

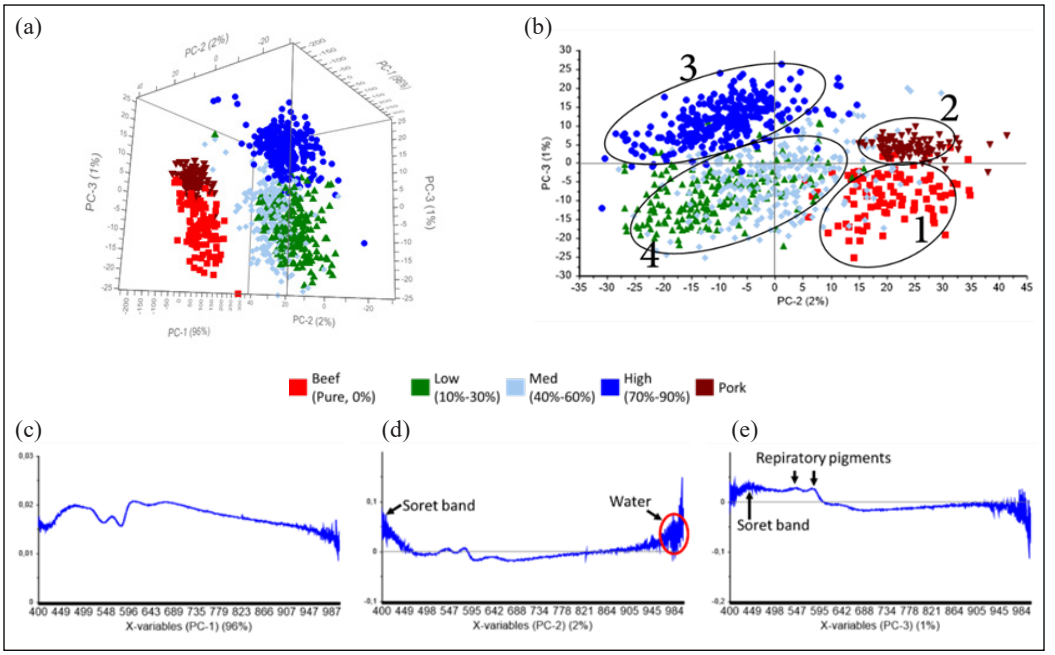

Figure 4. PCA score and loading plot of Beef+Pork using Vis-NIR spectra

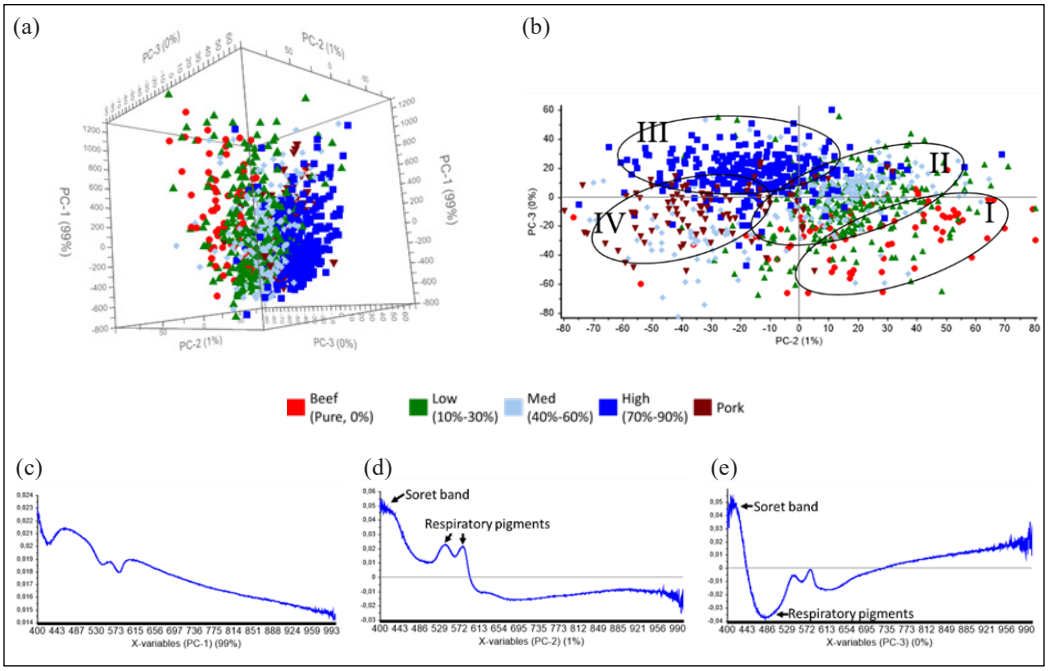

Figure 5. PCA score and loading plot of Mutton+Pork using Vis-NIR spectra

PC-3 could discriminate Category IV from Category III and Category II from Category I. Samples in Category III and Category II had positive values of PC-3, while samples in Category IV and Category I had negative values of PC-3. On the score plot of PC-2 vs. PC-3, Category I is in the fourth quadrant of the graph, Category II in the third quadrant, Category III in the second quadrant, and Category IV in the fourth quadrant of the graph. The loading plot of PC-2 (Figure 5d) and PC-3 (Figure 5e) shows that the Soret band influenced the classification at 400–440 nm in both PCs (Ayaz et al., 2020). Respiratory pigments influenced the PC-2 at 530–580 nm and 480 nm in the PC-3 (Weng et al., 2020).

Principal Component Analysis—Linear Discriminant Analysis (PCA-LDA) Using VisNIR Spectra

The PCA-LDA performances built using Vis-NIR spectra are shown in Table 1. The highest accuracies for Beef+Pork were 99.0% (calibration) and 91.3% (prediction), while for Mutton+Pork, they were 82.4% (calibration) and 73.7% (prediction). Those models were both obtained from raw spectra. The failure of preprocessing to improve accuracy in this study highlights the importance of careful selection and optimization of preprocessing techniques. While preprocessing aims to remove noise and enhance relevant spectral features, it can inadvertently remove or distort information crucial for discriminating between different adulteration levels. The PCA-LDA of Beef+Pork developed using original spectra has a misclassification rate of 1.0% for calibration and 8.7% for prediction. Table 1 also showed that preprocessed spectra could not improve model performance compared to the model with raw spectra. Lower performances of preprocessed spectra could be obtained because sometimes the preprocessed spectra may even omit information essential to the model.

Table 1
PCA-LDA Performances to classify adulteration levels in meat

Sample	Performance	Original		Normalization		SGD1	
		C	P	C	P	C	P
Beef+Pork	Accuracy	99.0%	91.3%	97.0%	90.7%	97.2%	90.0%
	Misclassification rate	1.0%	8.7%	3.0%	9.3%	2.8%	10.0%
Mutton+Pork	Accuracy	82.4%	73.7%	82.4%	70.3%	77.0%	75.0%
	Misclassification rate	17.6%	26.3%	17.6%	29.7%	23.0%	25.0%

Note: SGD1 = 1st order of Savitzky-Golay derivative, C = calibration, P = prediction

CONCLUSION

Vis-NIR spectroscopy, coupled with PCA-LDA, provides a simple, fast, and accurate method for determining the levels of pork adulteration in Beef+Pork and Mutton+Pork

mixtures. The best PCA-LDA model, utilizing the original Vis-NIR spectra, achieved a calibration accuracy of 99% for Beef+Pork and 82.4% for Mutton+Pork. SW-NIR yielded lower performance, with the best calibration accuracy of 91.4% and 86.2% for Beef+Pork and Mutton+Pork, respectively. The model built can predict adulteration levels in minced beef and mutton without requiring complex sample preparation and will be particularly beneficial to several stakeholders. Meat producers and processors can use it for quality control, ensuring product authenticity. Regulatory agencies can employ it for on-site screening and enforcing food labeling. Consumers, especially those with religious dietary restrictions, can use it to verify the absence of forbidden meats. Retailers can also leverage it to ensure product authenticity.

This study provides a strong foundation for future research, addressing a significant challenge in food authenticity and consumer protection. Further investigations could explore the application of this Vis-NIR PCA-LDA methodology to other meat types (e.g., poultry, fish) and processed food products. Furthermore, integrating this technique with emerging technologies, such as hyperspectral imaging, may offer enhanced analytical capabilities and potentially improve the accuracy and robustness of adulteration detection. Overall, this result shows the capability of using non-destructive methods for on-site testing, contributing to greater transparency and trust in the meat supply chain.

ACKNOWLEDGEMENT

We thank the Ministry of Higher Education, Research, and Technology of Indonesia through "Penelitian Dasar Unggulan Perguruan Tinggi 2022" for their support in conducting this research.

REFERENCES

Alamprese, C., Casale, M., Sinelli, N., Lanteri, S., & Casiraghi, E. (2013). Detection of minced beef adulteration with turkey meat by UV-vis, NIR and MIR spectroscopy. *LWT - Food Science and Technology*, *53*(1), 225–232. https://doi.org/10.1016/j.lwt.2013.01.027

Ayaz, H., Ahmad, M., Sohaib, A., Yasir, M. N., Zaidan, M. A., Ali, M., Khan, M. H., & Saleem, Z. (2020). Myoglobin-based classification of minced meat using hyperspectral imaging. *Applied Sciences (Switzerland)*, *10*(19), Article 6862. https://doi.org/10.3390/app10196862

Barbin, D. F., Elmasry, G., Sun, D. W., & Allen, P. (2013). Non-destructive determination of chemical composition in intact and minced pork using near-infrared hyperspectral imaging. *Food Chemistry*, *138*(2–3), 1162–1171. https://doi.org/10.1016/j.foodchem.2012.11.120

Bekhit, A. E. D. A., Morton, J. D., Bhat, Z. F., & Zequan, X. (2019). Meat colour: Chemistry and measurement systems. *Encyclopedia of Food Chemistry*, *2,* 211–217. https://doi.org/10.1016/B978-0-08-100596-5.22419-0

Cortés, V., Blasco, J., Aleixos, N., Cubero, S., & Talens, P. (2019). Monitoring strategies for quality control of agricultural products using visible and near-infrared spectroscopy: A review. *Trends in Food Science and Technology*, *85*, 138–148. https://doi.org/10.1016/j.tifs.2019.01.015

Cozzolino, D., & Murray, I. (2004). Identification of animal meat muscles by visible and near infrared reflectance spectroscopy. *LWT - Food Science and Technology*, *37*(4), 447–452. https://doi.org/10.1016/j.lwt.2003.10.013

Esteki, M., Memarbashi, N., & Simal-Gandara, J. (2023). Classification and authentication of tea according to their harvest season based on FT-IR fingerprinting using pattern recognition methods. *Journal of Food Composition and Analysis*, *115*, Article 104995. https://doi.org/10.1016/j.jfca.2022.104995

Hrbek, V., Zdenkova, K., Jilkova, D., Cermakova, E., Jiru, M., Demnerova, K., Pulkrabova, J., & Hajslova, J. (2020). Authentication of meat and meat products using triacylglycerols profiling and by DNA analysis. *Foods*, *9*(9), Article 1269. https://doi.org/10.3390/foods9091269

Hu, H., Cheng, J., Wei, C., Li, S., Yu, C., Meng, X., & Li, J. (2021). Pre-degassed microfluidic chamber-based digital pcr device for meat authentication applications. *Micromachines*, *12*(6), Article 694. https://doi.org/10.3390/mi12060694

Kucharska-Ambrożej, K., & Karpinska, J. (2019). The application of spectroscopic techniques in combination with chemometrics for detection adulteration of some herbs and spices. *Microchemical Journal*, *153*, Article 104278. https://doi.org/10.1016/j.microc.2019.104278

Lee, S. M., Buss, D. H., Holcombe, G. D., & Hatton, D. (1995). Nutrient content of retail cuts of beef, pork and lamb–preliminary results. *Journal of Human Nutrition and Dietetics*, *8*(1), 75–80. https://doi.org/10.1111/j.1365-277X.1995.tb00297.x

Li, Y., Wang, G., Guo, G., Li, Y., Via, B. K., & Pei, Z. (2022). Spectral preprocessing and multivariate calibration methods for the prediction of wood density in Chinese white poplar by visible and near infrared spectroscopy. *Forests*, *13*(1), Article 62. https://doi.org/10.3390/f13010062

Mabood, F., Boqué, R., Alkindi, A. Y., Al-Harrasi, A., Al Amri, I. S., Boukra, S., Jabeen, F., Hussain, J., Abbas, G., Nureen, Z., Haq, Q. M. I., Shah, H. H., Khan, A., Khalaf, S. K., & Kadim, I. (2020). Fast detection and quantification of pork meat in other meats by reflectance FT-NIR spectroscopy and multivariate analysis. *Meat Science*, *163*, Article 108084. https://doi.org/10.1016/j.meatsci.2020.108084

Masithoh, R. E., Amanah, H. Z., & Cho, B. K. (2020). Application of fourier transform near-infrared (FT-NIR) and fourier transform infrared (FT-IR) spectroscopy coupled with wavelength selection for fast discrimination of similar color of tuber flours. *Indonesian Journal of Chemistry*, *20*(3), Article 680. https://doi.org/10.22146/ijc.48092

Morsy, N., & Sun, D. W. (2013). Robust linear and non-linear models of NIR spectroscopy for detection and quantification of adulterants in fresh and frozen-thawed minced beef. *Meat Science*, *93*(2), 292–302. https://doi.org/10.1016/j.meatsci.2012.09.005

Nobari-Moghaddam, H., Tamiji, Z., Akbari-Lakeh, M., Khoshayand, M. R., & Haji-Mahmoodi, M. (2021). Multivariate analysis of food fraud: A review of NIR based instruments in tandem with chemometrics. *Journal of Food Composition and Analysis*, *107*, Article 104343. https://doi.org/10.1016/j.jfca.2021.104343

Peyvasteh, M., Popov, A., Bykov, A., & Meglinski, I. (2020). Meat freshness revealed by visible to near-infrared spectroscopy and principal component analysis. *Journal of Physics Communications*, *4*(9), Article 095011. https://doi.org/10.1088/2399-6528/abb322

Siddiqui, M. A., Khir, M. H. M., Witjaksono, G., Ghumman, A. S. M., Junaid, M., Magsi, S. A., & Saboor, A. (2021). Multivariate analysis coupled with m-svm classification for lard adulteration detection in meat mixtures of beef, lamb, and chicken using ftir spectroscopy. *Foods*, *10*(10), Article 2405. https://doi.org/10.3390/foods10102405

Silva, T. V., Pérez-Rodríguez, M., de Oliveira, N. R., de Santana, H., & de Almeida, L. C. (2021). Tracing commercial coffee quality by infrared spectroscopy in tandem with pattern recognition approaches. *Vibrational Spectroscopy*, *116*, Article 103295. https://doi.org/10.1016/j.vibspec.2021.103295

Weng, S., Guo, B., Tang, P., Yin, X., Pan, F., Zhao, J., Huang, L., & Zhang, D. (2020). Rapid detection of adulteration of minced beef using Vis/NIR reflectance spectroscopy with multivariate methods. *Spectrochimica Acta - Part A: Molecular and Biomolecular Spectroscopy*, *230*, Article 118005. https://doi.org/10.1016/j.saa.2019.118005

Zhang, J., Liu, G., Li, Y., Guo, M., Pu, F., & Wang, H. (2022). Rapid identification of lamb freshness grades using visible and near-infrared spectroscopy (Vis-NIR). *Journal of Food Composition and Analysis*, *111*, Article 104590. https://doi.org/10.1016/j.jfca.2022.104590

Zhao, N., Mio, W., & Liu, X. (2011). A hybrid PCA-LDA model for dimension reduction. In *The 2011 International Joint Conference on Neural Networks* (pp. 2184-2190). IEEE. https://doi.org/10.1109/IJCNN.2011.6033499

REFEREES FOR THE PERTANIKA
JOURNAL OF SCIENCE & TECHNOLOGY

Vol. 33 (S5) 2025

The Editorial Board of the Pertanika Journal of Science and Technology wishes to thank the following:

Apurav Koyande
UTP, Malaysia

Hasfalina Che Man
UPM, Malaysia

Jamarosliza Jamaluddin
UTM, Malaysia

Jarinah Mohd Ali
UKM, Malaysia

Khalina Abdan
UPM, Malaysia

Meng Wai Woo
University of Auckland, New Zealand

Mohammad Rezaul Islam Shishir
ZJU, China

Nadavala Siva Kumar
KSU, Saudi Arabia

Nik Nor Liyana Nik Ibrahim
UPM, Malaysia

Revathy Sankaran
UCSI, Malaysia

Siti Farah Md Tohid
UPM, Malaysia

Zainab T. Al-Sharify
Mustansiryiah University, Iraq

KSU	*- King Saud University*	*UTM*	*- Universiti Teknologi Malaysia*
UKM	*- Universiti Kebangsaan Malaysia*	*UTP*	*- Universiti Teknologi PETRONAS*
UPM	*- Universiti Putra Malaysia*	*ZJU*	*- Zhejiang University*

While every effort has been made to include a complete list of referees for the period stated above, however if any name(s) have been omitted unintentionally or spelt incorrectly, please notify the Chief Executive Editor, *Pertanika* Journals at executive_editor.pertanika@upm.edu.my

Pertanika Journal of Science & Technology
Vol. 33 (S5) 2025

Content

Pertanika Editorial Office, Journal Division,
Putra Science Park,
1st Floor, IDEA Tower II,
UPM-MTDC Center,
Universiti Putra Malaysia,
43400 UPM Serdang,
Selangor Darul Ehsan
Malaysia

http://www.pertanika.upm.edu.my
Email: executive_editor.pertanika@upm.edu.my
Tel. No.: +603- 9769 1622

PENERBIT UPM UNIVERSITI PUTRA MALAYSIA PRESS

http://penerbit.upm.edu.my
Email: penerbit@upm.edu.my
Tel. No.: +603- 9769 8855

e-ISSN 2231-8526